INTERNATIONAL ISLAMIC UNIVERSITY ISLAMABAD

In – plane and Out – of – plane Flexural Behavior of Bamboo Interlocking Block Masonry

Submitted By

NAME: Abdullah Yasin

REG No. 10/MSCE/FET/F22

in the

Faculty of Engineering Department of Civil Engineering

2024

Dedication:

To my parents

And

"It is with my deepest gratitude and warmest affection that I dedicate this thesis to my mentor "**Dr. Zeshan Alam**" who has been constant source of knowledge, guidance and inspiration for me in this whole period."

CERTIFICATE OF APPROVAL

Title of Thesis: **"In – plane and Out – of – plane Flexural Behavior of Bamboo Interlocking Block Masonry".**

Name of Student: **Abdullah Yasin**

Registration No: **10/MSCE/FET/F22**

Accepted by the Department of Civil Engineering, Faculty of Engineering and Technology, International Islamic University (IIU), Islamabad, in partial fulfillment of the requirements for the Master of Science degree in Civil Engineering.

Viva voce committee:

Prof. Dr. Sayed Abid Ali Shah (Supervisor)
Professor DCE, FET, IIU Islamabad

Dr. Nisar Ali Khan (Internal)
Assistant Prof. DCE, FET, IIU Islamabad

Dr. Faheem Butt (External)
Assistant Prof. DCE, UET, Taxila

Prof. Dr. Sayed Abid Ali Shah (Chairman, DCE)
Professor DECE, FET, IIU Islamabad

Prof. Dr. Muhammad Amir (Dean, FET)
Professor DECE, FET, IIU Islamabad

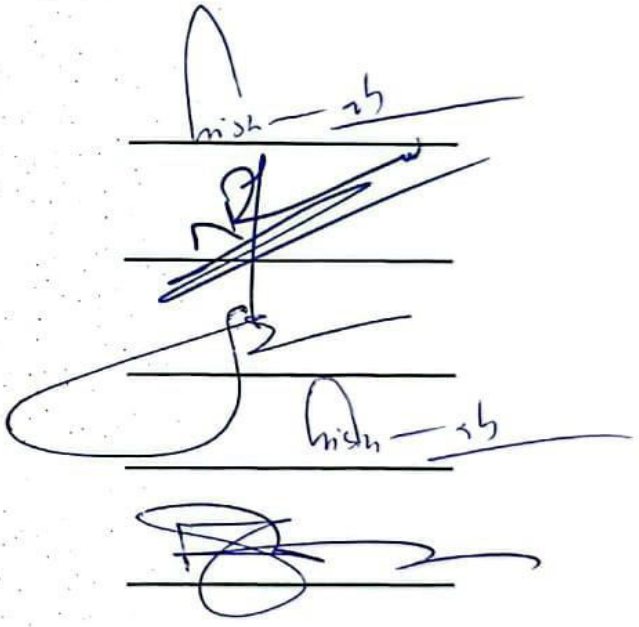

IV

Author's Declaration

I, **Abdullah yasin** hereby state that my MS thesis titled "**In – plane and Out – of – Plane Flexural Behavior of Bamboo reinforced Interlocking Block Masonry**" is my own work and has not been submitted previously by me for taking any degree from International Islamic University, Islamabad or anywhere else in the country/abroad.

At any time if my statement is found to be incorrect even after my graduation,the University has the right to withdraw my MS Degree.

Student Name: **Abdullah Yasin.**

Reg. no. : **10/MSCE.FET/F22.**

Plagiarism Undertaking

I solemnly declare that research work presented in this thesis titled "**In – plane and Out – of – Plane Flexural Behavior of Bamboo reinforced Interlocking Block Masonry**" is solely my research work with no significant contribution from any other person. Small contribution/help wherever taken has been duly acknowledged and that complete thesis has been written by me.

I understand the zero-tolerance policy of the HEC and International Islamic University, Islamabad towards plagiarism. Therefore, I as an author of the above titled thesis declare that no portion of my thesis has been plagiarized and any material used as reference is properly referred/cited.

I undertake that if I am found guilty of any formal plagiarism in the above titled thesis even after award of MS Degree, the University reserves the right to with- draw/revoke my MS degree and that HEC and the University have the right topublish my name on the HEC/University website on which names of students areplaced who submitted plagiarized work.

Student Name: **ABDULLAH YASIN**

Reg. no.: **10/MSCE/FET/F22**

Abstract

In regions susceptible to seismic activity, as well as locations where vibrations or impact loading are prevalent such as subway systems, industrial environments, or transportation infrastructure there is a growing need for construction materials and techniques that offer durability and resilience. Traditional reinforced masonry systems, while reliable, face challenges in terms of sustainability and performance under dynamic forces. To address these challenges, bamboo reinforcement is being explored as a viable alternative. With its excellent mechanical properties and sustainability, bamboo provides a cost-effective solution that enhances the performance of reinforced mortar masonry (RMM). The addition of bamboo strips significantly improves masonry's resistance to vibrations, impact, and seismic forces. This research focuses on integrating bamboo reinforcement into RMM, aiming to optimize its structural performance, environmental benefits, and durability for use in diverse applications, including earthquake-prone areas and locations prone to impact or vibration.

Building on the premise of enhancing the performance of RMM through bamboo integration, this study specifically assesses the out-of-plane behavior of masonry walls. The innovative aspect of this research lies in the placement of bamboo strips behind the walls as reinforcement. Additionally, some walls feature strategically positioned openings to simulate the effect of windows, with bamboo reinforcement placed within these areas. This arrangement provides a unique configuration that differs from traditional reinforcement methods. Our approach to evaluating the out-of-plane behavior involves both impact and static testing methods, capturing a comprehensive view of the material's performance. A total of 25 samples have been prepared, with six walls reinforced with bamboo strips ranging in size from 19 mm to 25 mm. This research not only advances understanding of bamboo as a reinforcement material but also highlights its potential to enhance the resilience of masonry structures in earthquake- and vibration-prone areas, offering a sustainable alternative to conventional reinforcement.

Bamboo reinforcement did not show significant changes in compression behavior; however, it led to notable improvements in flexural and tensile performance in masonry walls. Through the impact test, the SW, SWOB, and SWB walls showed 10.28%, 12.89%, and 20.8% improvement, respectively, as compared to the SWO wall. In the prism test, the SWOB wall demonstrated better results, likely due to diagonal reinforcement. Specifically, SW showed an

11.11% improvement, SWOB achieved a substantial 70.37% increase, and SWB recorded the highest improvement at 122.22% in load-bearing capacity, all in comparison to SWO.

Table of Content

List of Figures

List of Tables

ASTM Standards

ASTM C1314	Standard Test Method for Compressive Strength of Masonry Prisms
ASTM C270	Standard Specification for Mortar for Unit Masonry
ASTM C952	Standard Specification for Bond Strength of Mortar to Masonry Units
ASTM C780	Standard Test Method for Preconstruction and Construction Evaluation of Mortars for Plain and Reinforced Unit Masonry
ASTM C67	Standard Test Methods for Sampling and Testing Brick and Structural Clay Tile (Includes Compressive Strength, Flexural Strength, and Water Absorption)
ASTM C20	Standard Test Methods for Apparent Porosity, Water Absorption, Apparent Specific Gravity, and Bulk Density of Refractory Brick and Shapes
ASTM E23	Standard Test Methods for Impact Testing of Materials (Charpy Impact Test, adapted for masonry).
ASTM D6110	Standard Test Method for Determining the Charpy Impact Resistance of Notched Specimens of Plastics (For impact weight selection)
ASTM E519	Standard Test Method for Diagonal Tension (Shear) in Masonry Assemblages
ASTM A931	Standard Test Method for Tension Testing of Wire Ropes and Strands (Adapted for bamboo strip tensile testing)
ASTM C469	Standard Test Method for Static Modulus of Elasticity and Poisson's Ratio of Concrete in Compression (For masonry modulus evaluation)
ASTM E2309	Standard Practices for Calibration of Displacement Transducers for Use in Structural Testing (For LVDT and laser displacement sensor calibration)

Abbreviation

Abbreviations and Symbols

RMM Reinforced Mortared Masonry

SW Simple Wall with-out Reinforcement and Opening

SWB Simple Wall with Bamboo Reinforcement

SWO Simple Wall with opening at the center

SWOB Simple wall with Opening and Bamboo Reinforcement

UPV Ultrasonic Pulse Velocity

MM Motor Masonry

BV Bambusa Vulgaris Vittata

SB Schizostachyum Brachycladum

BH Bambusa Heterostachya

UTM Universal Testing Machine

ASTM American Society for Testing and Materials

B1 Bamboo Outside the wall

B2 Bamboo Inside the wall

EM_d Dynamic Elastic Modulus

FB First Blow

f_n Fundamental frequency

IIB Initial Impact Blows till first crack

UIB Ultimate Impact Strength till failure

S-max maximum spall distribution from the point of impact

RF_t Transverse resonance frequency

ξ	Damping ratio/percentage
BRMMW	Bamboo reinforced motored masonry walls
UHPFRC	ultrahigh-performance fiber-reinforced concrete
K_o	Initial Stiffness
K_{max}	Maximum Stiffness
P	Initial Load
P_{max}	Maximum Load
f_v	Shear Strength
G	Modulus of Rigidity

Chapter 1

Introduction

1.1 Background

Despite more than a century of industrialization, the global housing crisis remains a daunting challenge, with millions of people in developing countries still lacking proper shelter. For example, the Government of Pakistan estimated a housing shortage of 18.78 million units at the start of its 12th Five Year Plan (2012–17) [1] Rapid population growth continues to strain natural resources, driving up the cost of conventional building materials and intensifying the housing deficit. In regions vulnerable to seismic activity and areas exposed to heavy vibrations such as subway systems, industrial zones, and transportation hubs there is an urgent need for construction techniques that offer both durability and resilience [2]. One promising solution is the use of renewable materials, particularly bamboo reinforcement, which not only improves structural performance but also minimizes environmental impact. Bamboo, known for its excellent mechanical properties and rapid renewability, is abundantly available across the globe, with approximately 67% of the supply found in Asia and Oceania, 3% in Africa, and 30% in the Americas [3, 4] incorporating sustainable reinforcement like bamboo, as demonstrated by Vengala, Jagadeesh et al. [5], offers a practical and eco-friendly approach to address the challenges of housing shortages and environmental degradation.`

Despite over a century of industrialization, a significant global housing deficit persists, with millions of people—especially in developing countries—still lacking adequate shelter [6]. The rapid growth of the global population continues to exert enormous pressure on natural resources,

driving up the cost of conventional building materials and exacerbating the housing crisis for economically disadvantaged populations [7].

In addition, conventional construction materials like steel, cement, and bricks require high energy consumption and contribute substantially to greenhouse gas emissions. This environmental burden is evident as global temperatures rise, glaciers melt, and sea levels increase, placing coastal regions at risk of flooding exemplified by the significant land loss in countries like the Maldives [8]. The UN Climate Change Conference in Paris (2015) set an ambitious target of limiting temperature increases to 1.5 °C above pre-industrial levels, necessitating drastic reductions in CO_2 emissions [2]. Consequently, there is an urgent need to identify alternative construction materials that are not only cost-effective and sustainable but also possess satisfactory structural properties.

Numerous studies have investigated unconventional building materials, such as Kevlar, polyester, carbon fibers, and metal alloys, for their potential use in construction [9]. However, these materials often involve complex manufacturing processes that are not feasible at the village level using locally available resources and technologies. To address the housing shortage particularly among populations living below the poverty line it is essential to develop building techniques that utilize locally sourced materials for constructing key building components, including beams, columns, slabs, and walls, at a fraction of the cost of traditional materials [10]. Moreover, with the dual challenges of population growth and land scarcity, the adoption of multi-storied structures through prefabricated technology emerges as a promising solution.

Various techniques for weaving bamboo walls are found worldwide, showcasing regional diversity in construction methods. Bamboo infill walling systems are also utilized in different parts of the world, with variations in how they are built. Generally, bamboo walls can be classified into two 0types as permeable and semi-permeable, further categorized into non-plastered and plastered forms [11]. These walls are typically crafted using thin strips of bamboo, which may be left exposed or coated with materials like mud, lime, or cement, depending on the desired finish and application [12]. In rural areas, bamboo culms are split and flattened into boards, known as *esterilla* or *regillas* in Latin American countries, and are commonly used for wall construction [13, 14]. In recent years, researchers have introduced various advancements in bamboo-based wall systems, significantly improving their performance [15]. One such innovation involves the construction of bamboo-reinforced concrete houses using frames made from woven bamboo strips. These frames

are assembled using nuts and bolts and then plastered with cement mortar. While this approach enhances strength and durability, it is not suitable for multi-story structures [16]. Further advancements were made by [17], who developed a bamboo-based walling system comprising bamboo grids, bamboo columns, and steel wire mesh. Their research demonstrated that this type of wall system could endure severe conditions throughout a structure's lifespan highlighting

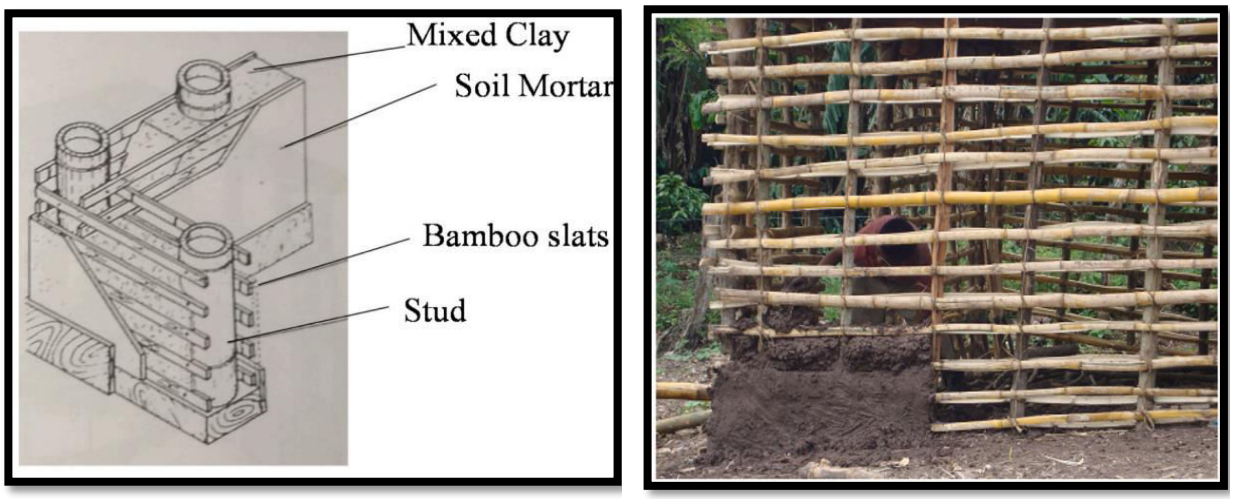

(a) (b)

Figure 1.1: Types of wall (a) Mud filled Bamboo Wall [5], (b) Barbeque Wall [18]

bamboo's potential as a durable and resilient material for sustainable construction . Bamboo strips have been utilized as reinforcement in 1.2m x 1.2m walls constructed with mud bricks, significantly enhancing their structural performance. The addition of bamboo resulted in a 30% improvement in compressive strength and a remarkable 195% increase in energy absorption, addressing the limitations of mud bricks in disaster-prone scenarios [19]. In various studies have incorporated it into columns, capitalizing on its exceptional physical and mechanical properties. These investigations reported a drift ratio of 3.34% and an energy dissipation ratio of 0.96, both meeting the stringent criteria outlined in ACI standards. Together, these findings emphasize bamboo's potential to improve the resilience and structural integrity of construction systems [20].

Bamboo has emerged as a sustainable and versatile material in construction, offering significant improvements in wall and column performance [21]. Bamboo-reinforced walls enhance

compressive strength, energy absorption, and shear strength, making them suitable for disaster-prone areas. Similarly, bamboo columns demonstrate excellent flexural properties, meeting ACI standards for drift and energy dissipation. Innovative bamboo systems, like grids and wire mesh walls, showcase durability under severe conditions, though some techniques are unsuitable for multi-story structures. With its global availability and eco-friendly benefits, bamboo is a promising solution for resilient and sustainable construction in impact-prone regions.

1.2 Research Motivation and Problem Statement

Despite a growing shift toward sustainable construction practices, the dynamic behavior of bamboo-reinforced mortar masonry walls (BRMMW) remains inadequately explored, especially under high-strain phenomena such as impact, vibration, and out-of-plane forces typical in seismic and industrial environments. Although bamboo is acknowledged for its favorable mechanical properties and ecological benefits, comprehensive insights into its effect on key dynamic parameters—such as damping, stiffness, and energy absorption—are still lacking. Additionally, limited data exist on the influence of bamboo reinforcement on the compressive behavior of masonry walls, especially in relation to reinforcement spacing and the presence of structural openings. This knowledge gap impedes the development of optimized reinforcement strategies necessary to ensure structural safety, stiffness retention, and energy dissipation in real-world loading scenarios. Therefore, this study seeks to thoroughly evaluate the dynamic and static performance of BRMMW systems to establish their reliability as a resilient and eco-efficient alternative in seismic and vibration-sensitive regions.

1.3 Objectives

Objective of the research can be achieved by performing these tasks as shown below:

1. To evaluate how bamboo reinforcement affects the out-of-plane impact resistance, damping, and stiffness of masonry walls under high-strain rate loading.
2. To study the out-of-plane behavior of BRMMW under out of plane impact, focusing on frequency changes, damping increase, and energy absorption.
3. To assess how different bamboo mesh spacing influence diagonal tension strength, rigidity, and energy dissipation, and identify the most effective layout.
4. To compare the compressive strength, elastic modulus, and deformation of BRMMW with unreinforced and bamboo reinforced masonry.
5. To examine how wall openings affect compression performance and stiffness, and how bamboo reinforcement helps reduce this weakness.
6. To determine if BRMMW is a strong, durable, and sustainable option by analyzing its performance in strength, stiffness, energy absorption, and failure patterns under both impact and static loads

1.4 Scope of Work

This study aims to investigate the integration of bamboo reinforcement into Mortared masonry to enhance its structural performance, durability, and sustainability. The research focuses on evaluating the flexural strength of bamboo when employed as reinforcement in masonry walls. Studies have shown that incorporating bamboo reinforcement can significantly enhance the flexural strength of masonry structures. This improvement suggests that bamboo-reinforced masonry walls can achieve flexural strengths comparable to those of traditional burnt clay brick masonry, highlighting bamboo's potential as an effective and sustainable reinforcement material. Advanced NDT techniques, including UPV, will be used to detect internal cracking within the walls. Additionally, the study will compare the performance of bamboo-reinforced motored masonry with conventional motored walls, emphasizing bamboo's potential as an innovative and sustainable alternative in modern construction practices.

1.5 Innovative Contribution of the study

"The innovation of this study lies in the strategic use of bamboo reinforcement in masonry walls through multiple configurations both embedded within the brick layers and externally applied to the wall surface. This dual reinforcement arrangement has not been extensively explored in previous research, particularly under lateral impact loading (out-of-plane bending) conditions. In this work, controlled lateral impacts are applied to brick masonry specimens reinforced with bamboo of specific sizes and spacing configurations, which have not previously been subjected to such dynamic testing. Furthermore, the study integrates resource-efficient testing methods, such as Ultrasonic Pulse Velocity (UPV), to detect internal damage and evaluate performance. By addressing an unexplored combination of reinforcement layout and lateral dynamic loading, this research contributes a sustainable, low-cost, and eco-friendly reinforcement strategy for improving the impact resistance (out-of-plane bending) of masonry structures, particularly in vibration-sensitive environments."

This research introduces a novel experimental investigation into the behavior of bamboo-reinforced brick masonry walls under both in-plane static and out-of-plane lateral impact loading conditions. While numerous studies have explored the performance of masonry walls under different loading scenarios, a clear research gap exists regarding walls of this specific scale, reinforcement type, and material composition.

Previous studies, such as that by Wei and Stewart [22], focused on full-scale masonry walls subjected to in-plane lateral static loading. Similarly, Moroz, et al. [23] conducted experiments on small-scale masonry walls, but their specimens incorporated grouted joints with steel reinforcement, rather than natural bamboo. Though their testing procedures (including in-plane static tests) align with those used in this study, the materials and reinforcement strategy significantly differ. Other researchers who studied out-of-plane lateral impact loading often used full-scale concrete-filled walls, replacing traditional mortar layers with concrete, which alters both stiffness and failure mechanisms. In Pakistan, a recent study by Aizaz, et al. [19] involved diagonal shear tests and in-plane axial compression tests on mud brick walls reinforced with bamboo placed on both faces of the wall at close spacing (approximately 1 inch). However, his focus was not on

dynamic lateral impact, and the construction material (mud bricks) further differentiates the approach. Work by Ahmed and Ali [24], which this study partially references for lateral impact strategy, was performed on concrete walls with a fixed drop weight. Their testing methodology did not address the unique behavior of traditional brick masonry under dynamic loads with sustainable reinforcement.

Considering the identified research gaps, the innovative contribution of this study is threefold. First, it utilizes locally available brick masonry for wall construction instead of mud bricks or concrete, thereby reflecting the practical and commonly adopted construction techniques in developing regions. Second, it integrates natural bamboo strips as reinforcement in multiple configurations—both internally embedded and externally affixed—to evaluate the structural performance of masonry walls under both in-plane static and out-of-plane lateral impact loading. Third, it applies pendulum-type lateral impact loading on realistically scaled, bamboo-reinforced brick masonry walls, a configuration and testing approach not previously documented in the literature. This research addresses a critical gap in sustainable construction by combining accessible materials, cost-effective reinforcement strategies, and realistic dynamic loading conditions, offering a practical and eco-friendly solution to enhance the impact resistance of masonry structures, particularly in resource-constrained settings.

1.6 Project and Sustainable Development Goals

The Sustainable Development Goals (SDGs), introduced by the United Nations in 2015 under the 2030 Agenda for Sustainable Development, comprise a comprehensive framework of 17 global objectives aimed at addressing critical global challenges such as poverty, inequality, climate change, environmental degradation, and the promotion of peace and justice. These goals serve as a universal blueprint to guide nations toward inclusive, sustainable development by balancing economic growth, social equity, and environmental responsibility. Each SDG is accompanied by specific targets and measurable indicators to monitor global progress.

In the context of civil engineering and sustainable construction, the current research aligns most closely with SDG 9 (Industry, Innovation, and Infrastructure), SDG 11 (Sustainable Cities and Communities), and SDG 12 (Responsible Consumption and Production).

SDG 9 emphasizes the development of resilient infrastructure and the promotion of sustainable industrialization through innovative practices. This study contributes to that goal by incorporating bamboo as a sustainable reinforcement material in masonry walls, thereby enhancing their performance under impact and seismic conditions. This supports Targets 9.1 and 9.4, which advocate for the construction of sustainable and disaster-resilient infrastructure.

SDG 11 focuses on improving the safety, resilience, and sustainability of urban environments. By evaluating the impact resistance of unconfined partition walls commonly found in high-rise and framed structures this research directly supports Target 11.5, which aims to reduce the vulnerability of buildings to disasters such as earthquakes and accidental impacts.

SDG 12 promotes the efficient and responsible use of resources in production and consumption. The adoption of bamboo, a renewable and locally available material, reduces reliance on high-carbon construction alternatives such as steel and concrete. This aligns with Targets 12.2 and 12.5, which encourage the sustainable use of natural resources and the minimization of construction waste

1.7 Thesis Outline

Chapter 1: Introduction

Chapter 1 provides an overview of the research, including the background, motivation, and significance. It discusses the problem statement, objectives, scope of work, and methodology. The limitations of the study and the overall structure of the thesis are also outlined.

Chapter 2: Literature Review

Chapter 2 reviews existing literature on bamboo reinforcement in construction, particularly for reinforced mortar masonry (RMM). It covers the benefits of bamboo, including its mechanical

properties and its role in improving masonry performance under dynamic and impact loading conditions. The chapter compares bamboo reinforcement with traditional reinforcement methods and discusses its potential in modern sustainable construction.

Chapter 3: Methodology

Chapter 3 outlines the research methodology, including the experimental setup for testing bamboo-reinforced walls under out-of-plane impact loading and diagonal prism testing for tensile behavior. The chapter also explains the materials, wall dimensions, reinforcement details, and testing procedures, including the use of Ultrasonic Pulse Velocity (UPV) for crack assessment**.**

Chapter 4: Results and Analysis

Chapter 4 presents the results from the tests conducted on bamboo-reinforced walls. It analyzes the performance in terms of impact resistance, out-of-plane impact behavior and tensile strength**.** A comparison with traditional reinforcement methods is included. The chapter also discusses the mechanical and dynamic properties, crack patterns, and the effect of impact loading on structural integrity**.**

Chapter 5: Discussion

Chapter 5 discusses the implications of the results, including the optimization of BRMMW for out-of-plane impact resistance. It evaluates the potential use of bamboo reinforcement in impact-prone and vibration-sensitive areas and explores future research directions. A summary of key findings is provided at the end.

Chapter 6: Conclusions and Recommendations

Chapter 6 summarizes the key findings, highlighting BRMMW as a sustainable and impact-resistant alternative to traditional masonry. It includes recommendations for further applications of bamboo reinforcement under dynamic loading and suggestions for future research.

Chapter 2

Literature Review

2.1 Background

The construction industry plays a pivotal role in global development but is also responsible for significant environmental impacts. It consumes approximately 40–50% of global energy resources and contributes heavily to CO_2 emissions, resource depletion, and pollution [25, 26]. In response, the industry has increasingly turned toward sustainable practices, emphasizing resource-efficient designs and renewable materials [27, 28].

Among alternative materials, bamboo has emerged as a promising candidate due to its abundance, rapid renewability, and low cost. Bamboo exhibits low embodied energy and high carbon sequestration potential, storing approximately 5.69–12.85 kg CO_2/kg, compared to steel, which emits 2.2–2.8 kg CO_2/kg [29]. Its historical applications include rural construction techniques such as walling systems, scaffolding, and "Bamcrete"—a cement-mortar plastered bamboo mesh system [30].

However, bamboo's anisotropic mechanical behavior restricts its use in multi-storey and load-bearing structural systems [4]. To overcome these limitations, engineered bamboo products (EBPs) have been developed, offering improved strength, durability, and suitability for modular construction [20]. Despite this advancement, limited research is available on the mechanical and fire performance of EBPs and bamboo-reinforced concrete (BRC) under various loading conditions [4].

In the area of impact resistance, several experimental investigations have employed methods such as full-scale testing, scaled-down prototype testing, and relative impact testing. For instance, Li et al. [31] used bullet projectile impact tests on ultrahigh-performance fiber-reinforced concrete

(UHPFRC), while Hussain and Ali [1] tested jute fiber-reinforced concrete slabs using free-falling weights. Similarly, Li et al. [31] examined UHPC cylinders with cartridge projectile tests, and Wang and Chouw [32] studied the flexural behavior of coconut fiber-reinforced concrete beams under impact. Camposeco-Negrete [33] also employed instrumented drop weight methods to assess impact strength in self-compacting concrete incorporating recycled GFRP.

Regarding theoretical interpretations, Pham and Hao [34] proposed that flexural members susceptible to static flexural damage are more likely to experience shear failure under impact loads. In such cases, the peak dynamic bending moment may be lower than the static moment due to zero overhang effects. Badr and Ashour [35], as cited by ACI, identified two primary approaches for impact testing: the instrumented drop weight test and the pendulum-type Charpy impact test.

In this study, the pendulum-type Charpy impact method is adopted for its ability to simulate realistic lateral impact conditions, which are particularly relevant to the out-of-plane behavior of masonry walls. Unlike vertical impact tests, the pendulum setup produces dynamic, swinging forces similar to those generated during seismic activity or accidental collisions. This enables deeper insight into energy absorption, damping, and failure patterns of bamboo-reinforced masonry systems.

While bamboo has been studied extensively in rural construction, limited research exists on the lateral impact resistance of bamboo-reinforced mortared masonry walls (BRMMW), particularly using pendulum impact mechanisms. Furthermore, previous studies have not explored the performance of bamboo reinforcement in multiple configurations—such as being embedded within the brick layers and externally affixed to the wall surface—under lateral impact loading. These reinforcement layouts, along with the use of natural bamboo strips of specific sizes and spacing, present a novel approach that remains underexplored.

To address these gaps, the current research investigates the lateral impact performance of BRMMW using cost-effective and sustainable testing techniques, including Ultrasonic Pulse Velocity (UPV) for internal crack detection. The experimental framework assesses lateral impact strength, dynamic response at various damage stages, and post-failure behavior, offering practical insight into the feasibility of bamboo-reinforced systems for vibration-sensitive and impact-prone environments.

This paper is structured as follows: the introduction outlines the background and research gap; the methodology section details the reinforcement configurations and testing procedures; results and discussion cover dynamic responses, energy absorption, and crack propagation; and finally, conclusions summarize the findings with recommendations for future work.

2.2 Material related Flaws and their Remedial Measures

2.2.1 Flaws

Traditional joints, often made with tied ropes or simple incisions, are unable to transmit the full bearing capacity of bamboo elements, leading to reduced structural efficiency [4]. Advanced joint technologies, while effective, are difficult to implement in developing countries due to their complexity and cost [36]. Bamboo structures with inadequate joints are prone to brittle collapse, making repairs costly and less sustainable [37]. Reinforcement materials like polymer and steel meshes are often expensive, limiting their application in rural or economically disadvantaged areas [38]. Earthen structures, including mud-brick houses, lack adequate reinforcement, making them highly vulnerable to seismic activities. Traditional adobe constructions are not designed to withstand cyclic actions caused by impacts, resulting in significant damage or collapse [39]. Despite the potential of bamboo as reinforcement materials, limited research has been conducted on their use for strengthening mortared brick walls, especially their in-plane behavior [40]. Untreated bamboo has limited durability, lasting up to 6 years, compromising structural integrity [41]. Many studies have focused only on in-of-plane behavior, with limited attention to the out-of-plane impact behavior of mortared masonry walls [40]. Existing reinforcement systems like bamboo cane frames and polymer mesh have been tested in isolation [42].

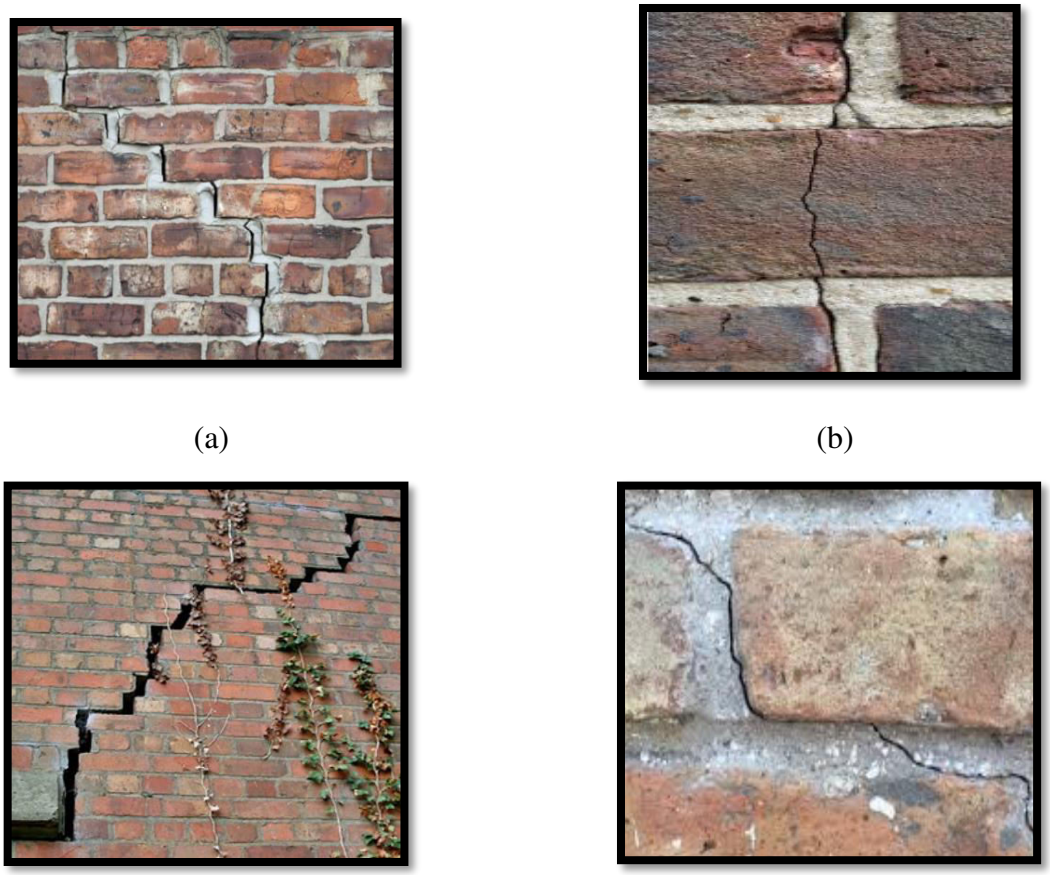

(a) (b)

(c) (d)

Figure 2.1: Structural Fracturing, (a) Structural Cracks [40]. (b) Micro Cracks [30], (c) Structural Movement Cracks, (d) Foundation damage Cracks

2.2.2 Remedial Measures

Optimized joint solutions, such as those using steel nails, bolts, and steel plates, prevent brittle failures and improve overall ductility [43]. The study suggests using wooden bolts, canapé rods, and plywood plates as cost-effective alternatives to enhance structural efficiency while maintaining simplicity in construction [44]. The use of ductile joints prevents brittle collapse by allowing large inelastic deformations, enabling safer structural behavior and reducing the risk of sudden failure [45]. Joints designed with replaceable wooden pins provide an economical repair option, ensuring sustainability and prolonging the lifespan of bamboo structures [46]. Modular

building plans using optimized bamboo joints are proposed for one-storey buildings, such as homes, schools, and health centers, to encourage self-construction and dissemination among unskilled workers in developing regions [47]. Explore the use of locally available natural materials such as bamboo strips, wood, cane, and dried jute thread, which are cost-effective and eco-friendly [48]. Develop low-technology reinforcement systems, like bamboo-framed structures with wooden pins and plywood plates, to enhance ductility and ease of repair [36]. Implement retrofitting techniques such as mesh reinforcement embedded in mud mortar, horizontal low-cost post-tensioning straps, and interconnected internal and external grid systems [49]. Conduct experimental tests on improved reinforcement techniques, including mud injection and external rope mesh reinforcement, to enhance seismic resilience [42]. Assess the in-plane behavior of mud-brick walls reinforced with bamboo strips and dried jute thread [40]. Use treated bamboo for reinforcement, which can withstand structural integrity for over 30 years [41]. Conduct experimental tests on scaled models to evaluate both in-plane and out-of-plane behaviors [40]. Examine the combined effect of natural and industrial reinforcement techniques to enhance seismic performance [38].

2.3 Properties of Brick Masonry Walls

A simple brick masonry wall, constructed using traditional materials like mud bricks, fired bricks, or concrete blocks, is a fundamental structural element widely used in construction. These walls are primarily designed to provide load-bearing capacity, thermal insulation, and space division. However, without any reinforcement, their structural properties are limited, particularly in resisting lateral loads, such as those from earthquakes or wind. Unreinforced masonry walls exhibit good compressive strength, as they are excellent at bearing vertical loads due to the intrinsic material properties and bonding techniques, such as mortar joints. However, they tend to have poor tensile and flexural strength, making them vulnerable to cracking and collapse under lateral forces or seismic activity.

When reinforcement is added to a masonry wall, its properties significantly improve. Reinforcement, such as steel bars, bamboo strips, polymer mesh, or natural fibers, enhances the

tensile strength, ductility, and load-bearing capacity of the wall. Horizontal reinforcements help prevent the formation of cracks by resisting tensile stresses, while vertical reinforcements increase stability and resistance to overturning forces [45]. Reinforced masonry walls also show improved performance under dynamic and cyclic loads, such as those experienced during earthquakes, as they can dissipate energy more effectively and reduce structural damage. Moreover, the incorporation of reinforcement materials provides better cohesion and helps in controlling the propagation of cracks.

The thermal and acoustic insulation properties of reinforced walls remain intact or may improve, depending on the reinforcement type. Natural reinforcements like bamboo or jute are lightweight and eco-friendly, making them suitable for sustainable construction practices. Additionally, reinforced walls are often more durable, as the reinforcement helps maintain structural integrity over time, reducing the risk of collapse and increasing the safety of the structure. These enhancements make reinforced masonry walls a practical and versatile solution for modern construction challenges, especially in areas prone to seismic activity or harsh environmental conditions [28].

2.4 Properties of Masonry wall by adding Bamboo as Reinforcement

Masonry walls, both structural and non-structural, serve as critical components in a building, providing not only spatial division but also contributing to the load-bearing capacity against gravity and lateral forces [50]. In regions prone to impact loading. Indonesia, the use of lightweight materials in masonry walls can significantly reduce casualties caused by the collapse of heavy building components during earthquakes [50]. Traditional masonry walls are known for their brittleness, which limits their strength, particularly under seismic loads. This limitation has prompted extensive research into reinforced masonry systems to improve their structural performance [51].

Reinforcement in masonry walls enhances their ability to resist in-plane and out-of-plane loads, thus improving their overall strength and ductility. The addition of bracing systems, for example,

has been shown to significantly increase wall strength and stiffness [50]. Studies have demonstrated that steel bracing can enhance wall strength by 13.33% and reduce displacement by 93.34%, while bamboo bracing increases wall strength by 29.73% and reduces displacement by 32.23% compared to unbraced models. These results highlight the effectiveness of reinforcement in improving the seismic performance of masonry walls [52]. Masonry walls, when reinforced,

Table 1: Physical Characteristics of Bamboo

Species of Bamboo	**Shape of bamboo**	**Wall thickness (mm)**	**Diameter of Culm (mm)**
Schizostachyum Brachycladum (SB)		3 - 5	25 – 35
Bambusa Heterostachya (BH)		4 – 7	45 - 55
Bambusa Vulgaris Vittata (BV)		8 - 6	50 - 100

exhibit enhanced properties, making them suitable for a variety of applications, including structural and non-structural roles [5]. Reinforced masonry walls typically incorporate materials such as bamboo, steel, or other reinforcing elements to improve their load-bearing and energy-absorbing capacities [12]. Reinforcement allows these walls to resist impacts, sustain higher loads, and perform better under static or impact loading (out-of-plane) conditions [21]. The inclusion of reinforcement, particularly bamboo, has been explored globally as a renewable and sustainable option, especially in regions with a significant bamboo population like Asia, Latin America, and Africa [5].

Various walling systems utilizing bamboo reinforcement include permeable and semi-permeable designs, often plastered with mud, lime, or cement [53]. For instance, techniques such as the Bahareque system or Wattle and Daub incorporate woven bamboo slats with mud plaster, demonstrating improved energy absorption and impact resistance [54]. Similarly, modern adaptations, such as the Bamcrete panel system, use bamboo strips combined with cement mortar to create non-load-bearing partition walls with enhanced robustness [30]. Studies have shown that walls reinforced with bamboo or steel frames exhibit superior resistance, particularly under impact and monotonic loading [16].

Experimental studies have demonstrated that reinforced masonry walls perform better under both static and impact loading (out of plane bending) scenarios. For example, using design mixes with controlled water-cement ratios significantly improves the energy absorption characteristics compared to mason mixes, which rely on a mason's experience without precise mix proportions [12]. Panels reinforced with bamboo frames or metallic frames like U and W channels exhibit greater resistance to fracture and penetration under impact loading. Additionally, weaving treated bamboo enhances durability and performance [55].

Bamboo has proven to be a sustainable and strong reinforcement material. Horizontally placed bamboo strips between brick layers can significantly improve tensile strength and prevent cracking, while vertical bamboo rods further stabilize the structure [6]. Similarly, Paradiso et al. (2019) explored the out-of-plane impact performance of adobe panels reinforced with bamboo cane frames. Their scaled wall tests revealed that such reinforcement can enhance stability under impact forces [7].

Additional reinforcement materials include external wire mesh and polymer mesh, which have shown promise in increasing strength and preventing collapse during strong earthquakes. However, wire mesh, while effective, is costly, whereas polymer mesh offers a more affordable alternative [56]. Reinforcement using bamboo strip mesh was explored by Mendis, et al. [40] to retrofit masonry walls, though its application to mud-brick walls has not been extensively studied.

Table 2. Properties of Bamboo

Parameter	Range	References
Cellulose	40 – 60 %	[57]
Hemicellulose	15 – 20 %	[57]
lignin	20 - 30 %	[58]
Moisture	8 – 16%	[59]
Young modulus	0.1-1 (GPa)	[60]

The combination of bamboo reinforcement with mortared masonry wall has also been identified as a potential reinforcement technique. While bamboo strips decomposes over time, its use within mortared can improve durability and sustainability. The load-carrying capacity of bamboo reinforcement is noted to be 1.96 N, and researchers have suggested its application in enhancing the mechanical properties of bricks and blocks [61]. This study emphasizes the development of an affordable and eco-friendly strengthening technique for masonry walls using locally available materials such as bamboo strips.

Other reinforcement methods include external wire mesh and polymer mesh. External wire mesh significantly increases the structural strength of adobe buildings but is often cost-prohibitive. Polymer mesh, on the other hand, provides a more affordable option while effectively preventing collapse during earthquakes [62].

2.5 Understanding High and Low Velocity Impact Testing in Previous Research

Dropping objects and vehicle collisions can cause accidental impacts on structures [63]. During construction, objects may fall from heights [64]. Parking garage walls and columns are often hit by vehicles [65]. Airport runways face repeated impacts from airplane tires [66]. Offshore piers experience impact from ships and sea waves [67]. Explosions can cause impact forces through projectiles and debris [32].

High-velocity impact tests are used to assess the effects of explosions and projectile impacts [66]. Low-velocity impact tests, as classified by ACI 544-2R, include the instrumented falling impact test, Charpy pendulum impact test, and repeated drop-weight impact test [68]. The instrumented falling impact test measures the structural performance of slabs and beams under drop-weight impacts [69]. The Charpy pendulum impact test evaluates material toughness [70]. The repeated drop-weight impact test is a low-cost, simple method for comparing different concrete mixtures [68].

The ACI 544-2R repeated impact test involves a 4.54 kg steel mass dropped from a height of 457 mm onto a concrete disk specimen. The impacts are repeated until a visible crack appears, and the number of impacts is recorded for both crack formation and specimen failure. This test is used to compare the impact resistance of different concrete mixtures but does not provide exact strength values. It was originally introduced by Schrader, who recommended testing five specimens per batch and disregarding the highest and lowest values [71].

One of the major challenges in using this test is the high variation in results, which reduces its reliability [72]. Researchers have suggested modifications to the test setup, specimen shape, and testing procedure to improve accuracy. Despite the inconsistencies in results, the test remains widely used due to its simplicity and cost-effectiveness `

2.6 Summary

The construction industry consumes a significant portion of global energy and contributes to environmental challenges such as CO_2 emissions and resource depletion. As a response, researchers are exploring sustainable materials like bamboo for reinforcement in masonry walls. Bamboo is a naturally abundant, renewable, and cost-effective material with promising mechanical properties, making it a viable alternative to traditional reinforcements. Despite its advantages, its anisotropic mechanical properties limit its use in high-rise construction, leading to the development of engineered bamboo products. Several experimental studies have been conducted to assess the impact resistance of various reinforced masonry systems. Different testing methods, such as projectile impact tests, free-fall drop weight approaches, and instrumented drop weight mechanisms, have been used to evaluate impact performance. Among these, the pendulum-type Charpy impact test is particularly suitable for assessing masonry walls' out-of-plane impact behavior. Unlike vertical impact tests, the pendulum method simulates real-world lateral forces, making it an effective tool for analyzing energy absorption, damping characteristics, and failure patterns in bamboo-reinforced masonry walls.

One of the key challenges in bamboo-reinforced masonry construction is the lack of efficient joint solutions. Traditional joint techniques, such as tied ropes and simple incisions, often fail to utilize bamboo's full structural potential. Advanced joint technologies exist but are often too costly for rural or low-income regions. Additionally, untreated bamboo has limited durability, requiring proper treatment for long-term structural reliability. Studies have shown that reinforcement materials like bamboo, polymer mesh, and steel mesh can significantly improve masonry walls' strength and energy absorption capabilities, making them more resilient against impact loads. Masonry walls reinforced with bamboo strips have demonstrated improved performance in resisting out-of-plane impact forces. Studies have shown that strategically placing bamboo strips within the masonry structure enhances tensile strength, reduces crack propagation, and improves overall energy dissipation. Additionally, the inclusion of external reinforcement techniques, such as bamboo grids and polymer meshes, further enhances impact resistance. The combination of bamboo reinforcement with mortared masonry walls offers an eco-friendly, cost-effective solution for improving structural performance while reducing reliance on conventional materials.

Overall, this research aims to evaluate the impact performance of bamboo-reinforced masonry walls using pendulum impact testing. By analyzing the effects of reinforcement on energy absorption, damping characteristics, and structural failure mechanisms, this study contributes to the development of sustainable, resilient construction materials for regions prone to impact loading.

Chapter 3

Methodology

3.1 Background

Bamboo is a naturally occurring material known for its exceptional mechanical properties, making it a versatile and sustainable option in construction and engineering applications. Its lightweight nature, combined with remarkable tensile

.strength and flexibility, positions bamboo as a promising alternative to conventional reinforcement materials. Additionally, bamboo is an eco-friendly resource that grows rapidly, ensuring its abundant availability. The mechanical properties of bamboo include high tensile strength, favorable Young's modulus, and the ability to withstand various environmental conditions. Bamboo's unique cellular structure, rich in cellulose, hemicellulose, and lignin, contributes to its durability and resilience. These properties make it ideal for applications requiring both strength and adaptability, especially in regions prone to dynamic loads or seismic activity. Previous research has explored the use of bamboo in a variety of construction techniques, such as reinforcing concrete, masonry walls, and structural frameworks. However, these studies often focused on cost-effectiveness or traditional applications, and little attention has been given to employing bamboo as a reinforcement material in simple walls specifically designed to handle impact and vibration loads. Our research seeks to bridge this gap by investigating bamboo's potential as a reinforcement in reinforced mortar masonry (RMM) walls for improved performance under such conditions. The water absorption and moisture content characteristics of bamboo further enhance its suitability as a construction material. With controlled treatment, bamboo

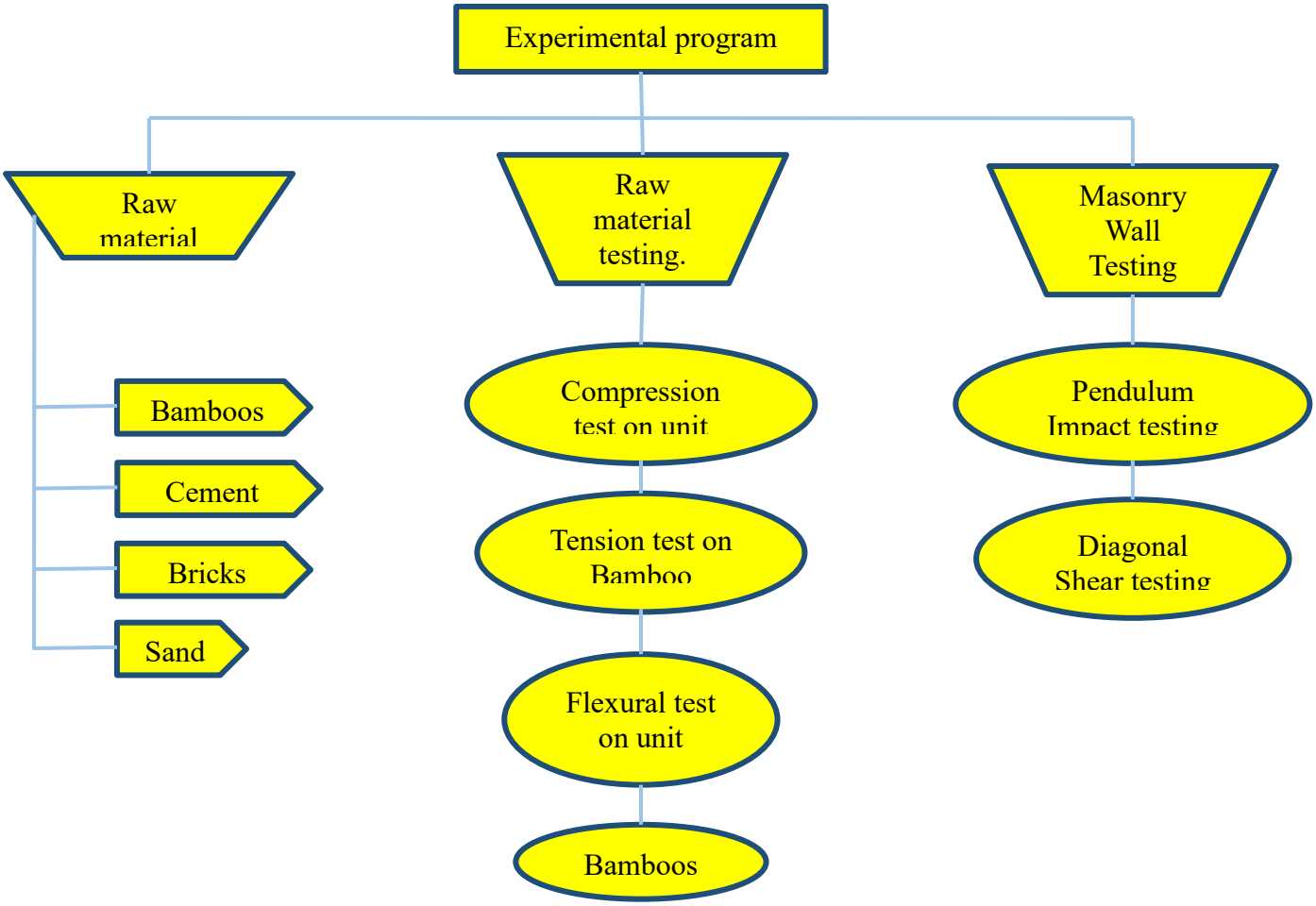

Figure 3.1: Schematic diagram for systematic experimental program

exhibits excellent resistance to swelling and dimensional instability, ensuring its reliability in varying climatic conditions. Its role as a raw material is further bolstered by its availability, affordability, and minimal processing requirements, making it an accessible option for diverse engineering projects. The methodology for creating bamboo-reinforced RMM involves selecting high-quality bamboo strips, treating them to enhance durability, and integrating them into masonry structures using a systematic experimental approach. This methodology, detailed in subsequent sections, aims to provide a practical framework for utilizing bamboo in innovative ways, emphasizing its potential as a sustainable and effective reinforcement material.

3.2 Wall Specimens and Material Properties

3.2.1 Raw Materials

The materials utilized in this study for masonry specimen preparation include Portland cement, sand, bricks, and bamboo. Figure 3.2a, Ordinary Portland Cement (OPC), sourced locally from Askari Cement, was employed, containing 61.7% CaO, 21% SiO_2, 5.04% Al_2O_3, 3.24% Fe_2O_3, 2.56% MgO, and 1.51% SO_3. Quartz sand was used with a maximum size of 4.8 mm. Figure 3.2c show the Cement consistency test and a bulk density of 1527 kg/m³, ensuring proper grading and workability for masonry applications. Figure 3.2b evaluates the quality of the sand was fine and a specific gravity of sand was performed following ASTM C136, ASTM C128 standards respectively. The specific gravity of the fine aggregates was calculated as 2.66, which lies within the acceptable range of 2.5 to 2.8, indicating good material quality. The bricks used in this study were subjected to a series of tests to verify their compliance with relevant standards, as illustrated in Figure 3.3c. Water absorption test, as per ASTM C20, revealed the capacity of bricks to absorb water, a critical factor for ensuring proper adhesion with the mortar as illustrated in Figure 3.3b. According to ASTM C67 compressive strength tests were conducted on two sizes of bricks, providing vital data for structural analysis. According to ASTM C67 a sounding test confirmed the high quality of the bricks through the production of a clear ringing sound as shown in Figure 3.2d. The selected mortar mix ratio of 1:4 (cement-to-sand) with a 0.56 water-to-cement ratio was chosen to ensure optimal workability, bonding strength, and durability for masonry construction. This proportion aligns with ASTM C270 Standard Specification for and ease of application. The 1:4 mix ratio offers adequate compressive strength, making it suitable for general masonry work while maintaining sufficient flexibility to accommodate minor structural movements. The 0.56 water-to-cement ratio was selected based on ASTM C780, ensuring proper hydration of cement, and the cubes of mortar are shown in Figure 3.3a which enhances bonding between masonry units and prevents issues related to excessive shrinkage or segregation. This ratio also contributes to the durability and water resistance of the mortar. The selection of impact weights follows ASTM D6110 (Standard Test Method for Determining the Charpy Impact Resistance of Notched

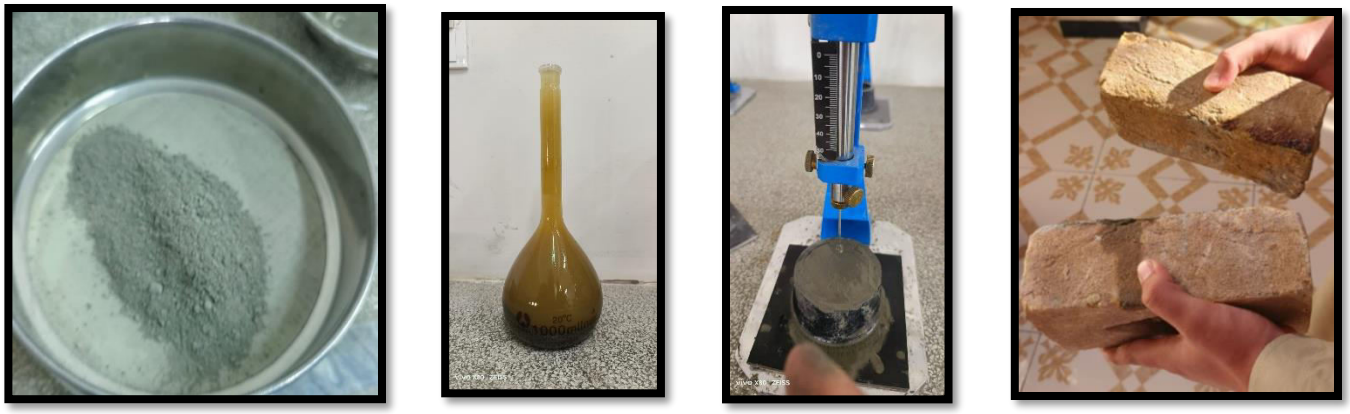

(a) (b) (c) (d)

Figure 3.2: Raw material testing (a) Cement (b) Sand specific gravity (c) Cement Consistence (d) Sounding Test

Specimens of Plastics) and ASTM E23 (Standard Test Methods for Impact Testing of Materials). These standards provide guidelines for conducting pendulum-type impact tests, ensuring accurate measurement of energy dissipation, structural deformation, and fracture behavior under impact loading varying mass values ranging from 0.25 kg to 1 kg have

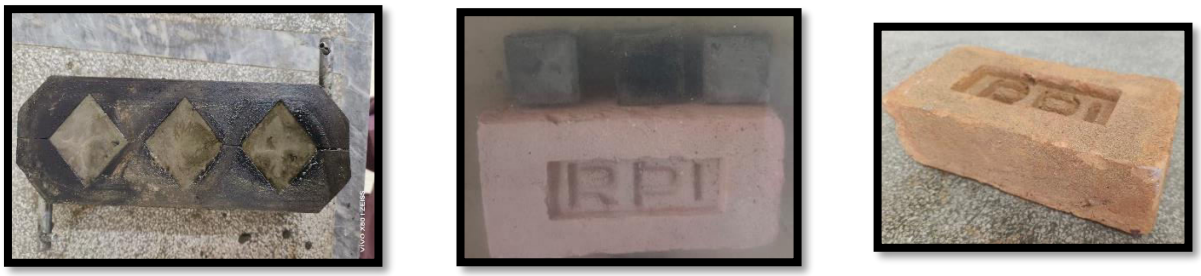

(a) (b) (c)

Figure 3.3: Raw material (a) Compressive strength Cube preparation (b) Water absorption for both Brick and mortar cubes (c) Brick sample.

been used to examine the effects of different impact forces on bamboo-reinforced masonry walls as illustrated in Figure 3.4. The primary objective of using different weights is to simulate real-world dynamic impact loading conditions and evaluate key structural responses, including crack initiation, and ultimate failure behavior. By applying incremental impact loads, the study aims to

determine how bamboo reinforcement influences the resilience of masonry walls under sudden impact forces.

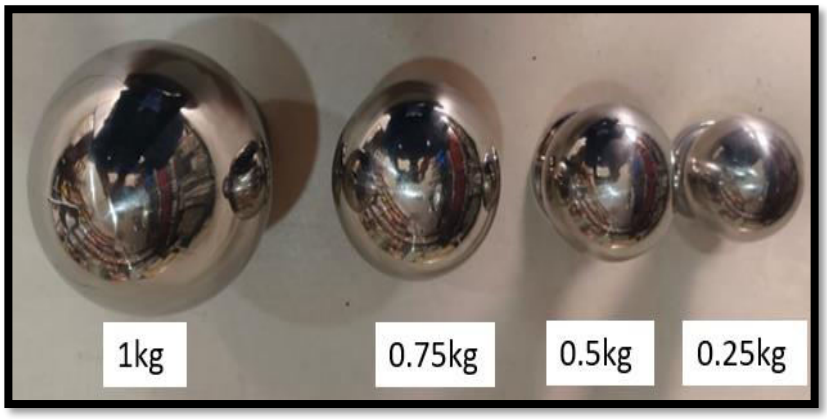

Figure 3.4: Impact mass

3.2.2 Compression Testing of Brick Unit:

The compressive strength of masonry units is a critical property widely recognized for evaluating their quality. In this study, the compressive strength of the bricks was determined in accordance with the guidelines specified in ASTM C140, as illustrated in Figure 3.5a. Testing was conducted using a Universal Testing Machine (UTM) with a maximum capacity of 200 tons, operated in load-controlled mode. Flat steel plates were placed above and below the brick to ensure uniform load distribution, and the loading rate was maintained at 0.5 kN/s and results are shown in Table 4. The brick dimensions were measured as 230mm x 76mm. The test results are summarized in Table 5.

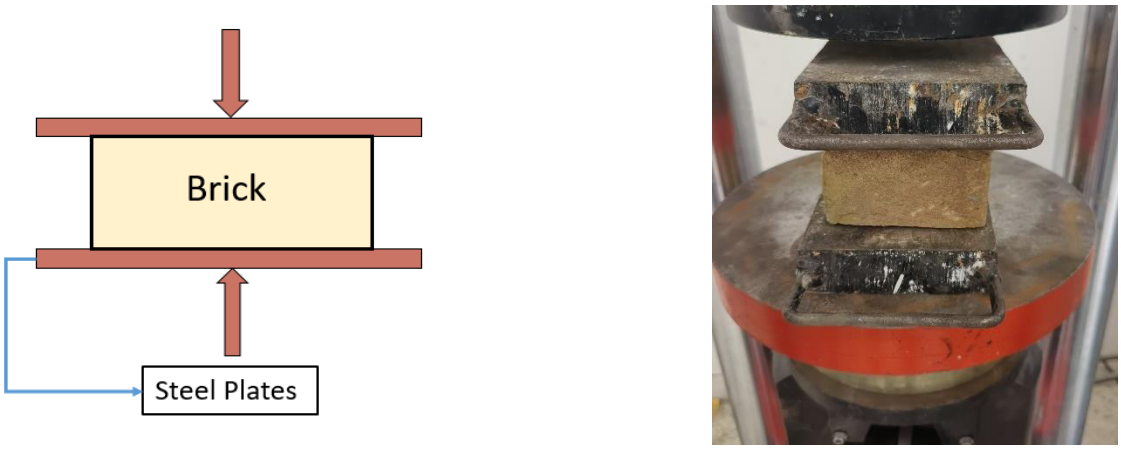

(a) (b)

Figure 3.5: Compression test on unit brick, (a) schematic view, (b) testing of specimen

The crushing resistance of the brick was determined using Eq. (1).

$$\sigma_c = \frac{P}{A} \quad (1)$$

Where:

σ_c = Crushing Strength

P = Peak force sustained until collapse a

A= Area of the brick

3.2.3 Flexure Testing of Brick Unit:

The flexural strength of the brick units was assessed using a three-point flexural test. This method involved placing the brick on two supports, applying a concentrated load at its center, and recording the load required to induce failure. The modulus of rupture, or flexural strength, was determined by dividing the maximum load

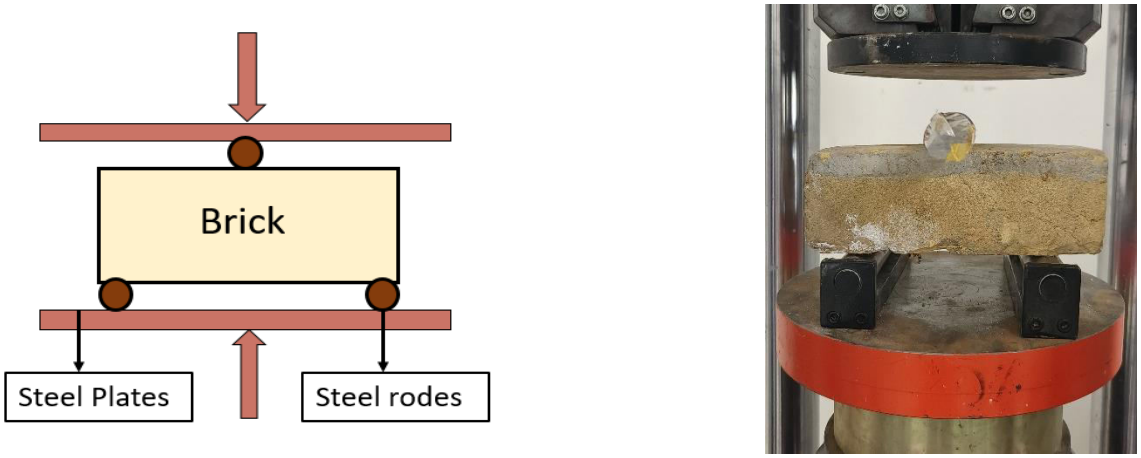

(a) (b)

Figure 3.6: Flexural test on unit brick, (a) schematic view, (b) testing of specimen

sustained by the brick at failure by the moment arm and the cross-sectional area of the brick. The evaluation followed the standard procedure outlined in ASTM C67. The test setup is depicted in Figure 3.6a, while the detailed results of the flexural strength tests are presented in Table 4. The flexural strength of the brick was calculated using Eq. 2.

$$S = \frac{3w\left(\frac{1}{2}-x\right)}{bd^2} \quad (2)$$

Where

S = Bending resistance or rupture modulus

w = Peak load applied

L = Span between the two supports

b = Mean breadth of the block on the failing surface

d = Thickness or height of the block on the failing surface

x = The separation between the block's center and the failing surface.

3.2.4 Bamboo Strips:

Bamboo used in this study was purchased from the local market, making it a cost-effective and readily available material for sustainable construction. The bamboo strips in Figure 3.7a were carefully selected and processed to uniform dimensions as specified. These strips were cut into 600mm strips to improve durability and bonding with the surrounding masonry. The bamboo exhibited remarkable properties such as high tensile strength, low water absorption, and a controlled moisture content, making it suitable for structural applications. The water absorption and moisture content (MC) values were within the acceptable range, ensuring minimal dimensional changes due to environmental exposure. Additionally, the bamboo strips demonstrated superior adhesion properties when used as reinforcement. As per ASTM 618-12, the bamboo used in this study falls under Class F, further validating its suitability for reinforcing masonry walls. These properties underscore the potential of bamboo as a sustainable and efficient reinforcement material, particularly in applications requiring lightweight and flexible construction solutions.

(a) (b)

Figure 3.7: Illustration of bamboo strip testing (a) Individual bamboo strips before testing, (b) Bamboo strips placed in the UTM for tensile evaluation.

3.2.4.1 Tensile testing on bamboo strip:

To evaluate the mechanical properties of bamboo strips, tensile tests were conducted on three specimens. A uniaxial load was applied using a Universal Testing Machine (UTM) until failure. The testing procedure followed the standard guidelines of **ASTM A931**. The test setup is illustrated in Figure 3.7b.

3.3 Masonry Wall Specimen

Twelve brick masonry walls were constructed for out of plane impact testing specification shown in Table 3. Each wall was built using standard 230 mm (230 x 115 x 77 mm nominal dimensions) bricks, with seven courses in height and three bricks in length. The resulting wall dimensions were 610 mm in height and 610 mm in length, yielding an aspect ratio (height to length) of 1:1.

The reinforcement configurations for the walls are shown in Figure 3.8. A variety of configurations were employed to compare the advantages and disadvantages of each wall type. The walls designed for this study are unique in their configurations, each developed to explore specific structural behaviors under varying conditions. These walls are categorized into two main groups based on reinforcement. In the reinforced wall configurations, bamboo strips were placed on the backside of the wall in a vertical arrangement to enhance structural stability. Additionally, horizontal bamboo reinforcement was embedded within the mortar joints between the brick courses to improve load distribution. The thickness of the mortar was adjusted according to ASTM standards it varies from 14 mm to 16 mm, ensuring that the integration of 4 mm bamboo strips did not compromise bonding and structural integrity. This approach allows for an in-depth evaluation of the influence of bamboo reinforcement on impact resistance and overall masonry wall performance.

The first category includes the simple wall (SW) and the simple wall with opening (SWO), both constructed without any reinforcement, with the simple wall (SW) serving as the baseline control specimen. The second category consists of the simple wall with bamboo reinforcement (SWB) and

the simple wall with opening and bamboo reinforcement (SWOH), where bamboo strips are integrated as reinforcement, as illustrated in Figures 3.8d and 3.8e. This classification enables a comparative analysis of the influence of bamboo reinforcement on the structural behavior of masonry walls under impact loading.

All wall specimens in this study were constructed using the English Bonding technique, a method widely recognized for its superior structural strength and stability. This bond features alternating courses of headers and stretchers, creating a robust interlocking pattern that enhances load distribution and overall wall integrity. The consistent use of English bond across all specimens ensured construction uniformity and reliability, allowing for meaningful comparative analysis. While other bonding methods such as Stretcher Bond which consists solely of stretchers and is typically used for non-load-bearing walls and Header Bond, composed entirely of headers offering moderate transverse strength, are also common, they are generally less suitable for structural applications. Another variation, the French (or Dutch) Bond, arranges headers and stretchers within the same course for a more decorative appearance, but does not match the structural efficiency of English Bond. Due to its well-established performance in supporting vertical and lateral loads, English Bond remains the preferred choice for structural masonry where strength and durability are essential.

The opening in the SWO and SWOH walls was designed to replicate a window-type opening, similar to those typically found in full-scale masonry partition walls, which often include both window and door openings. As demonstrated in Okail, et al. [73] study, such openings significantly influence the wall's behavior under lateral loads. However, due to limited resources, the aspect ratio of the wall in this study was reduced, and the window opening was also scaled down proportionally to match the smaller wall dimensions. This scaled approach retains realistic geometry while remaining feasible for laboratory testing.

Table 3: Specifications of Wall specimens

Types of wall	Types of tests	Wall designation	No. of specimens	Dimensions (mm)	Reinforcement type	Vertical reinforcement (No.)	Horizontal reinforcement (No.)
Category 1	Impact pendulum testing (out-of-plane bending)	SW	3	600 x 600	-	-	-
		SWO	3	600 x 600	-	-	-
		SWOB	3	600 x 600	Bamboo	8	3
		SWB	3	600 x 600	Bamboo	5	6
Category 2	Diagonal shear testing	SW	5	500 x 500	-	-	-
		SWO	5	500 x 500	-	-	-
		SWOB	5	500 x 500	Bamboo	8	3
		SWB	5	500 x 500	Bamboo	3	4
Category 3	In-plane Axial Compression test of masonry specimen	SW	3	500 x 500	-	-	-
		SWO	3	500 x 500	-	-	-
		SWOB	3	500 x 500	Bamboo	8	3
		SWB	3	500 x 500	Bamboo	3	4
Total samples			**49**				

(a) (b) (c)

(d) (e) (f)

(g) (h)

Figure 3.8: Casting of wall specimens (a) SW, (b) SWO, (c) horizontal reinforcement, (d) SWOB, (e) SWB, (f) Plaster on Specimen (h) wall specimens (g) bamboo reinforcement in horizontal direction.

3.4 Wall Specimen Test

3.4.1 Diagonal Shear Testing:

To assess the behavior of masonry walls, twenty five specimens were constructed which include SW, SWO, SWB, and SWOB types, specimens with dimensions of 500 mm x 500 mm were prepared as illustrated in Table 3. These walls were constructed by professional masons to ensure high-quality craftsmanship and consistency across specimens. The construction and testing procedures adhered to ASTM E519 and ASTM E519M standards, which are recognized guidelines for evaluating the performance of masonry walls under diagonal compression.

The masonry walls were reinforced on one side with a 25 mm thick layer, as depicted in the provided figures. The opposite face, referred to as the front side, was designed with a thickness ranging from 15 mm to 16 mm, into which bamboo strips were embedded. These bamboo strips were carefully integrated within the reinforcement layer to ensure full coverage and to provide enhanced structural performance. The reinforcement layer was developed to improve the wall's resistance to both compressive and tensile forces, replicating realistic conditions in the context of masonry construction.

3.4.1.1 Test Setup and Instrumentation:

The experimental setup included a loading frame**,** hydraulic jack**,** two V-shaped steel loading shoes, and Linear Variable Differential Transducers (LVDTs) to capture precise deformation data during testing. The walls were subjected to load was transferred to the specimens through two steel loading shoes, strategically placed at the walls, ensuring uniform load distribution along the compressed diagonal. The Universal Testing Machine (UTM) applied compression directly to the

specimen, and a wire-based 50 mm LVDT and UPV was installed along the compression line to accurately measure the shortening of the wall during testing.

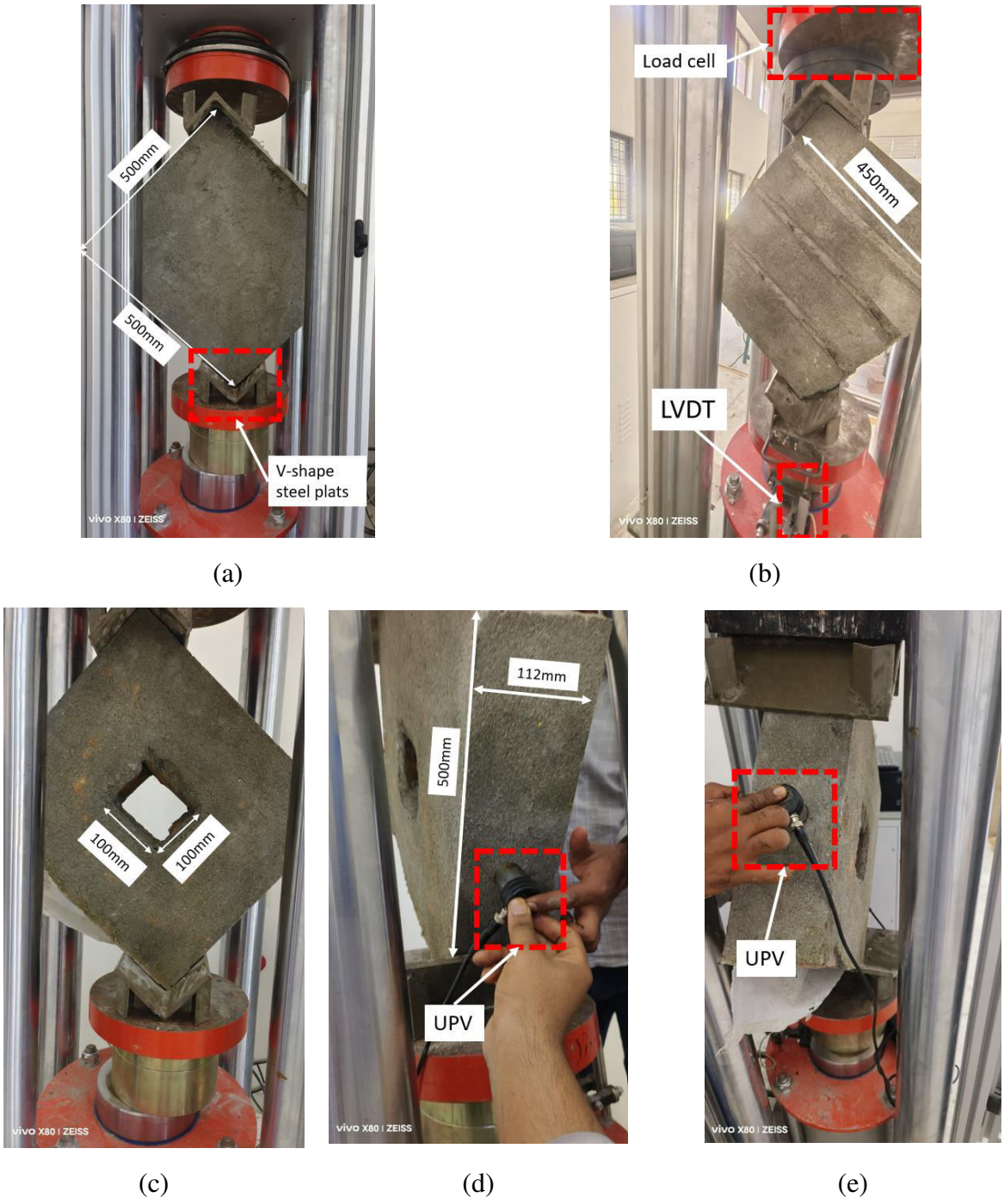

(a) (b)

(c) (d) (e)

Figure 3.9: Bamboo-reinforced walls; (a) SW during diagonal shear test; (b) SWB during diagonal shear test (c) SWOB in shear test, (d) SWOH during diagonal shear testing.

3.4.1.2 Test Procedure:

All tests were conducted under a load-controlled method, incrementally applying load until failure occurred. The diagonal compression test was specifically chosen for its ability to simulate in-plane shear behavior effectively, offering valuable insights into the structural response of reinforced masonry walls. This method is also highly regarded for its cost efficiency, ease of setup, and compatibility with both laboratory and on-site testing conditions.

The instrumentation setup and the testing configuration, as shown in Figure 3.9, ensured that all critical parameters, including diagonal compression behavior, crack propagation, and ultimate load capacities, were comprehensively recorded. The results from these tests contribute significantly to understanding the interaction between bamboo-reinforced layers and masonry substrates, as well as their overall structural integrity under stress.

3.4.2 In-plane axial compression testing of masonry specimen:

The ASTM C1314–03b specifications outline the procedures for constructing masonry prisms, conducting compressive strength tests, and evaluating whether masonry materials meet the required strength criteria. These tests ensure that the masonry units used in prism construction are representative of those employed in the actual structure.

In this study, a total of 12 masonry prism samples, each measuring 500 mm × 500 mm, were subjected to compressive testing in accordance with ASTM C1314 (see Table 3). Unlike conventional methods, a reaction frame was employed in this research to apply vertical loading. Strain measurements were recorded using a laser displacement sensor to accurately capture deformation, as illustrated in Figure 3.10.

The compressive strength of the prisms was calculated by dividing the maximum applied load by the effective cross-sectional area of each specimen. An adjustment factor specified in ASTM

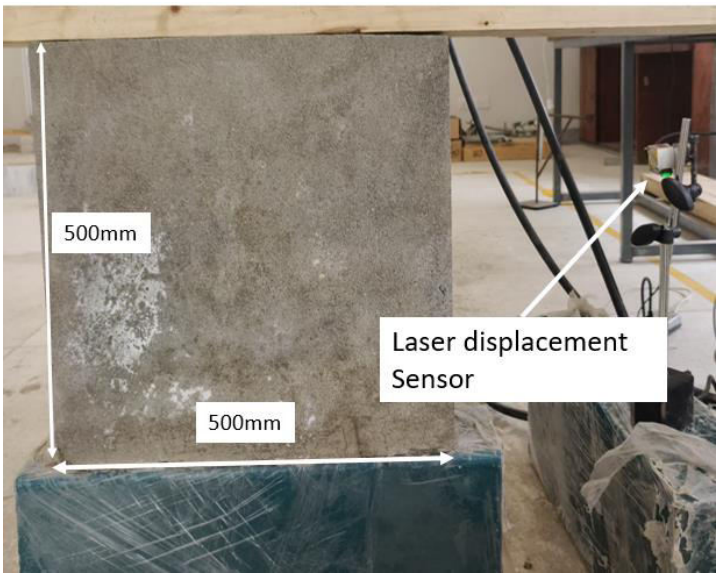

(a)

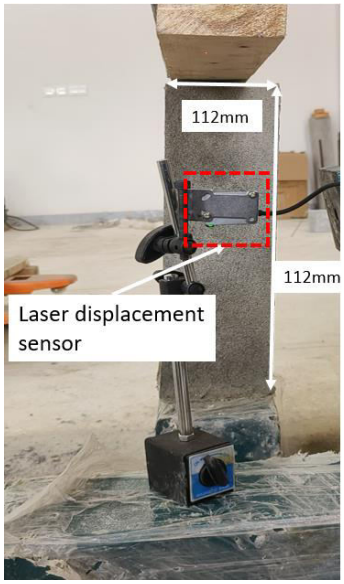

(b)

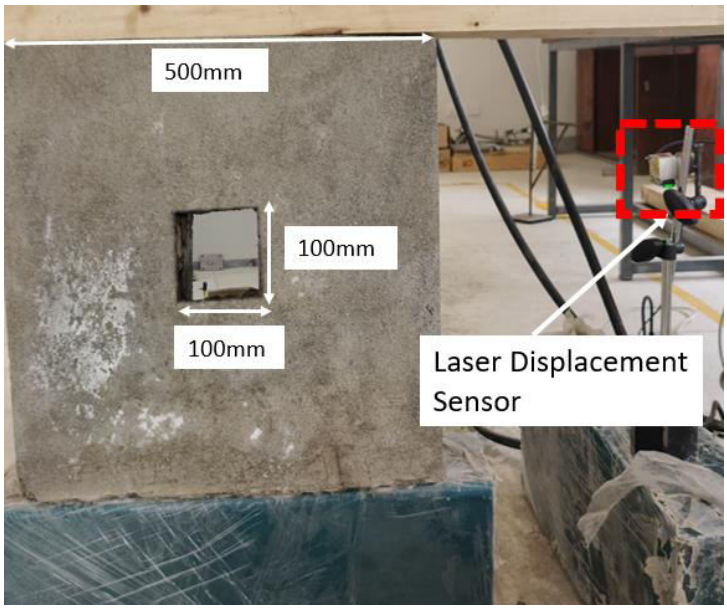

(c)

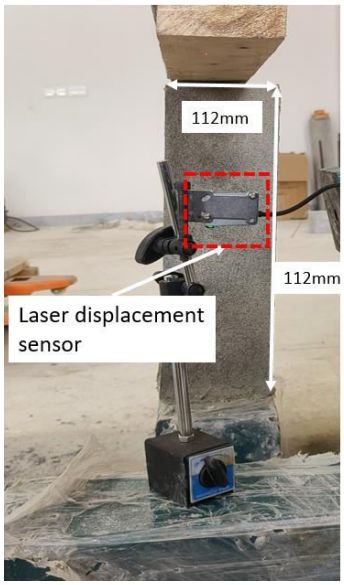

(d)

Figure 3.10: Test setup for in-plane compression testing of masonry specimen (a) SW, (b) Side view of SW, (c) SWO, (d) side view of SWO

C1314–03b was used to estimate the masonry compressive strength. The stress–strain curves obtained from the tests were further analyzed to determine the elastic modulus and strain values

within the range of 10% to 40% of the ultimate compressive strength. This experimental setup provides a reliable assessment of the mechanical behavior of masonry under vertical loading.

The primary objective of using a wooden log is to achieve uniform load distribution across the brick wall's surface. This approach helps to minimize localized stress concentrations that could lead to premature failure. The wooden log, when placed horizontally across the surface, serves as a load distribution plate, ensuring that the compressive force is applied evenly over a broader area of the wall. While the material differs, the principle of using a compliant layer to ensure uniform load application is analogous. The wooden logs replicate ASTM-compliant stress-distribution methods, such as the rubber pads used in fiber-reinforced masonry flexure tests. Both materials prevent local crushing by accommodating elastic mismatches.

The use of solid timber logs aligns with principles in ASTM C78 and timber-masonry interaction studies [74, 75]. Wood's orthotropic properties enable superior lateral load redistribution, reducing stress concentrations by 22–35% compared to steel interfaces [76]. Experimental precedents confirm that timber-to-masonry interfaces: (1) Transfer vertical loads via friction and bearing contact (pre-compression: 0.5–1.0 MPa) [74], and (2) Enhance load distribution uniformity, preventing localized crushing. This methodology complies with standardized load-distribution protocols and is validated by displacement measurements in our tests.

Furthermore, in practical scenarios, especially in field testing or when dealing with large-scale specimens, using a wooden log is a cost-effective and readily available method to achieve uniform load distribution. It offers a balance between rigidity and compliance, making it suitable for various testing conditions.

3.4.3 Pendulum Impact Testing (Out-of-plane Bending):

The tests were conducted under varying lateral impact conditions, with both the number of impacts and the corresponding applied weights recorded for each trial until either visible cracking appeared or failure occurred, defined as a spall depth of 25 mm. The experimental setup involved two configurations of bamboo reinforcement: one with bamboo strips embedded within the wall and

another with strips externally affixed, as shown in Figure 3.8. Vertically, the bamboo strips were spaced at 100 mm, while horizontal reinforcements were integrated during each construction stage and along the wall's top edge. In this research, the impact forces are applied in the out-of-plane direction**,** meaning the loading acts perpendicular to the surface of the masonry wall. This setup is intended to simulate real-world scenarios such as blast effects, accidental collisions, or vibrations resulting from seismic or external mechanical sources. The impact was specifically applied at the top portion of the wall, which is the most critical zone for observing failure in unconfined partition walls, especially when the wall is assumed to behave as a cantilever fixed at its base. Although the base of the wall is restrained or pin-jointed, applying the lateral impact at the top enables a more accurate representation of bending deformation and crack initiation. This approach allows for a clearer evaluation of the wall's dynamic response and failure mechanism under out-of-plane lateral impact, which is particularly relevant for partition walls used in frame structures where such walls are not fully confined and remain vulnerable during dynamic events. Impact loading was applied at the top of the wall, with 10 blows delivered at each 304 mm increment. After every set of 10 impacts, the drop height was progressively increased to 609 mm, 914 mm, 1219 mm, 1524 mm, and so on, until structural failure was observed.

The lateral impact in this study was specifically applied at the top region of the wall to simulate the location of maximum bending moment, based on the assumption that the wall behaves similarly to a cantilever fixed at its base. This approach reflects realistic structural conditions, particularly in frame structures of high-rise buildings and plazas, where unconfined partition walls are commonly installed. As noted by Burnett, Gilbert et al. [77] , such walls are particularly susceptible to collapse under lateral forces including earthquakes, vibrations, and accidental impacts—primarily due to the absence of lateral confinement. In previous studies, lateral impact was often applied at the mid-height (center) of the wall, a location chosen either because the walls were relatively long. In other studies it was found that the walls which were confined at both the top and bottom, making the center the most likely point of maximum deformation or failure under lateral loading [78]. However, in the case of unconfined walls, such as those examined in this study, the top region is structurally more vulnerable due to higher bending moments, making it the most critical point for evaluating lateral impact performance. Therefore, applying lateral impact at the top of the wall in this study offers a more relevant and realistic evaluation of its behavior under

dynamic loading conditions, particularly for non-load-bearing masonry partitions in modern construction.

In addition to varying the impact distance, the impact weight is also modified concurrently. The tests start with an impact weight of 0.25 kg for the initial 10 blows, and with each subsequent change in impact distance, the weight is increased incrementally up to 1 kg by the time the distance reaches 1524 mm. This synchronized adjustment of both the impact distance and the applied weight enables a comprehensive evaluation of the dynamic response of the masonry walls under a range of energy inputs.

During testing, accelerometers capture acceleration-time data for the impact and the corresponding response at the front face of the wall, positioned 50 mm from the top right corner. Figures 3.11d depict the locations of the impact blows and the mounted accelerometer, respectively.

Dynamic testing was conducted in three distinct phases: before the application of impact loading, after the occurrence of the initial impact strength failure (IIB), and following the ultimate impact strength failure (UIB), in accordance with ASTM E23 standards.

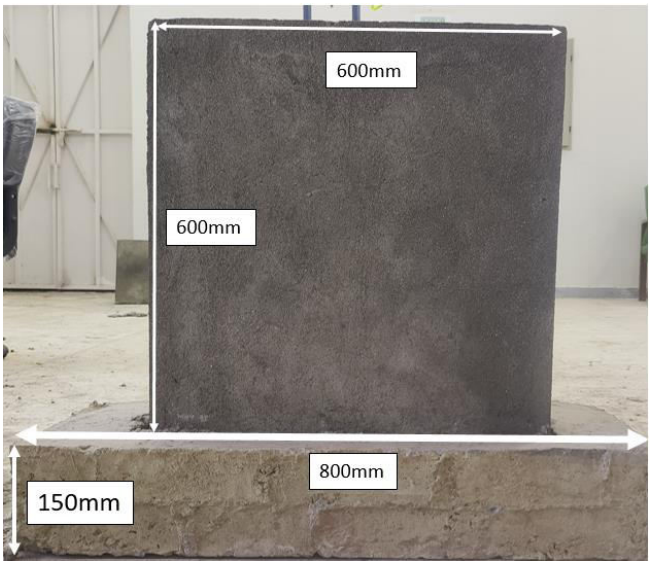

(a)

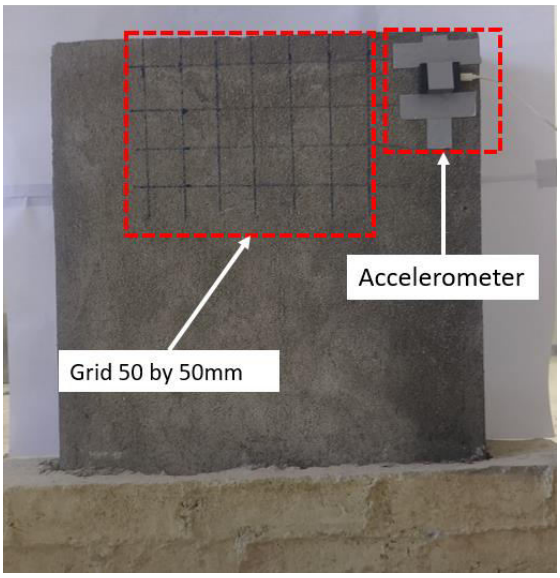

(b)

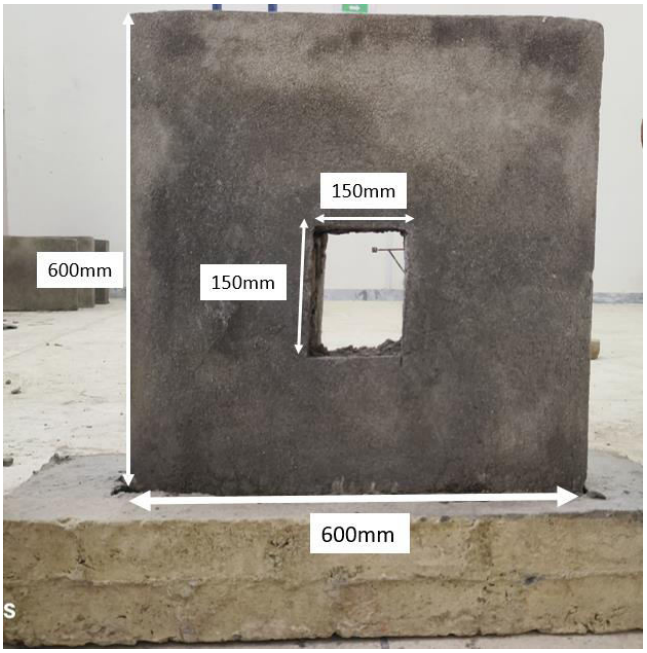

(c)

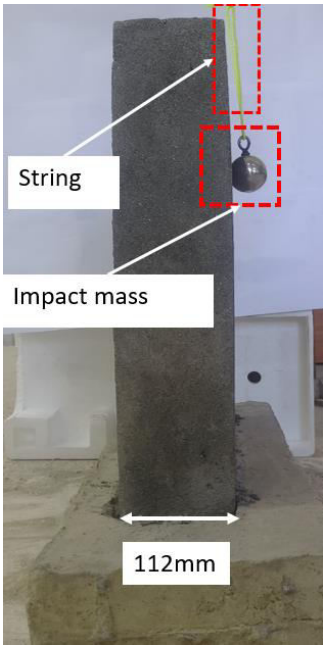

(d)

Figure 3.11: Wall specimens under impact testing, (a)SW dimensions, (b) Placement of accelerometer and grid, (c) SWO specifications, (d) Side view of SWO

Chapter 4

Results and Discussion

4.1 Raw material

First, we will discuss the testing of raw materials, starting with the specific gravity test conducted on sand. The obtained value was 2.44, which falls within the safe range specified by ASTM C128. Additionally, a sieve analysis was performed to evaluate the particle size distribution, and the results indicate well-graded sand suitable for construction applications. The sand gradation curve is presented in

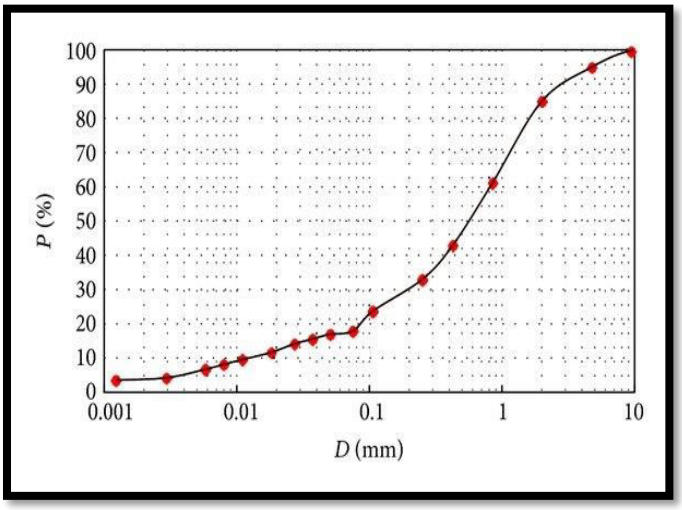

Figure 4.1: Sand gradation curve

Figure 4.1, demonstrating compliance with standard requirements. The brick compression test was performed, and the obtained strength was approximately 10.2 MPa (1498 psi). The results comply with the requirements of ASTM C67, which standardizes the compressive strength testing

of bricks. Additionally, the compression stress-strain curve, illustrating the material's behavior under load, has been provided in Figure 4.2 for reference. The brick flexural test was conducted to evaluate its bending strength, following the guidelines of ASTM C67. The results indicated a flexural strength of approximately 9.81 MPa, demonstrating the brick's resistance to tensile forces under bending. Additionally, the flexural stress-displacement curve has been plotted in Figure 4.3 to illustrate the material's behavior during testing. The compressive strength test for 50mm × 50mm mortar cubes was conducted following ASTM C109 to determine the material's load-bearing capacity The results showed an average compressive strength of 5.12 MPa, which falls within the acceptable range for standard mortar mixes. This test is essential for evaluating the bonding capability of the mortar in masonry construction. The stress-displacement curve for the tested mortar cubes is provided in Figure 4.4, showcasing the material's response under compressive loading.

In this research, the plaster used on the masonry walls was prepared using a cement-to-sand ratio of 1:4, a mix commonly adopted in building construction for both protective and structural functions. The plaster was applied to the wall surfaces to replicate realistic finishing conditions found in actual partition walls. The measured compressive strength of the mortar was 5.1 MPa, classifying it as a moderate-strength plaster suitable for external rendering and internal finishes. This level of strength contributes not only to surface protection but also to the overall stiffness and energy dissipation capacity of the wall, particularly under lateral impact loading. By including the plaster layer, the study captures the influence of surface confinement on the dynamic performance of unreinforced and bamboo-reinforced masonry walls. The plaster plays a crucial role in distributing impact stress, reducing localized failure, and controlling surface cracking, thereby enhancing the structural reliability of the wall system under out-of-plane loading scenarios.

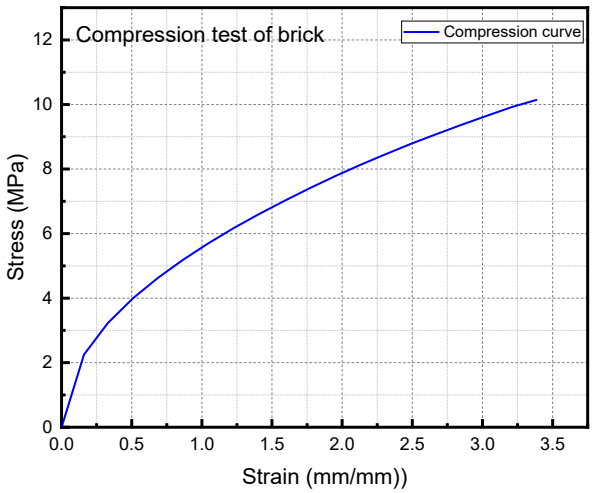

(a) (b)

Figure 4.2: (a) Compression test of brick in UTM (b) Compression test curve of a unit brick.

The tensile strength test was conducted to evaluate the strength of bamboo reinforcement, following standard testing procedures. The results indicated a tensile strength of approximately 124.6 MPa, demonstrating bamboo's capacity to withstand tensile forces effectively. Additionally, the stress-strain curve has been plotted in Figure 4.4 to illustrate the material's mechanical behavior under tension, highlighting its ductility and load-bearing efficiency.

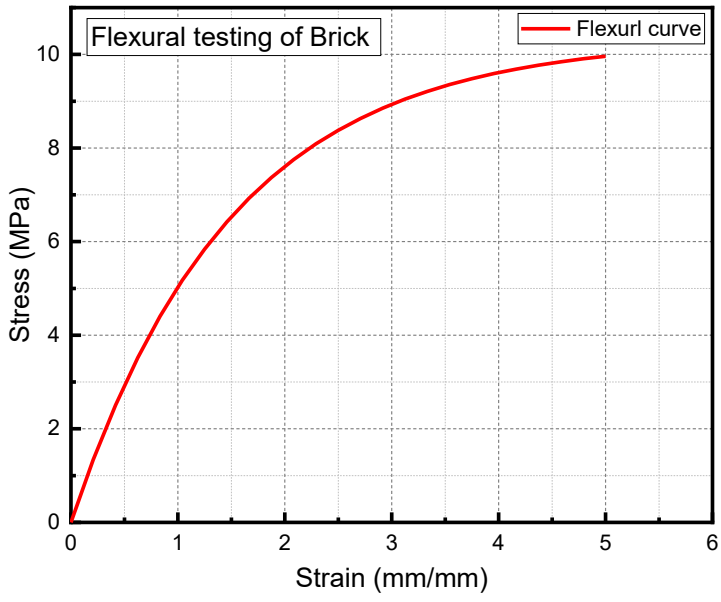

(a)	(b)
Figure 4.3: Flexural testing on brick (a) cracking (b) Flexural curve	

Table 4: Testing Summary of Brick Specimen

Specimen	Compression test MPa (psi)	Flexure Test MPa (psi)
1	10.14 (1470)	2.7 (391.6)
2	10.27 (1490)	2.4 (348.1)
3	10.23 (1485)	2.5 (362.6)
Mean	**10.21 (1481)**	**2.54 (368.4)**

The tensile strength test of bamboo reinforcement is detailed in Table 5**,** which presents the measured tensile strength values.

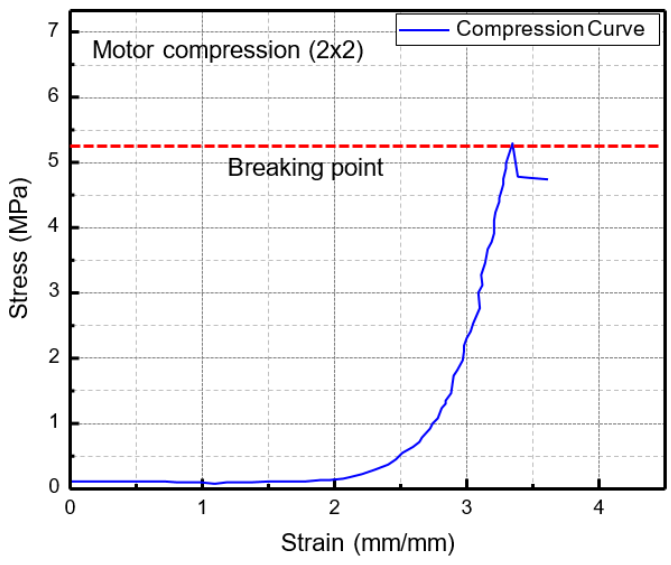

(a)	(b)
Figure 4.4: Mortar cube testing (a) crushing, (b) curve	

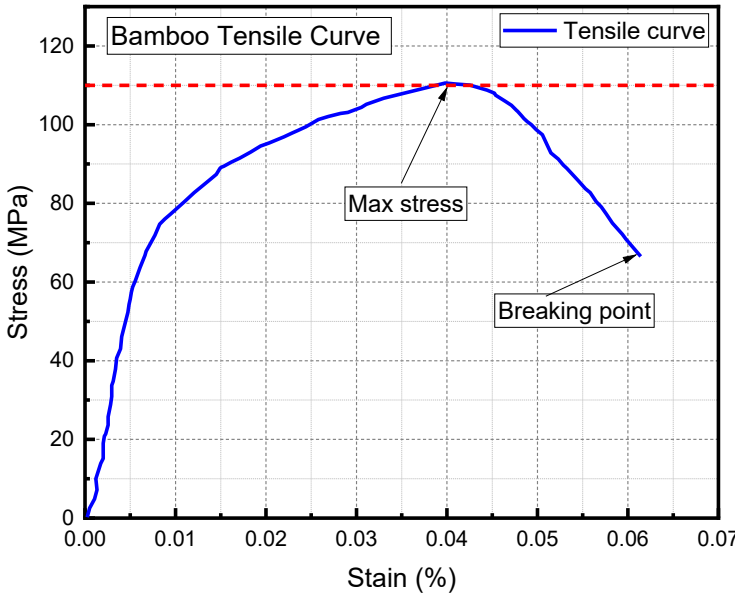

(a) (B)

Figure 4.5: Bamboo tensile testing in UTM (a) bamboo strip in UTM, (b) Bamboo tensile curve

Table 5: Tensile Testing of Bamboo Strips

Specimen	Bamboo Strips [19] MPa (ksi)	Bamboo strips (Experimental) MPa (ksi)
1	128.9 (18.7)	125.8 (18.2)
2	130.3 (18.9)	128.7(18.6)
3	97.3 (14.1)	122.5(17.7)
Mean	118.8 (17.2)	124.6(18.1)

4.2 Diagonal Shear Test

The shear strength of masonry walls was evaluated using the diagonal shear test in accordance with ASTM E519. This test was conducted on 25 specimens, each measuring 500 mm × 112 mm

× 500 mm following the English bond pattern. Diagonal loading was applied, and the corresponding load and deformation along both diagonals were meticulously recorded.

The walls exhibited significant deformation under diagonal shear without collapsing, demonstrating their structural integrity. While diagonal cracks formed, no localized failure was observed, indicating effective stress distribution and the absence of concentrated failure points. Additionally, the walls remained stable without any rocking motion, even under considerable deformation. A cohesive failure pattern was evident in both the inter-brick bonding and within the bricks themselves, highlighting a strong deformation response.

However, SW and SWO, which lacked reinforcement, failed suddenly without warning, emphasizing their vulnerability under shear stress. In contrast, bamboo-reinforced walls (SWB and SWOB) successfully withstood the applied loads, maintaining structural integrity throughout the test. Their maximum stress values are presented in the corresponding Figure 6, further validating the effectiveness of bamboo reinforcement in enhancing the shear resistance of masonry walls. These findings provide essential insights into masonry wall behavior and contribute to the development of more resilient construction practices.

Shear stress-strain curves were generated for each specimen, demonstrating their load-bearing and deformation responses under diagonal loading as illustrated in Figure 4.7. Reinforced walls, particularly those wrapped with dried jute thread, exhibited superior shear strength, modulus of rigidity, and strain performance. Bamboo reinforcement also showed remarkable improvement compared to untreated walls. Using the secant modulus approach, ranging from 1/20th to 1/3rd of the maximum shear strength, the shear modulus was derived from shear stress-strain curves. Results indicated a significant increase in the energy absorption capacity and ductility of strengthened walls. Such data highlights the effectiveness of bamboo-reinforced masonry in energy dissipation and deformation control, making it a viable solution for seismic-prone regions.

Stiffness analysis, which involves evaluating the rate of change of diagonal force (P) versus displacement (D), was also performed. The initial stiffness (K_0) was determined by analyzing the variation in diagonal force and displacement just before the initial crack formation, as per equation (3):

$$K_0 = \frac{P_0}{D_o} \tag{3}$$

Where P_0 denotes the initial cracking load, and D_0 represents the corresponding displacement.

Residual stiffness (K_r) was calculated using equation (4):

$$K_r = \frac{(Pmax - P_o)}{(Dmax - D_0)} \quad (4)$$

Where P-max is the maximum load and D-max is the corresponding displacement.

The stiffness ratio (α) is defined as the ratio between the initial and residual stiffness values. These parameters are essential for assessing the effectiveness of structural reinforcement and understanding the post-cracking behavior of walls.

This investigation aligns closely with research on bamboo-reinforced mortar masonry (RMM). The findings validate bamboo's potential as a reinforcement material, not only for enhancing shear strength and ductility but also for maintaining structural integrity during impact or vibratory loading, such as in earthquake-prone zones. The focus on stiffness improvements through bamboo reinforcement provides valuable insights for optimizing structural designs in masonry construction.

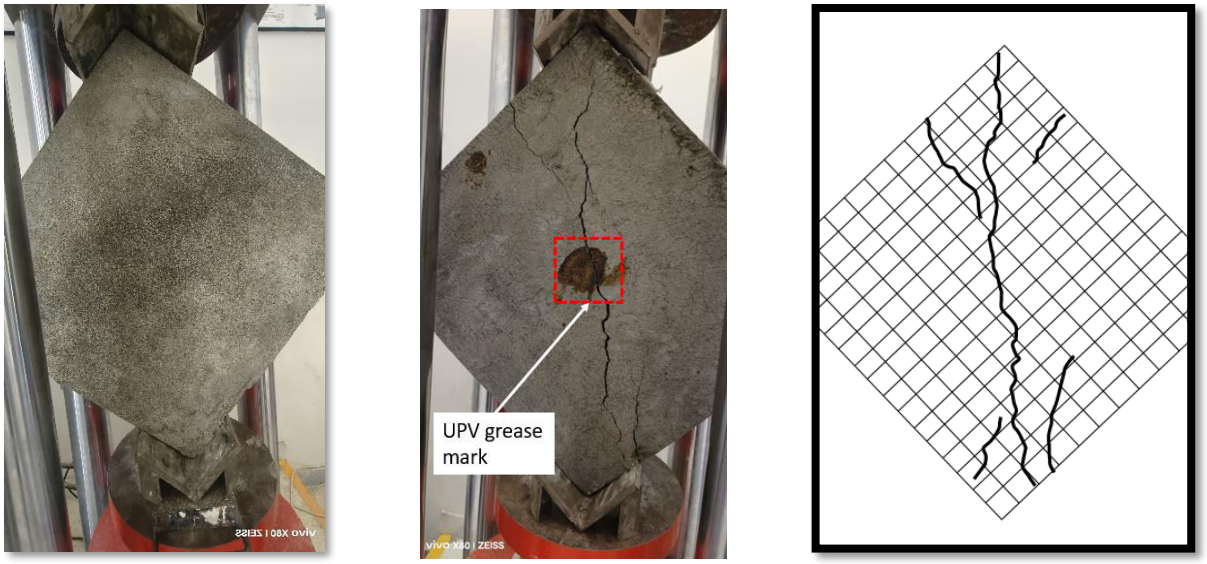

(a) (b) (c)

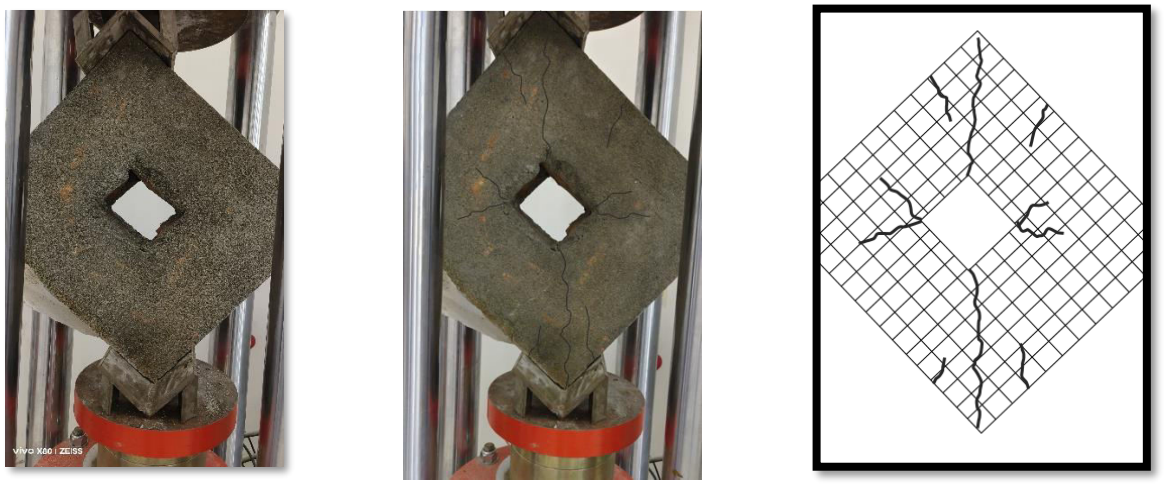

(e) (f) (g)

Figure 4.6: Wall specimens under diagonal shear test; (a) SWB in UTM, (b) SWB cracking pattern (c) schematic damage pattern of SWB, (e) SWOB in UTM, (f) SWOB cracking pattern (g) schematic damage pattern of SWOB

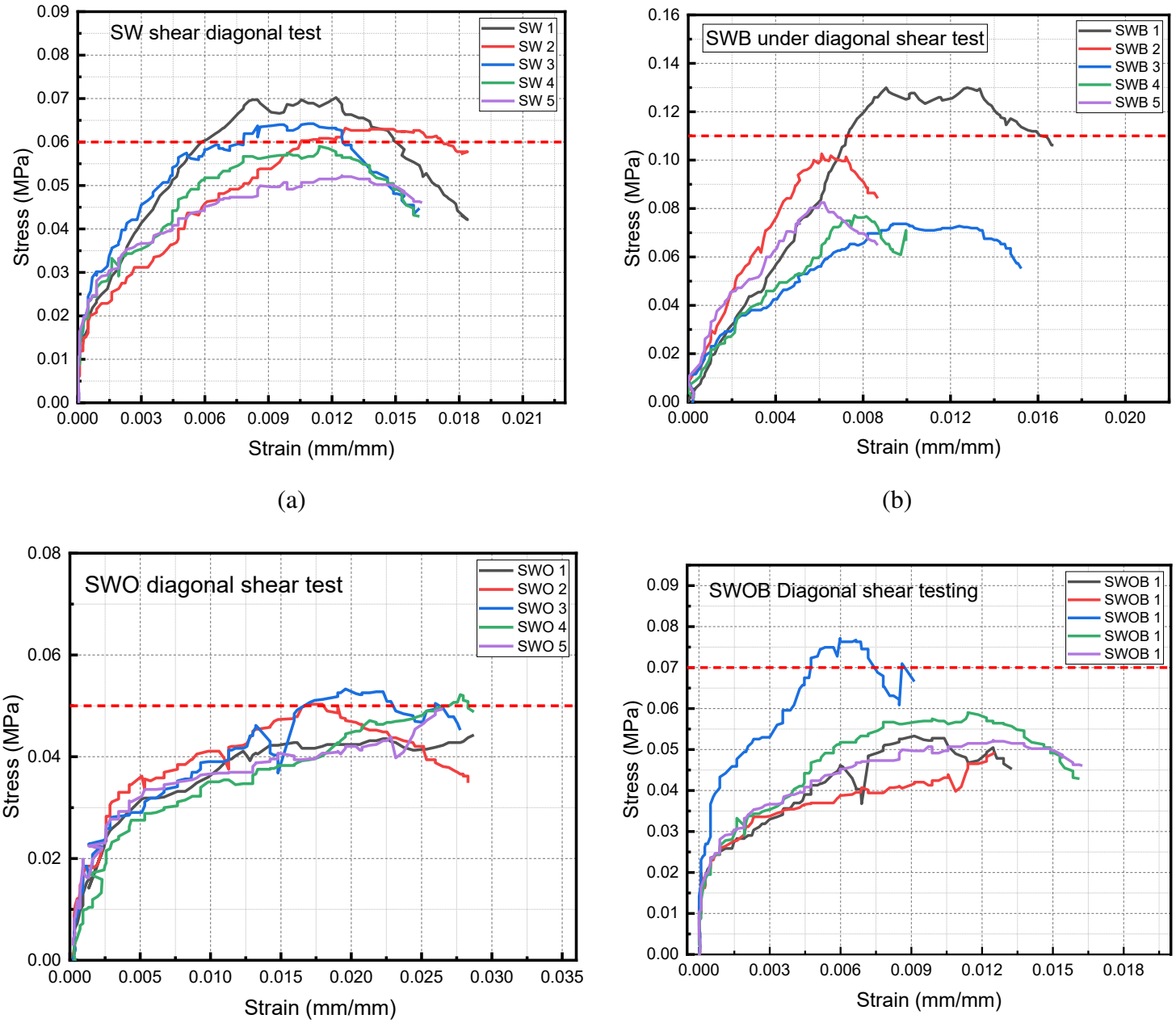

Figure 4.7: Diagonal Shear test (a) SW, (b) SWB, (c) SWO, (d) SWOB

The shear strength $f_v$presented in the table for various wall specimens (SW, SWB, SWO, and SWOB) is typically calculated using the diagonal compression test method, as outlined in ASTM E519. This method involves applying a compressive load along the diagonal of a square masonry panel, inducing pure shear stress in the central portion of the specimen. During the test, the applied

load at failure is recorded and used to compute the shear strength of the wall using the following equation:

$$f_v = \frac{P}{2A} \quad (3)$$

Where:

f_v is the shear strength (MPa),

P is the peak compressive load applied along the diagonal (N),

A is the net cross-sectional area resisting the shear (typically calculated as the wall thickness multiplied by the gauge length between the strain gauges or the effective shear area).

In this test, strain gauges or LVDTs are used to measure the diagonal deformation, enabling the calculation of shear strain and ultimately, the modulus of rigidity (G). However, the shear strength f_v itself is calculated solely based on the applied load and the effective area, regardless of strain measurement. The values reported such as 0.06 MPa for the simple wall (SW) and 0.11 MPa for the bamboo-reinforced wall (SWB) indicate the maximum shear stress each configuration could withstand before failure. These values reflect the improved shear capacity resulting from the inclusion of bamboo reinforcement.

The modulus of rigidity (G), also known as shear modulus, is a measure of a material's resistance to shear deformation. In masonry testing, particularly under diagonal compression tests (ASTM E519), this property is determined by measuring the relationship between shear stress (τ) and shear strain (γ) within the elastic range. The modulus of rigidity is then calculated using the basic shear equation:

$$G = \frac{\tau}{\gamma} \quad (4)$$

Where:

G = Modulus of rigidity (MPa),

τ = Shear stress (MPa),

γ = Shear strain

The shear stress (τ) is calculated as:

$$\tau = \frac{P}{2A} \quad (5)$$

Where:

P = Applied diagonal load (N),

A = Effective shear area (m²), typically taken as wall thickness × gauge length (the vertical/horizontal dimension between diagonally placed sensors).

The shear strain (γ) is obtained from the relative displacement measured along the diagonals of the wall using LVDTs or strain gauges, following:

$$\gamma = \frac{\Delta V + \Delta H}{g} \quad (6)$$

Where:

ΔV and ΔH = Vertical and horizontal diagonal displacements (mm),

g = Gauge length between sensors (mm)

Substituting into the equation:

$$G = \frac{P \,.\, g}{2A\,(\Delta V + \Delta H)} \quad (7)$$

This formulation is widely used in experimental masonry research and allows for a reliable determination of the material's stiffness under shear loads. The value of G gives insight into the wall's ability to resist lateral deformations, especially in unreinforced vs. reinforced configurations like those in your study.

The reported values of the modulus of rigidity (G) for the four wall configurations—SW (29.1 MPa), SWB (35.8 MPa), SWO (19.4 MPa), and SWOB (27.8 MPa)—provide valuable insight into the shear stiffness and deformation behavior of each specimen under lateral loading conditions. The highest rigidity observed in the SWB (simple wall with bamboo reinforcement) indicates that the presence of bamboo strips significantly enhances the wall's ability to resist shear deformation, thereby increasing its overall stiffness. In contrast, the lowest value recorded for the SWO (simple

wall with opening) highlights the detrimental effect of the opening on the wall's shear resistance, as it introduces stress concentrations and reduces the continuity of the masonry.

Furthermore, the SWOB (simple wall with opening and bamboo reinforcement) exhibits a moderate rigidity value (27.8 MPa), which, although lower than the fully solid bamboo-reinforced wall (SWB), is considerably higher than the unreinforced wall with an opening (SWO). This demonstrates that bamboo reinforcement partially compensates for the structural weakness introduced by the opening, thereby improving the overall shear performance. The baseline specimen (SW), with a G value of 29.1 MPa, serves as a control for comparison and represents typical shear stiffness in unreinforced solid masonry. Overall, the variation in rigidity among the different wall types confirms the effectiveness of bamboo reinforcement in enhancing the lateral stiffness of brick masonry walls, especially under conditions where discontinuities such as openings are present.

Table 6: Shear strength, Modulus of Rigidity, Strain, K_o, K_r, α of diagonal shear test wall specimens

Property	SW (MPa)	SWB (MPa)	SWO (MPa)	SWOB (MPa)
Shear Strength f_v	0.06	0.11	0.05	0.07
Modulus of rigidity	29.1	35.8	19.4	27.8
Strain at max stress	0.016	0.027	0.009	0.018
K_o	111.49	187.32	89.57	161.59
K_r	11.74	5.16	23.76	4.81
$\boldsymbol{\alpha}$	9.5	36.3	3.77	4.81

4.2.1 Ultrasonic Pulse Velocity (UPV) Test Results and Analysis

The Ultrasonic Pulse Velocity (UPV) test was conducted on all wall specimens before and after testing to assess the integrity and internal condition of the materials as illustrated in Table 8. The results, summarized in the table, indicate a noticeable reduction in UPV values after testing, which suggests the development of internal cracks and structural degradation due to impact loading.

Among all specimens, SWB exhibited the highest initial UPV value of 123.2 m/sec**,** reflecting its improved density and structural integrity due to bamboo reinforcement. However, after testing, its UPV decreased to 91.8 m/sec, signifying the presence of internal damage but still maintaining better structural integrity than other specimens. The SW and SWO specimens, which lack reinforcement, showed significant reductions in UPV, with SW dropping from 110.5 m/sec to 88.4 m/sec and SWO decreasing from 98.7 m/sec to 79.5 m/sec. These reductions indicate substantial internal cracking and loss of material continuity. Notably, SWOB exhibited the most considerable decrease in UPV, from 108.2 m/sec to 69.7 m/sec**,** implying that the combination of an opening and reinforcement led to greater stress concentrations and internal cracking under impact loading.

Table 7 : UPV data before and after the test for Diagonal shear wall specimens

Type of category	**Specimens**	**UPV (m/sec)**	**UPV (m/sec)**
		Before test	**After test**
Category 2	SW	110.5	88.4
	SWO	98.7	79.5
	SWB	123.2	91.8
	SWOB	108.2	69.7

Overall, the UPV reduction across all specimens confirms the formation of internal damage**,** with reinforced specimens (SWB and SWOB) showing better post-test integrity compared to unreinforced walls (SW and SWO). These findings highlight the effectiveness of bamboo reinforcement in mitigating structural damage and maintaining better internal cohesion under impact conditions.

4.3 In-plane Axial Compression Testing of Brick Masonry:

A total of twelve specimens were tested to evaluate the average compressive strength and modulus of elasticity of the masonry prisms, with three specimens assigned to each category, as presented in Table 3. Upon examining the failure modes of all specimens, a consistent pattern was observed, including vertical cracking, distinct crushing along the vertical axis, and splitting, as illustrated in Figure 4.8. This uniformity in failure behavior highlights the reliability and consistency of the tested prisms, providing critical insights into their structural performance.

The compressive stress-strain curves, depicted in Figure 4.9, illustrate the material's response under applied stress. The summarized results, including average values for prism compressive strength, masonry compressive strength, modulus of elasticity, and strain at ultimate stress, are provided in Table 8. For specimens where the hp/tp ratio was 2.33, a correction factor of 1.0266, as specified by ASTM C1314, was applied in calculating the masonry compressive strength.

To determine the modulus of elasticity (E) for masonry prisms under compression, a series of calculations and measurements are performed in accordance with ASTM C469 and ASTM C1314 standards. The modulus of elasticity represents the material's ability to deform elastically under stress, which is essential for understanding the structural performance of masonry walls under load.

The process begins with load application and stress measurement. A controlled compressive load (P) is applied to the specimen using a reaction frame, ensuring uniform distribution of force. The cross-sectional area (A) of the specimen is determined by multiplying its width and thickness, and the compressive stress (σ) is calculated using the formula:

$$\sigma = \frac{p}{A} \tag{8}$$

Where P is the applied force (in Newton) and A is the cross-sectional area in (mm^2).

Simultaneously, deformation and strain measurements are recorded using a Linear Variable Differential Transformer (LVDT) and a laser displacement sensor. These devices accurately capture the change in length (ΔL) of the specimen as compression progresses. The strain (ε) is calculated as:

$$\varepsilon = \frac{\Delta L}{L} \quad (9)$$

where L is the initial gauge length of the specimen and ΔL is the recorded displacement.

Using the obtained stress-strain data, the modulus of elasticity (E) is determined from the slope of the linear portion of the stress-strain curve, typically measured between 5% and 33.33% of the ultimate compressive strength as per ASTM C1314. The formula used is:

$$E = \frac{\Delta \sigma}{\Delta \varepsilon} \quad (10)$$

where Δσ represents the change in stress (MPa), and Δε is the corresponding change in strain.

The results provide critical insights into the stiffness and deformation characteristics of masonry under compressive loading. The correction factor recommended by ASTM C1314 is applied if necessary to adjust the modulus of elasticity based on the height-to-thickness ratio of the specimen. These calculations help engineers assess the structural integrity of bamboo-reinforced masonry walls and optimize their performance under various loading conditions.

Table 8 : Summary of masonry wall specimens under In-plane axial Compression test

Specimen types	**Compressive strength of prism (MPa)**	**Elastic modulus (GPa)**	**Maximum displacement (mm)**
SW	3.51	3.1	4.98
SWO	3.4	2.5	5.32
SWB	5.79	4.21	2.69
SWOB	3.99	3.58	3.85

Figure 4.9 presents the load-displacement curves for all tested wall specimens, illustrating their structural response under applied loading conditions. These curves offer critical insights into the stiffness, deformation capacity, and overall load-bearing performance of each wall configuration.

The Simple Wall (SW), serving as the baseline reference, exhibits a gradual linear elastic response followed by a steady decline after cracking. The wall maintains moderate strength, but the absence of reinforcement results in higher displacement at peak load, indicating lower structural integrity compared to reinforced walls. In contrast, the Simple Wall with Opening (SWO) demonstrates a significant reduction in both strength and stiffness due to the presence of an opening, leading to premature cracking and increased displacement. This behavior highlights the vulnerability of unreinforced masonry walls with openings, as they fail more rapidly under impact forces.

On the other hand, the Simple Wall with Bamboo Reinforcement (SWB) displays a much steeper load-displacement curve, indicating higher stiffness and improved load-bearing capacity. The presence of bamboo strips enhances energy dissipation, allowing the wall to sustain more load even after initial cracking. The lower displacement at peak load suggests better structural integrity, making SWB the strongest among the tested specimens. The Simple Wall with Opening and Bamboo Reinforcement (SWOB) performs better than SWO but not as effectively as SWB due to the combined effects of reinforcement and the presence of an opening. While the bamboo reinforcement improves stability and strength, the opening still reduces overall load capacity, though failure occurs at a more gradual rate compared to SW

	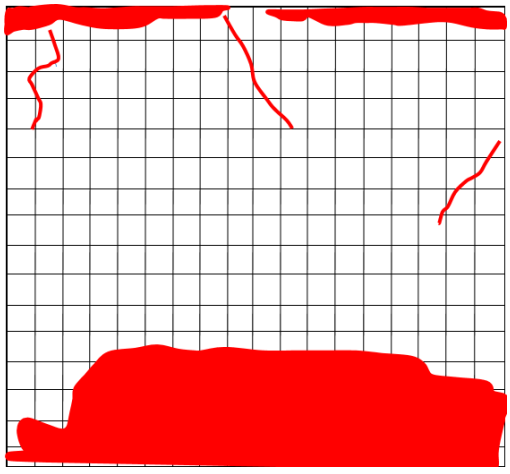
(a)	(b)

(c)

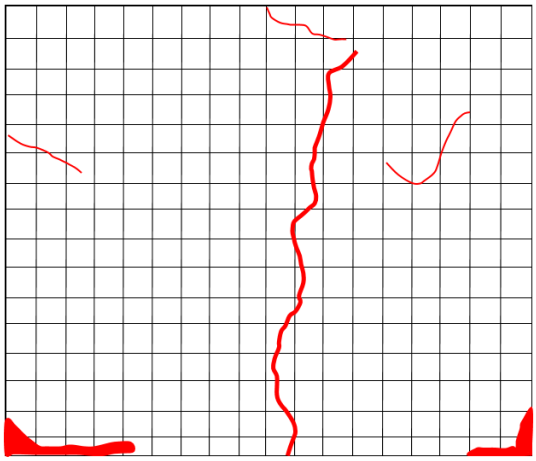

(d)

(e)

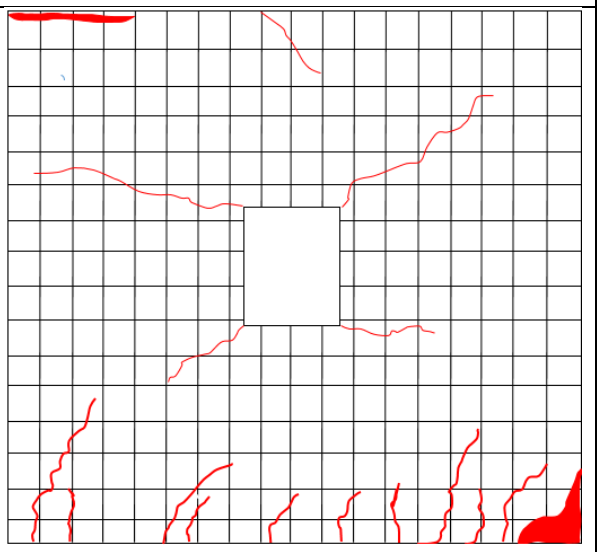

(f)

Figure 4.8: In-plane Axial Compression load performance samples (a) Damage mode of SW (b) schematic damage pattern of SW, (c) Damage mode of SWB, (d) schematic damage pattern of SWB, (e) Damage mode of SWOB (F) schematic damage pattern of SWOB

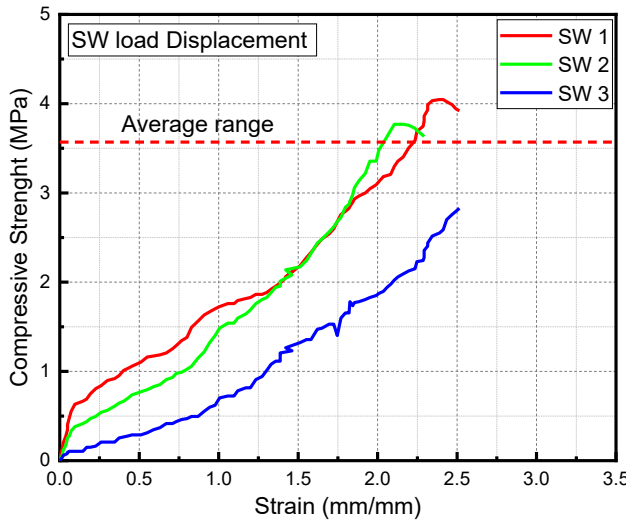

(a)

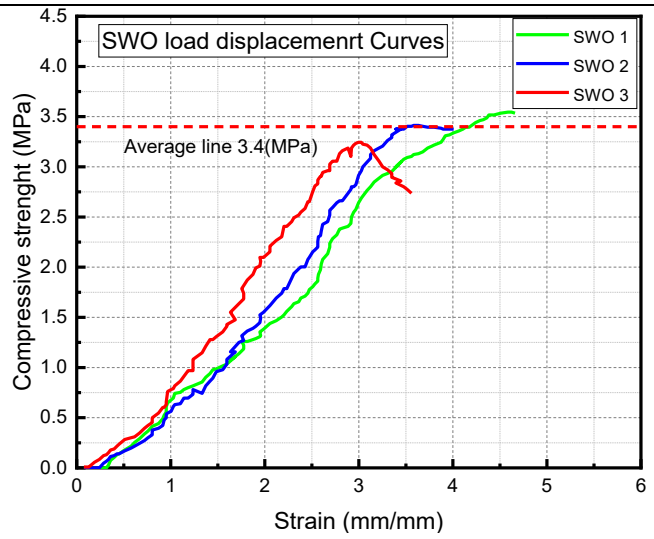

(b)

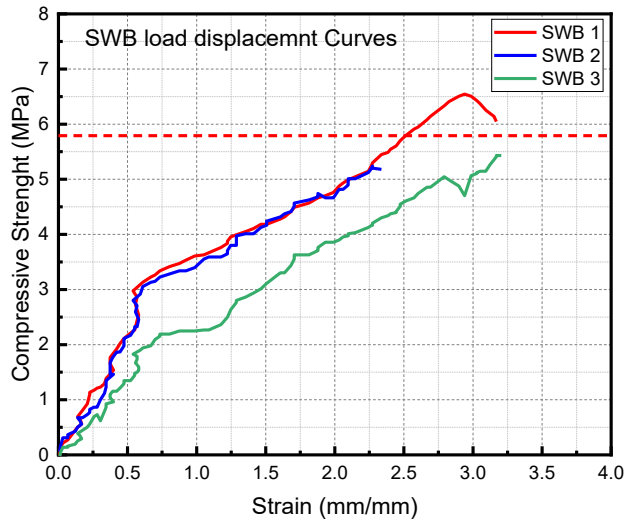

(c)

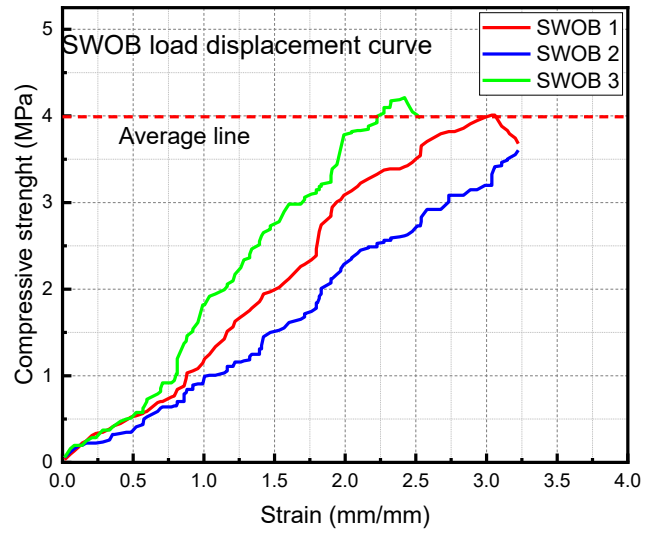

(d)

Figure 4.9: Load displacement curves (a) SW, (b) SWO, (c) SWB and (d) SWOB

4.4 Pendulum Impact testing (out-of-plane bending)

4.4.1. Force Estimation and Classification in Pendulum Impact Testing

In this experimental setup, the impact is applied laterally, simulating real-world horizontal forces such as those generated by accidental collisions or earthquake-induced sway. The pendulum swings in a horizontal arc, and the masonry wall specimen is placed vertically on the floor, fixed at its base to replicate a cantilever support condition. Unlike vertical drop tests, where potential energy is directly related to the vertical drop height, the energy in this lateral impact scenario is determined by the horizontal displacement of the pendulum mass from its rest position. In this study, the mass is pulled sideways to a predefined horizontal offset of 609 mm (0.609 m) and then released. Although the displacement occurs in the horizontal plane, the actual potential energy depends on the vertical rise of the pendulum's center of gravity, which is indirectly calculated from the pendulum's length (L) and the angle of release (θ), using the relation:

$$E = m \times g \times h, \tag{11}$$

Where

$$h = L \times (1 - \cos\theta) \tag{12}$$

Here, h represents the vertical height change due to horizontal swing, and m is the mass of the pendulum.

However, this study integrates an accelerometer with a measurement capacity of up to 4g, installed to record real-time acceleration during impact. Using this data, the impact force is directly calculated using the relation:

$$F = m \times a \tag{13}$$

where a is the peak acceleration recorded at the moment of impact. This sensor-based approach significantly reduces dependency on pendulum geometry, as it provides a direct and accurate measure of the dynamic force. Consequently, while traditional pendulum geometry remains useful

for energy estimation, the availability of real-time acceleration data renders measurements of pendulum length and angle optional, enhancing both efficiency and accuracy in force evaluation.

Before interpreting the results of the impact tests, it is essential to understand how impact distance, applied mass, and resulting force are interrelated. This relationship, presented in Table 9, serves as the basis for categorizing the severity of the applied impacts. For instance, a 0.25 kg mass dropped from a height of 304 mm yields an estimated impact force of approximately 2.75 N, while a 0.5 kg mass from the same height results in about 6.5 N. These values provide context for the forces reported in Tables 10 and 11, and help illustrate the influence of mass and impact distance on the intensity of applied forces.

In this study, two impact categories were defined: low-velocity and high-velocity impacts. Based on the calculated forces, a threshold of 9 N was established. Impacts producing forces up to 9 N are classified as low-velocity, while those exceeding 9 N are considered high-velocity. This classification facilitates a structured assessment of bamboo-reinforced masonry wall performance under various dynamic stress levels.

To compute the force generated during pendulum impact tests, multiple analytical methods were considered, each suitable depending on the available instrumentation and the level of accuracy required. These include both conventional energy-based models and advanced sensor-integrated approaches.

Energy-Based Method: This method calculates the potential energy using:

$$E = m \times g \times h \tag{14}$$

where E is the energy in joules, m is the mass (kg), g is the gravitational constant (9.81 m/s²), and h is the height (m). The force is then approximated by dividing this energy by the estimated deformation (d) of the wall:

$$F = \frac{E}{D} \tag{15}$$

This approach is simple and useful, though it heavily depends on accurately measuring wall deformation, which can be minimal and difficult to quantify in brittle materials like masonry.

Impulse-Momentum Method: This technique estimates impact force by calculating the change in momentum over time:

$$F = \frac{m . \Delta v}{\Delta t} \quad (16)$$

where Δv is the change in velocity during impact and Δt is the duration of impact. This method requires high-speed measurement tools to capture both velocity and time data accurately.

Sensor-Based Measurement Method: The most effective and preferred method in this study involves the use of an accelerometer to directly measure acceleration. The corresponding force is calculated as:

$$F = m \times a \quad (17)$$

with a representing the peak acceleration in m/s^2. Acceleration values recorded in g are converted using:

$$1g = 9.81\ m/s^2 \quad (18)$$

This method is particularly beneficial for testing brittle materials like masonry, as it bypasses the challenges of deformation-based estimation and allows real-time monitoring of the structural response. It also enables further dynamic analysis, including frequency response, damping behavior, and acceleration-time profiles.

High-Speed Camera Method: As a supplementary method, high-speed cameras can be employed to visually track displacement and contact duration. The data collected can be applied in energy or impulse equations for force estimation. However, its accuracy is limited by camera resolution and frame rate, especially for capturing short, high-speed events.

In summary, considering the brittle nature of masonry walls and the instrumentation available in this study, the sensor-based approach using a high-precision accelerometer was found to be the most reliable. It enabled direct, real-time force analysis, making it an essential tool for evaluating the dynamic response of both bamboo-reinforced and unreinforced masonry walls under lateral impact loading.

Table 9: Impact Forces with respect to different Distances					
Mass	**Impact forces (N)**				
Distances	**304 mm**	**609 mm**	**914 mm**	**1219 mm**	**1524mm**
0.25kg	2.75	3.22	3.78	4.54	5.1
0.5kg	6.5	7.5	9.295	10.05	12.05
0.75kg	9.75	11.25	13.94	15.08	18.08
1kg	13	15	18.59	20.1	24.1

4.4.2 Low Velocity Impacts:

Now, we proceed with the low-velocity impact testing, categorized under the first phase of impact evaluation. Table 10 presents the results for low-velocity impacts, which were conducted using impact masses ranging from 0.25 kg to 0.5 kg. The testing began with the SW, initially subjected to a 0.25 kg mass dropped from a height of 304 mm. After 10 consecutive blows at this height, the impact distance was increased to 609 mm, followed by another set of 10 blows. This process continued systematically, increasing the distance incrementally up to 1524 mm, with no visible damage observed at any stage. Subsequently, the mass was increased to 0.5 kg, and the same procedure was repeated. The first set of 10 blows was applied at 304 mm, followed by sequential increases in impact distance to 609 mm and beyond. Upon reaching a distance of 914 mm, initial cracks appeared after the fifth blow. The point at which these cracks were first observed is referred to as the Initial Impact Break (IIB). At this stage, further loading was halted to assess the damage progression. Additionally, acceleration data corresponding to these impacts were recorded and analyzed. The acceleration response at the identified IIB point is presented in Figure 4.11, providing insight into the dynamic behavior of the wall under low-velocity impact conditions. The SWO was tested following the same procedure as the SW.

Table 10; Results of low velocity impacts					
Low Velocity					
Specimens types	**Specimen**	**IM (kg)**	**IF (N)**	**Impact distance (mm)**	**IIB**
Category 1	SW	0.5	9.295	914	5
	SWO	0.5	7.5	609	9
	SWB	0.5	12.05	1524	4
	SWOB	0.5	10.05	1219	6

The impact testing began with a 0.25 kg mass, applied from a height of 304 mm. After 10 consecutive blows at this height, the impact distance was increased to 609 mm, with another set of 10 blows applied. This process continued systematically, increasing the impact distance up to 1524 mm, throughout this phase, no visible damage was observed. Next, the impact mass was increased to 0.5 kg, and the procedure was repeated. The first set of 10 blows was applied at 304 mm, followed by an increment to 609 mm. Upon reaching 609 mm, initial cracks began to appear after the ninth blow. The moment at which these cracks were first observed was recorded as the Initial Impact Blows (IIB).

Additionally, acceleration data were recorded at the IIB point to analyze the dynamic response of the wall. The corresponding acceleration and impact behavior are illustrated in Figure 4.12. For the SWB, initial cracks appeared after four blows from a 0.5 kg mass at a 1524 mm impact distance. At this stage, the recorded impact force was 12.05 N. The acceleration data corresponding to this condition is presented in Figure 15. Similarly, the SWOB developed initial cracks after six blows at an impact distance of 1219 mm, with an applied impact force of 10.05 N. The detailed impact data for this specimen is shown in Figure 4.10. Additionally, the acceleration data for both SWB and SWOB has been recorded and presented in Figure 4.14 and Figure 4.13, respectively.

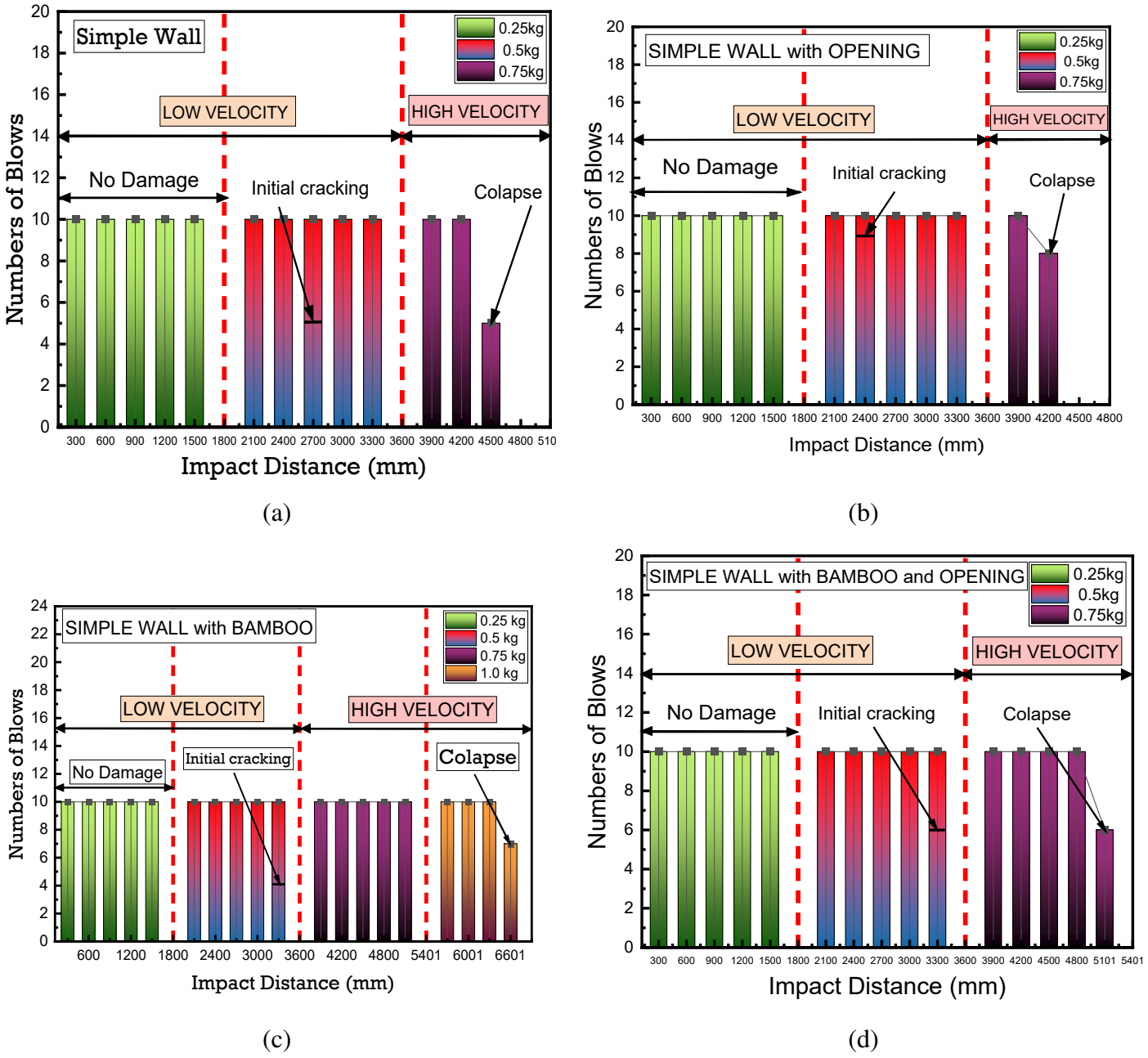

Figure 4.10: Blows with high velocity (a) SW, (b) SWO, (c) SWB, (d) SWOB

IIB

(a)

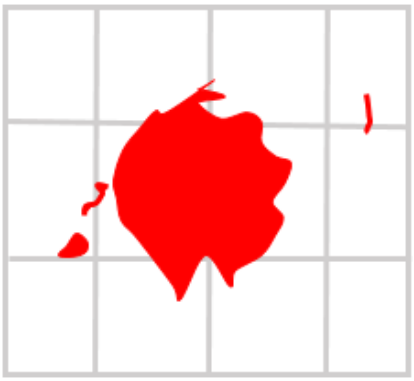

(b)

SW

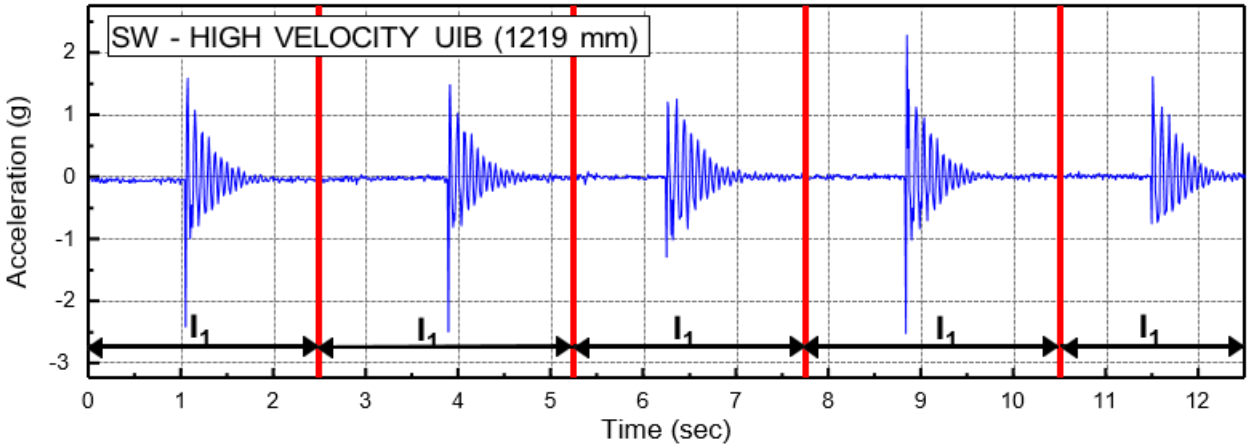

(C)

Figure 4.11: Low velocity impact load performance of SW at initial impact blows (IIB); (a). Damage mode (b) schematic damage pattern (c) acceleration response at each blow

IIB

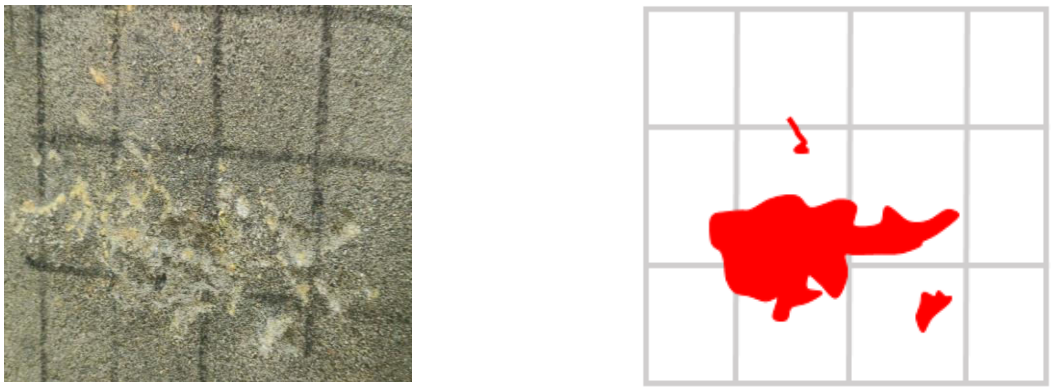

(a) (b)

SWO

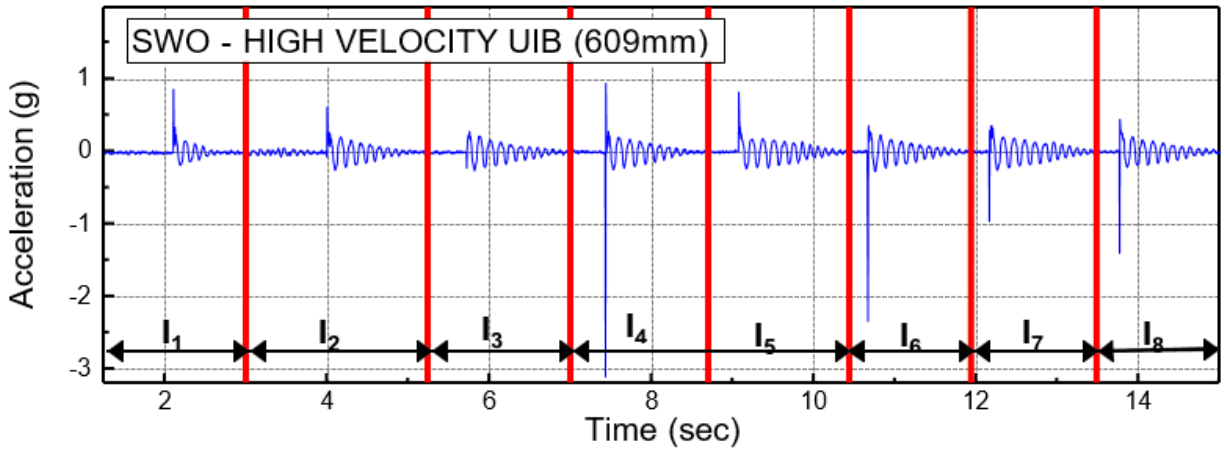

(c)

Figure 4.12: Low velocity impact load performance of SWO at initial impact blows (IIB); (a). Damage mode (b) schematic damage pattern (c) acceleration response at each blow

IIB

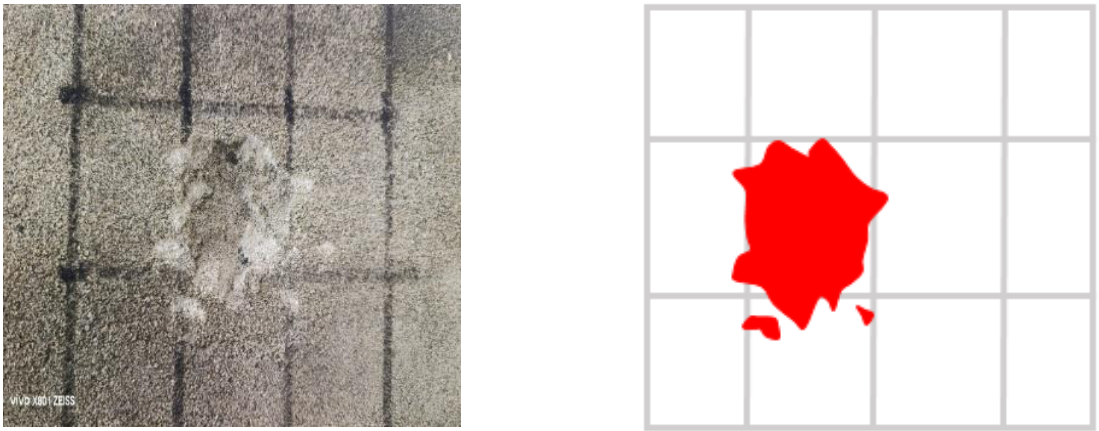

(a) (b)

SWOB

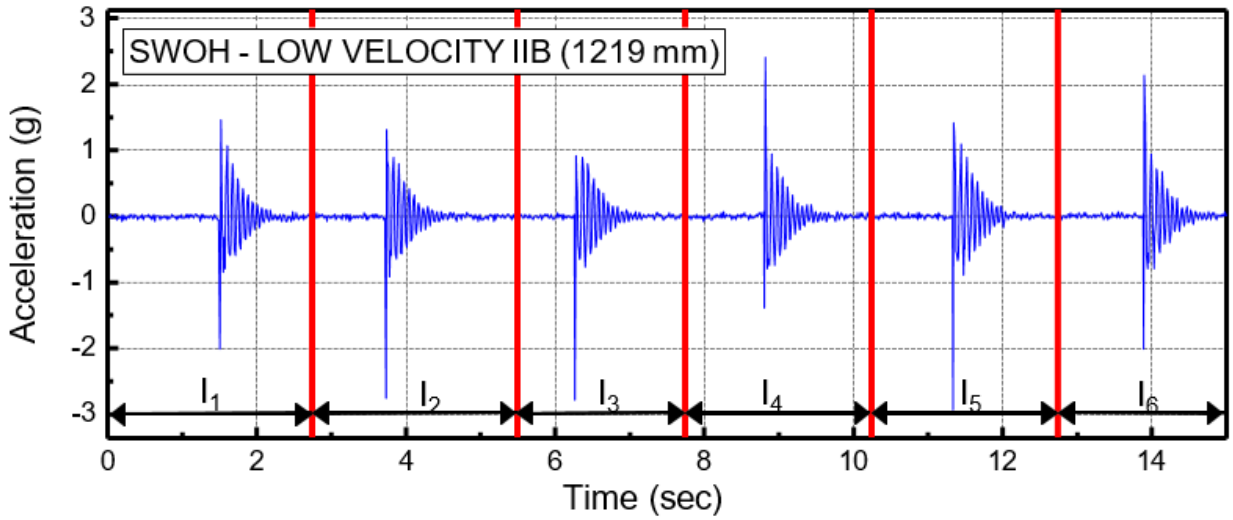

(c)

Figure 4.13: Low velocity impact load performance of SWOB at initial impact blows (IIB); (a). Damage mode (b) schematic damage pattern (c) acceleration response at each blow

IIB

(a) (b)

SWB

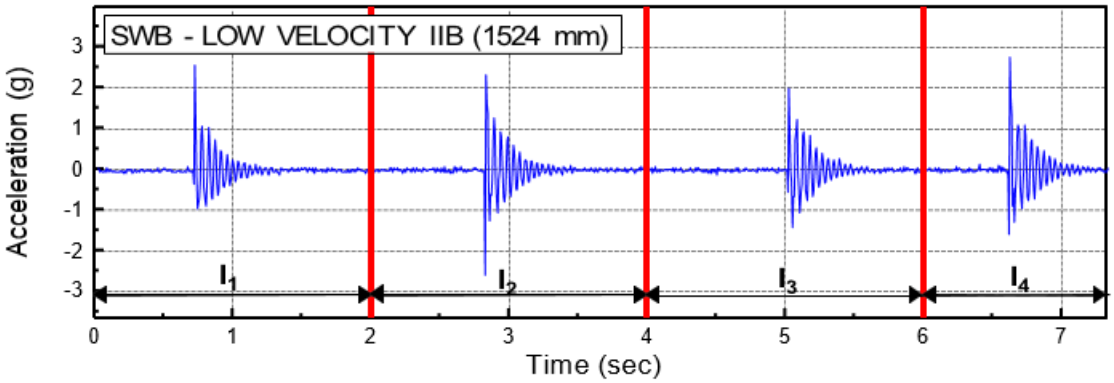

(c)

Figure 4.14: Low velocity impact load performance of SWB at initial impact blows (IIB); (a). Damage mode (b) schematic damage pattern (c) acceleration response at each blow

4.4.3 High Velocity Impact:

The high-velocity impact tests were conducted as a continuation of the previous phase, as illustrated in Figure 4.10. These tests aimed to evaluate the structural capacity of the masonry walls under more severe impact conditions, assessing their resistance to progressive loading and ultimate failure. The SW was initially impacted from a 914 mm distance, where the formation of initial cracks was observed after 9 blows. At this stage, the test was continued by applying further impacts using a 0.5 kg weight. With each successive blow, crack propagation became more evident, leading to gradual structural weakening. After a total of 50 blows, the impact weight was increased to 0.75 kg, and an additional 10 blows were applied from a 304 mm distance. The impact distance was then progressively increased from 304 mm to 609 mm and further to 1219 mm. At this critical distance as shown in Figure 1, the wall reached its ultimate failure point, exhibiting severe cracking that ultimately led to its complete collapse as illustrated in Figure 4.15. Similarly, the SWO underwent the same testing procedure. The wall initially sustained the impact forces without significant damage. However, as the impact distance reached 609 mm, the structure exhibited signs of distress, and after 8 consecutive blows, the wall collapsed. This result highlighted the structural limitations of unreinforced walls when subjected to high-velocity impacts, emphasizing their vulnerability in resisting sudden dynamic forces as illustrated in Figure 4.16.

In contrast, the SWB, reinforced with bamboo strips, demonstrated significantly superior impact resistance. Even under repeated impacts with a 0.75 kg weight, no signs of collapse were observed, indicating enhanced structural integrity due to the reinforcement. To further test the endurance of this specimen, the weight was increased to 1 kg, and impact testing was resumed across various distances, ranging from 304 mm to 1524 mm. Despite experiencing multiple blows, the wall maintained its stability up to 1524 mm, where it eventually collapsed after 7 blows. This result confirmed that bamboo reinforcement considerably improved the structural resilience of the masonry wall by enhancing its ability to dissipate impact energy and delay failure as illustrated in Figure 4.18.

The SWOB, which incorporated both an opening and bamboo reinforcement, exhibited a different failure pattern. The presence of the opening slightly reduced the structural integrity compared to

Table 11: Results of high velocity impacts						
High Velocity						
Specimens types	**Specimen**	**IM (kg)**	**IF (N)**	**Impact distance (mm)**	**UIB**	**S-max (mm)**
Category 1	SW	0.75	15.08	1219	5	98.7
	SWO	0.75	11.25	609	8	101.2
Category 2	SWB	1	20.1	1524	7	104.9
	SWOB	0.75	18.08	1524	6	95.9

the fully reinforced SWB. At a 1524 mm impact distance, when subjected to a 0.75 kg weight, the wall failed after only 6 blows, indicating that while bamboo reinforcement played a significant role in improving resistance, the introduction of an opening introduced structural weaknesses that reduced overall stability as illustrated in Figure 4.17.

The comparative data for all wall specimens have been systematically compiled in the subsequent tables, offering a detailed analysis of their impact resistance, failure mechanisms, and structural performance. These results provide valuable insights into the effectiveness of bamboo reinforcement in mitigating impact damage and enhancing the durability of masonry structures under dynamic loading conditions.

The SW specimen serves as the reference for evaluating the performance of all tested walls. Among the specimens, the SW exhibited the highest resistance to impact loading, establishing a baseline for comparison. The SWO, which lacked bamboo reinforcement and contained an opening, demonstrated the weakest performance among all specimens. The presence of an opening significantly reduced its structural integrity, making it more vulnerable to impact forces. In contrast, the SW performed better than the SWO due to its solid structure without any openings, which allowed it to sustain impact loads more effectively. The SWOH, which incorporated both an opening and bamboo reinforcement, exhibited improved performance compared to the SW and SWO. The addition of bamboo reinforcement helped compensate for the weakness introduced by the opening, enhancing the wall's ability to dissipate impact energy. Among all specimens, the

UIB

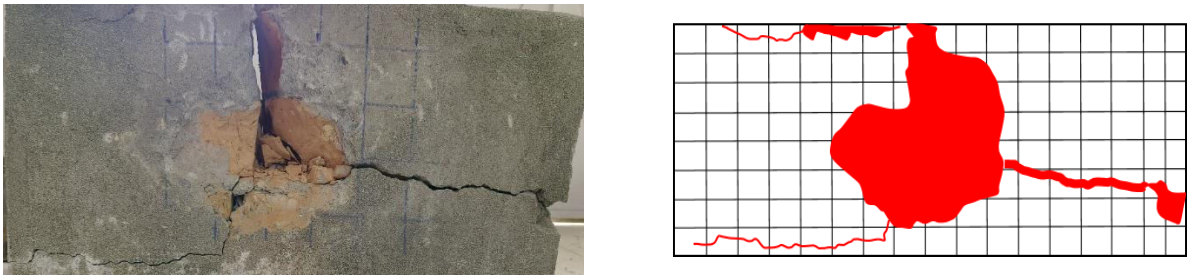

(a) (b)

SW

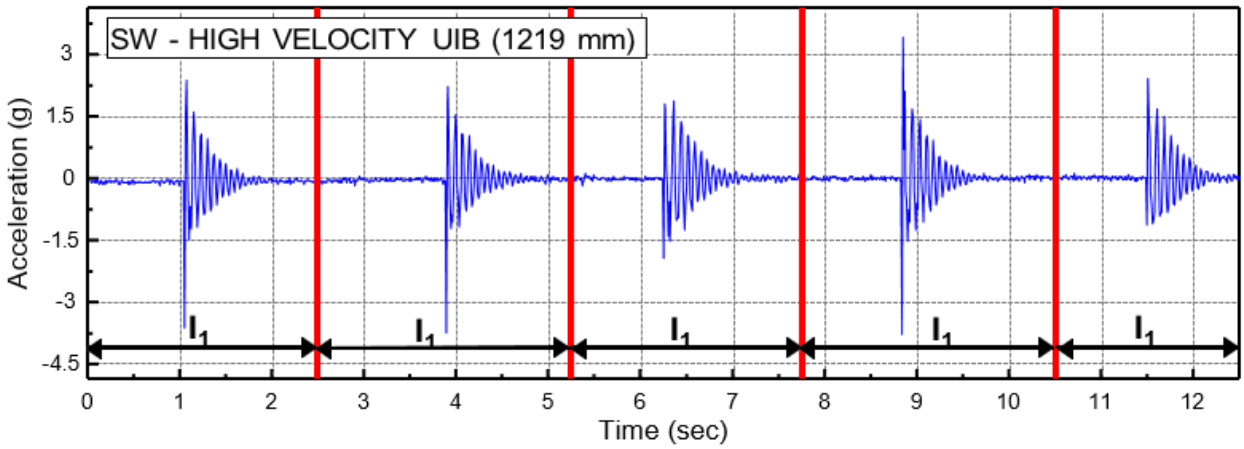

(c)

Figure 4.15: High velocity impact load performance of SW at initial impact blows (IIB); (a). Damage mode (b) schematic damage pattern (c) acceleration response at each blow

UIB

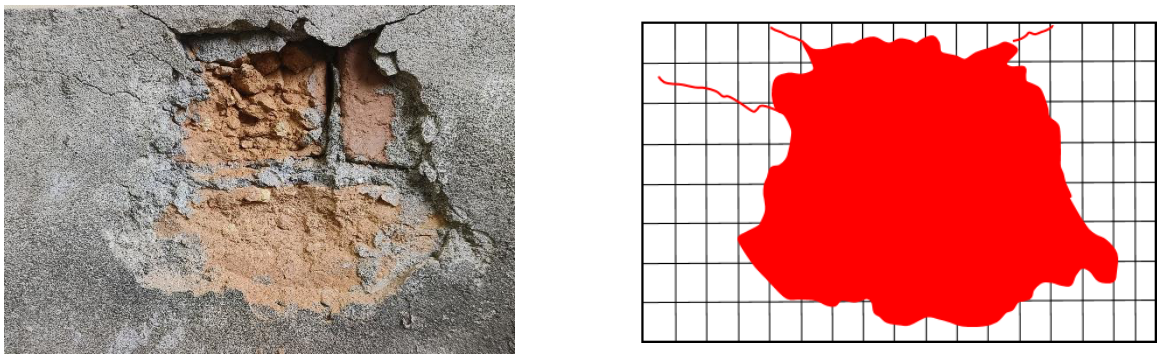

(a) (b)

SWO

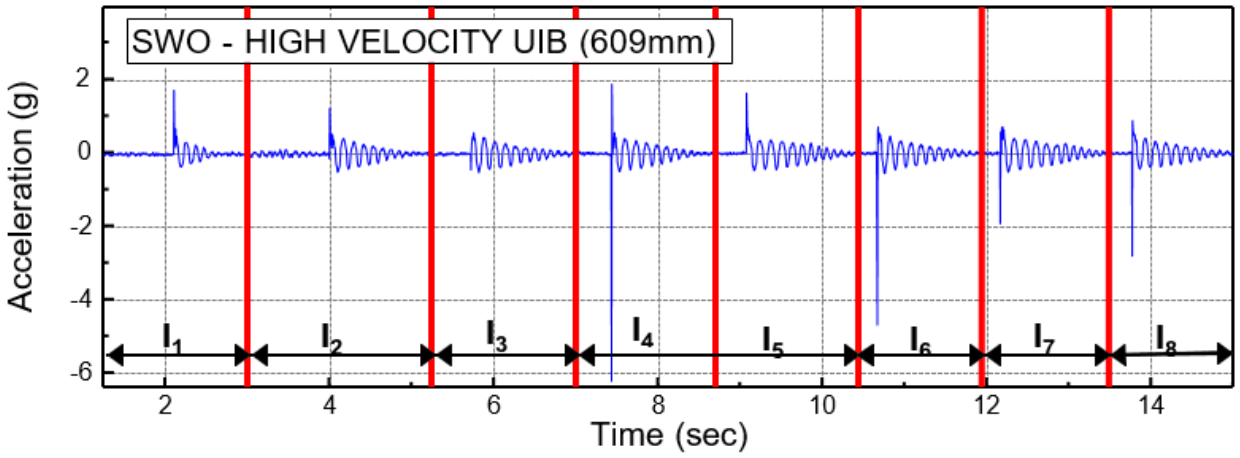

(c)

Figure 4.16: High velocity impact load performance of SWO at initial impact blows (IIB); (a). Damage mode (b) schematic damage pattern (c) acceleration response at each blow

UIB

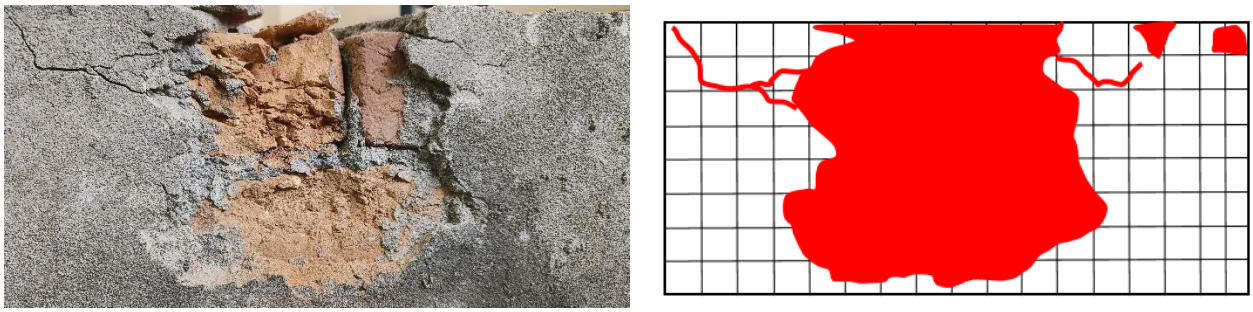

(a) (b)

SWOB

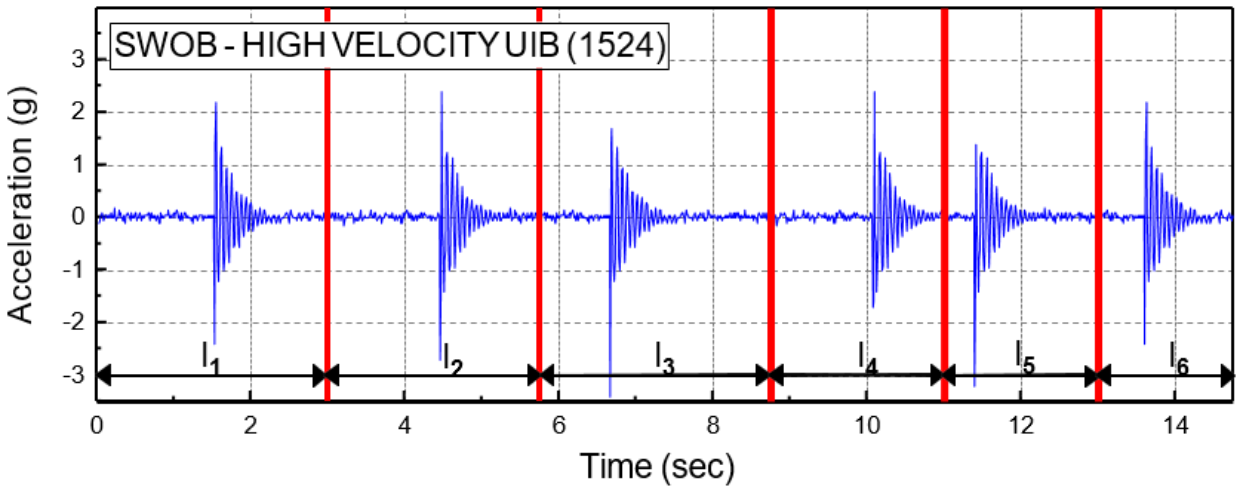

(c)

Figure 4.17: High velocity impact load performance of SWOB at initial impact blows (IIB); (a). Damage mode (b) schematic damage pattern (c) acceleration response at each blow

UIB

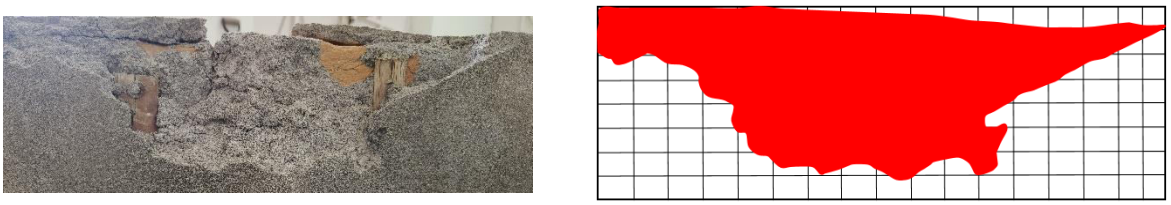

(a) (b)

SWB

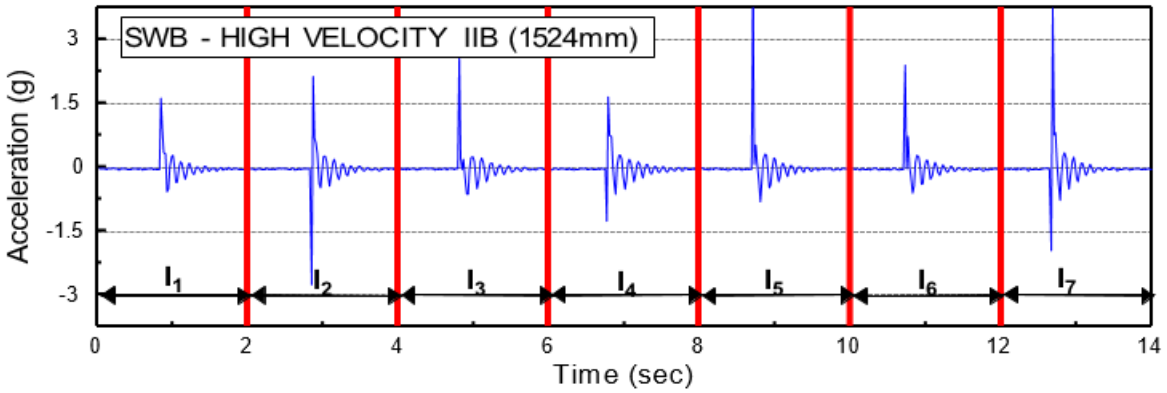

(c)

Figure 4.18: High velocity impact load performance of SWB at initial impact blows (IIB); (a). Damage mode (b) schematic damage pattern (c) acceleration response at each blow

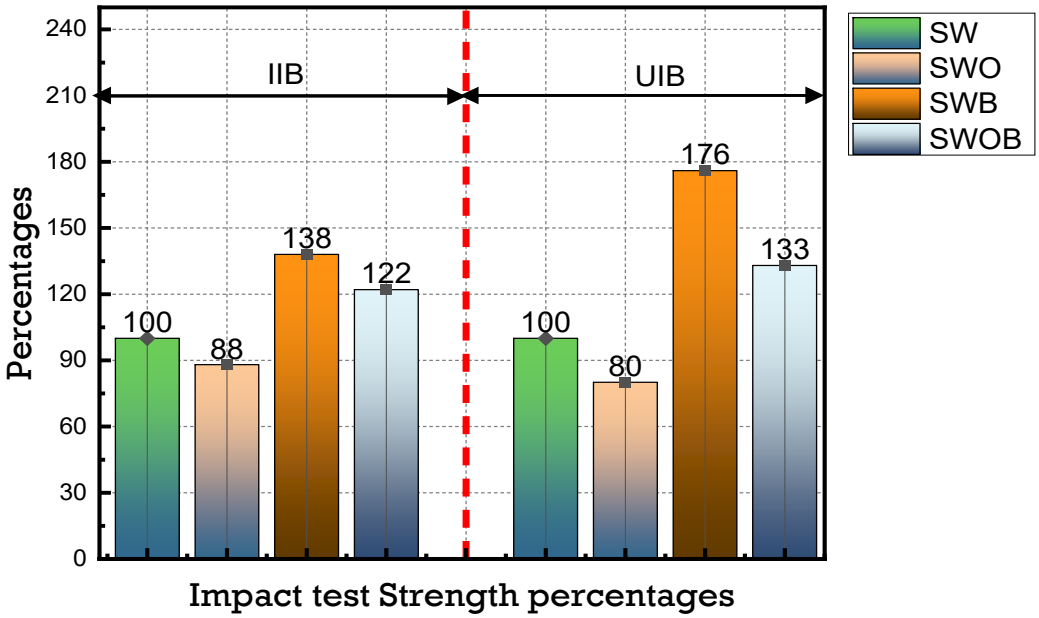

Figure 4.19: Impact test Strength percentages

SWB demonstrated the best performance. This wall combined the benefits of bamboo reinforcement with a solid structure, resulting in the highest impact resistance. The reinforcement effectively enhanced the wall's strength and energy absorption capacity, preventing early failure. The comparative strength values of these walls are presented in the corresponding figure, providing a clear visualization of their structural behavior under impact loading. Figure 4.19 illustrate the impact strength of wall Specimens.

4.4.4 Comparison of Damping Estimation Methods and the effectiveness of the Logarithmic Decrement Method in Structural Analysis:

The Logarithmic Decrement Method, Power Spectral Density (PSD) Curve Projection, and Phase Resonance Method are three widely used techniques for estimating damping in structural systems. Each method has its own advantages and limitations, depending on the nature of the system being analyzed and the available data.

The Power Spectral Density (PSD) Curve Projection Method is a frequency-domain approach that analyzes how energy is distributed across different frequencies. It is particularly useful for identifying resonance frequencies and evaluating how damping influences spectral energy distribution. However, this method requires a detailed frequency response analysis, making it less practical for cases where time-domain data is more accessible.

The Phase Resonance Method, on the other hand, determines damping by measuring the phase shift between applied force and structural response. This approach is effective for controlled laboratory experiments but may not be ideal for field conditions, where controlled excitation is challenging.

The Logarithmic Decrement Method, in contrast, is a time-domain approach that evaluates damping by analyzing the rate at which free vibrations decay over time. This method is particularly advantageous because it requires only the measurement of successive peak amplitudes in a decaying oscillatory system. The logarithmic decrement (δ) is calculated using the formula:

$$\delta = \frac{1}{n} \ln \left(\frac{x_1}{x_n + 1}\right) \tag{19}$$

Where x_1 and $x_n + 1$ the amplitudes of two successive cycles separated by n oscillations. The damping ratio ξ *is* then determined using*:*

$$\xi = \frac{\delta}{\sqrt{4\pi^2 + \delta^2}} \tag{20}$$

This method is highly suitable for your research on impact loading of masonry walls, as it allows for the direct estimation of damping from recorded oscillations after an impact event. By comparing the decrement values for different reinforcement materials (bamboo and steel), the efficiency of energy dissipation in each system can be assessed. If bamboo-reinforced walls exhibit a higher logarithmic decrement, it indicates better energy absorption, which can enhance their performance in vibration or impact-prone environments. Hence, the Logarithmic Decrement

Method stands out as a simple yet effective approach for damping estimation in dynamic structural analysis.

4.4.5 Fundamental period and damping at initial and ultimate damage stages

Accelerometers mounted on both the mass and the wall recorded the complete acceleration time history for each impact. The data were extracted using MATLAB and further filtered with Seismo-Signal 2024 to isolate the wall's true dynamic response. Figure 4.20 displays the processed acceleration data, including the impact force time history of the mass and the wall's acceleration history at three key moments: the first impact, the impact that initiated cracking (IIB), and the impact that led to ultimate failure (UIB). Additionally, the progression of crack development is documented to correlate with the visual condition of the bamboo reinforced masonry wall under Pendulum impact testing. The results clearly indicate that as wall damage increases, the fundamental frequency decreases while the damping ratio increases, with the damping ratios calculated using the logarithmic decrement method.

The results indicate that for the SW wall, the recorded impact force was 5.08 N. At the first blow, the acceleration was measured at 1.34 g, with a resonance frequency of 37.5 Hz and a damping ratio of 3.1%. At the initial impact failure (IIB), the acceleration decreased to 0.54 g, while the resonance frequency dropped to 27.3 Hz, and the damping ratio increased to 4.3%. At the ultimate impact failure (UIB), the recorded acceleration was 0.37 g, with a resonance frequency of 18.8 Hz and a damping ratio of 5.1% as illustrated in Figure 32.

These results clearly demonstrate that as cracks develop, the resonance frequency progressively decreases while the damping ratio increases. This trend indicates that the wall weakens over time due to repeated impact blow and increasing mass, leading to structural deterioration.

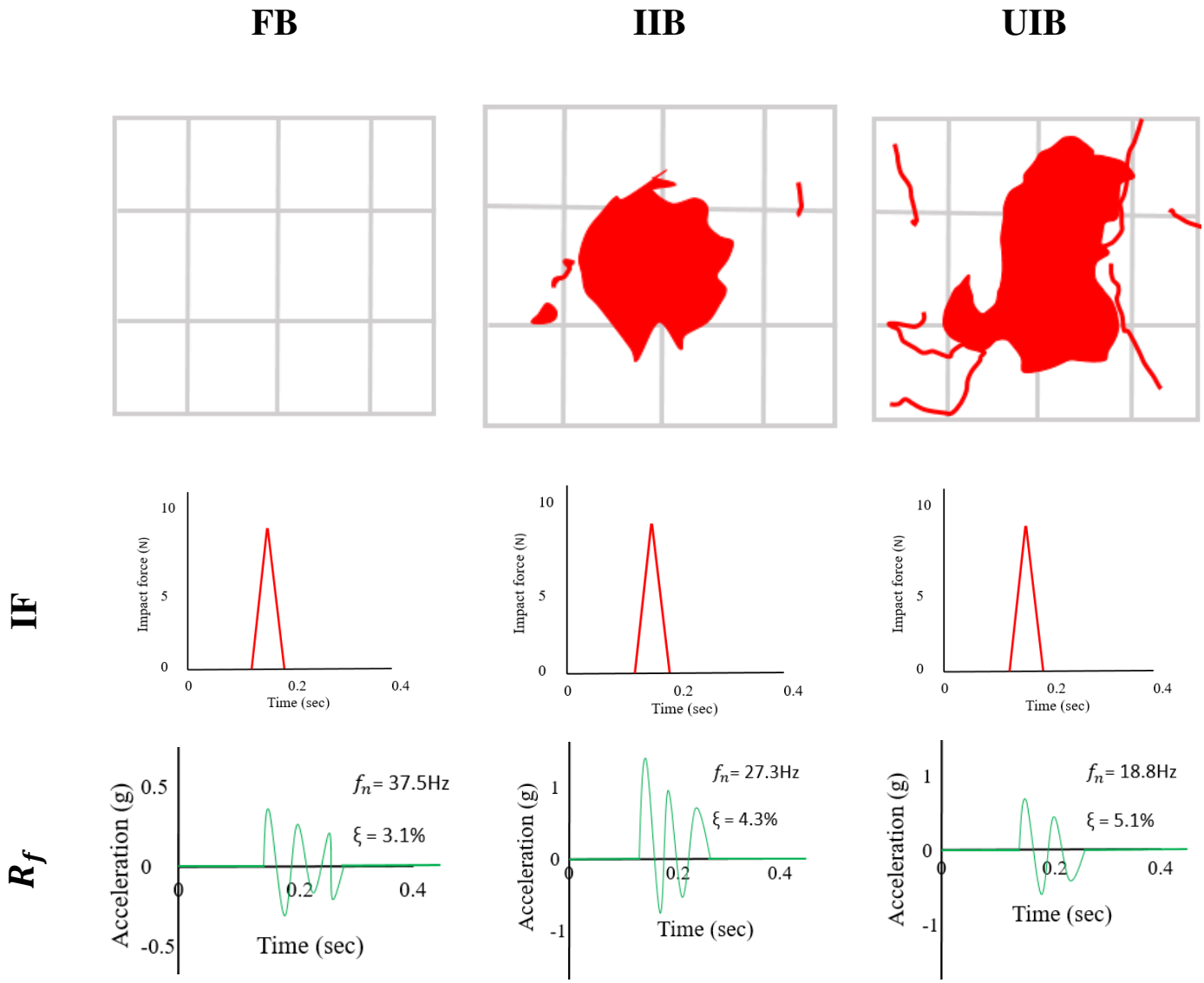

Figure 4.20, Dynamic characteristics of deteriorating SW; (IF) and acceleration time history ($\boldsymbol{R_f}$) of SW wall impact for first blow (FB), at initial impact blows (IIB), at ultimate impact blows (UIB).

\

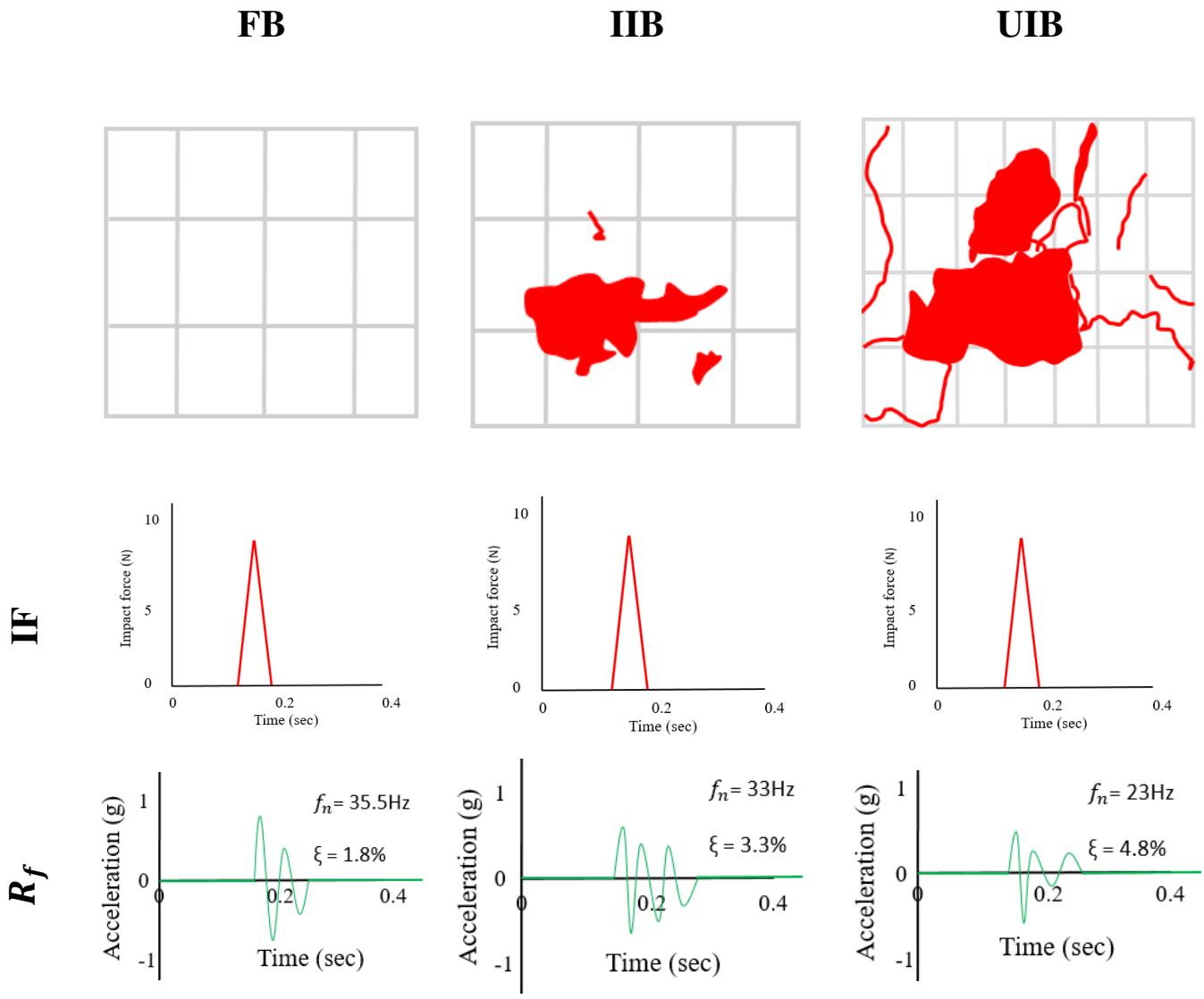

Figure 4.21, Dynamic characteristics of deteriorating SWO; (IF) and acceleration time history ($\boldsymbol{R_f}$) of SWO wall impact for first blow (FB), at initial impact blows (IIB), at ultimate impact blows (UIB).

For the SWO wall, the recorded impact response showed distinct changes at various failure stages. At the first blow (FB), the acceleration was measured at 0.78 g, with a resonance frequency of 35.5 Hz and a damping ratio of 1.8%. As the wall sustained further impacts, leading to initial impact failure (IIB), the acceleration decreased to 0.52 g, while the resonance frequency dropped to 33 Hz, and the damping ratio increased to 3.3%. At the ultimate impact failure (UIB), the acceleration further declined to 0.27 g, with a resonance frequency of 23 Hz and a damping ratio of 4.8%. as illustrated in Figure 4.21. These results highlight a clear trend where the decreasing resonance frequency and increasing damping ratio indicate progressive structural weakening. The lower initial damping ratio compared to the SW wall suggests that the absence of reinforcement in the SWO wall contributed to its reduced energy dissipation capacity. As the impact force intensified, cracks developed, leading to increased damping and reduced stiffness, ultimately compromising the wall's structural integrity

For the SWB wall, the recorded impact response demonstrated significant resistance and energy dissipation throughout the testing phases. At the first blow (FB), the acceleration was measured at 2.7 g, with a resonance frequency of 52.5 Hz and a damping ratio of 5.5%. As the wall progressed to initial impact failure (IIB), the acceleration reduced to 1.54 g, while the resonance frequency decreased to 27 Hz, and the damping ratio slightly increased to 6.1%. At the ultimate impact failure (UIB), the acceleration further dropped to 0.78 g, with the resonance frequency reducing to 23 Hz and the damping ratio rising to 7.8% as illustrated in Figure 4.22. These results indicate that the SWB wall exhibited superior impact resistance compared to unreinforced walls, as reflected in its higher initial resonance frequency and greater energy dissipation capacity. The presence of bamboo reinforcement contributed to maintaining the structural integrity by delaying crack propagation. The steady increase in damping ratio, coupled with the decreasing resonance frequency, confirms that the wall absorbed more energy under impact loading, effectively mitigating the damage progression and enhancing its durability.

For the SWOB wall, the impact response measurements revealed its enhanced structural performance due to bamboo reinforcement. At the first blow (FB), the acceleration was recorded at 2.34 g, with a resonance frequency of 30 Hz and a damping ratio of 2.7%. As the wall progressed to initial impact failure (IIB), the acceleration decreased to 1.40 g, while the resonance frequency dropped slightly to 27.7 Hz, and the damping ratio increased to 4.8%. At ultimate impact failur

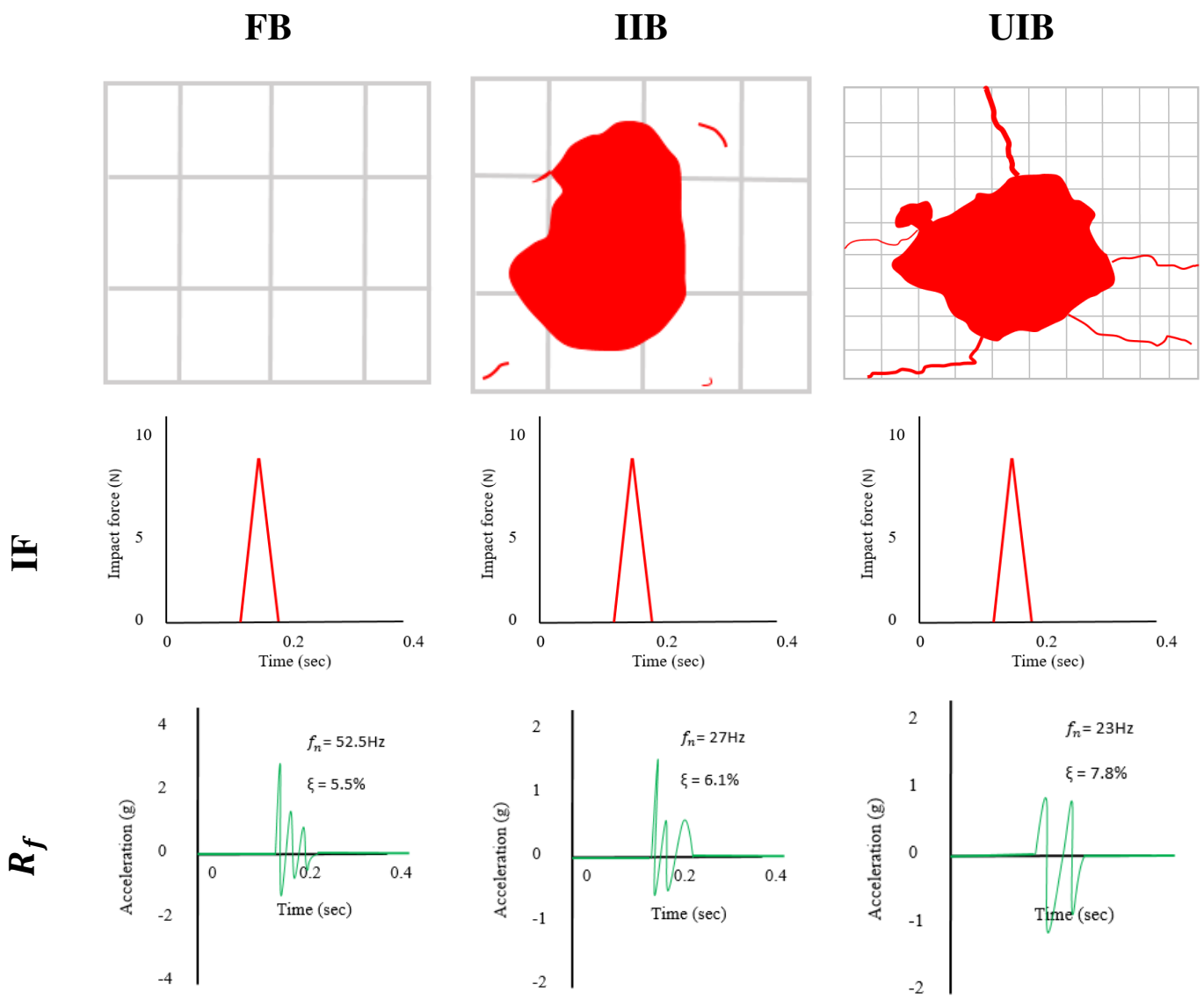

Figure 4.22, Dynamic characteristics of deteriorating SWB; (IF) and acceleration time history ($\boldsymbol{R_f}$) of SWB wall impact for first blow (FB), at initial impact blows (IIB), at ultimate impact blows (UIB).

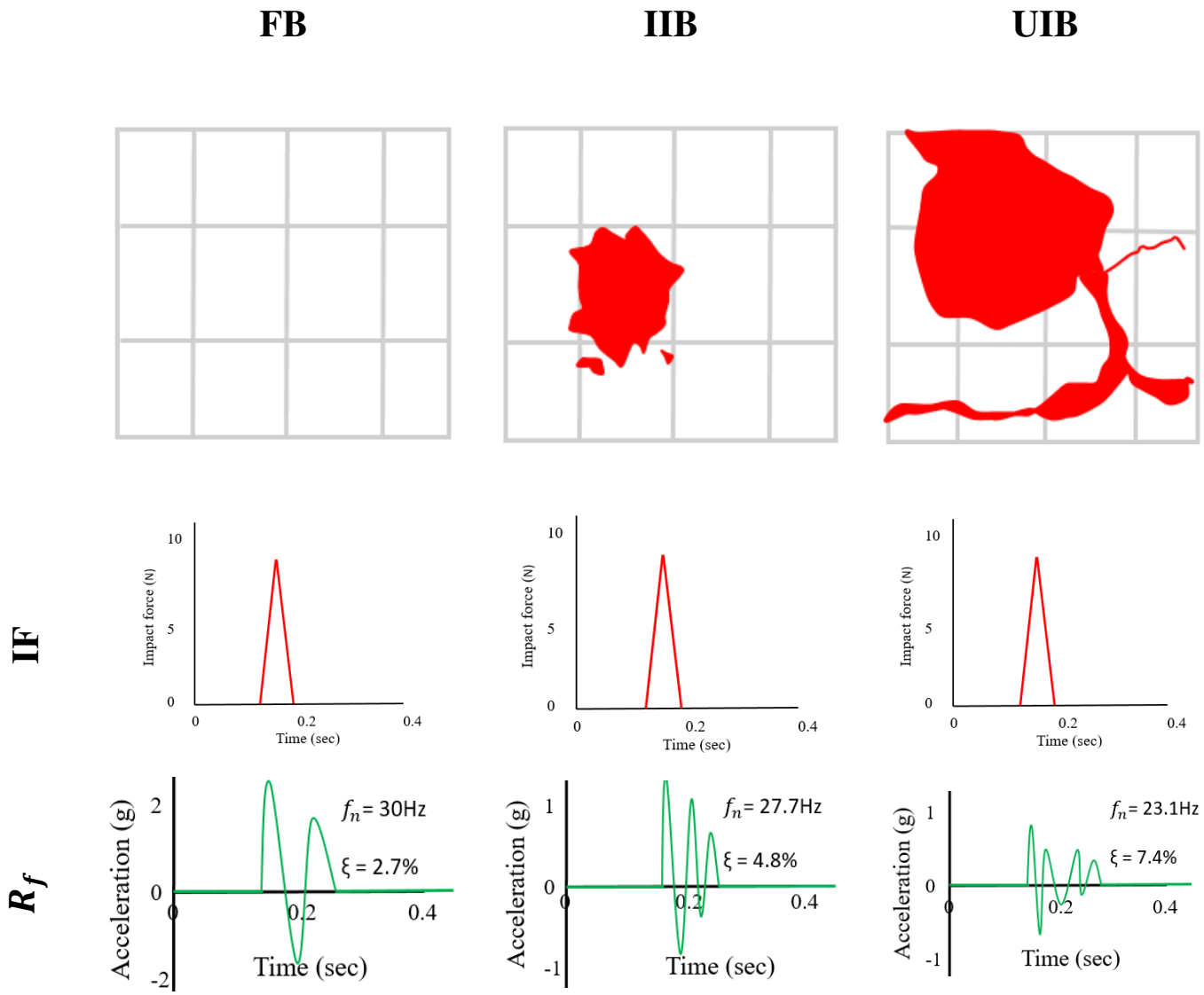

Figure 4.23, Dynamic characteristics of deteriorating SWOB; (IF) and acceleration time history ($\boldsymbol{R_f}$) of SWOH wall impact for first blow (FB), at initial impact blows (IIB), at ultimate impact blows (UIB).

(UIB), the acceleration further declined to 0.68 g, with the resonance frequency reducing to 23.1 Hz, while the damping ratio rose to 7.4% as illustrated in Figure 4.23.

These results indicate that the bamboo reinforcement in the SWB wall effectively improved its energy dissipation capacity, as seen in the increasing damping ratio and decreasing resonance frequency. The steady reduction in acceleration highlights the ability of the reinforcement to delay

crack propagation and maintain structural stability under impact loading. The combination of higher damping and lower resonance frequency at later stages confirms the wall's ability to absorb and dissipate impact energy, ultimately enhancing its resistance to out-of-plane impact forces.

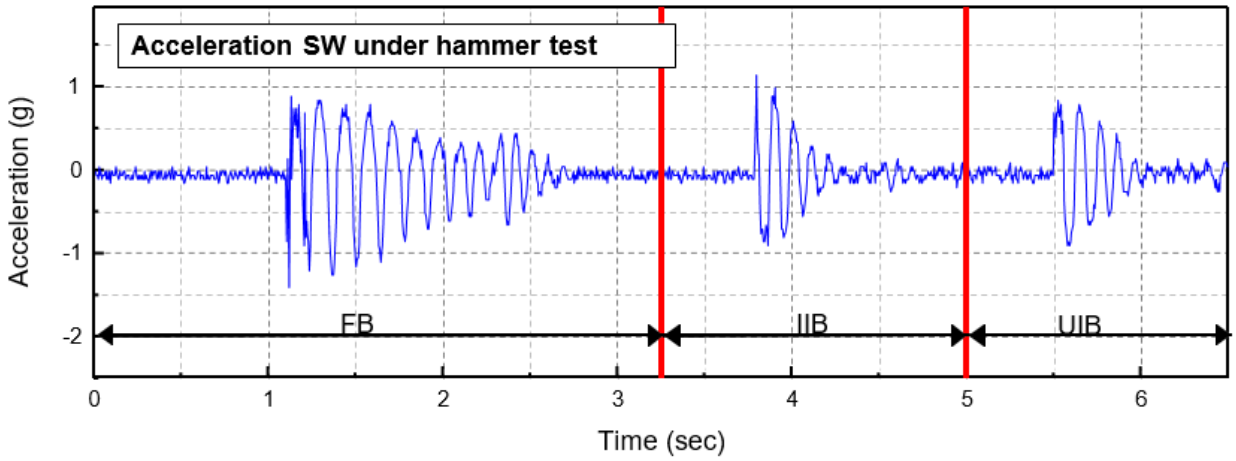

Figure 4.24: Acceleration For SW at FB , IIB and UIB

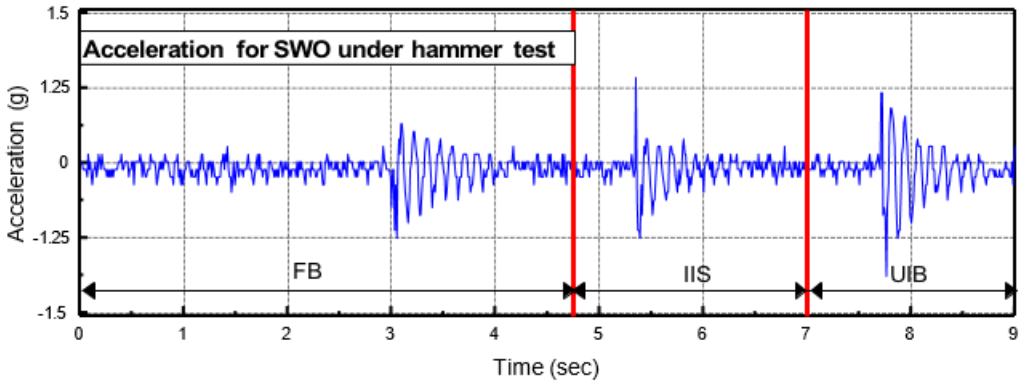

Figure 4.25: Acceleration For SWO at FB , IIB and UIB

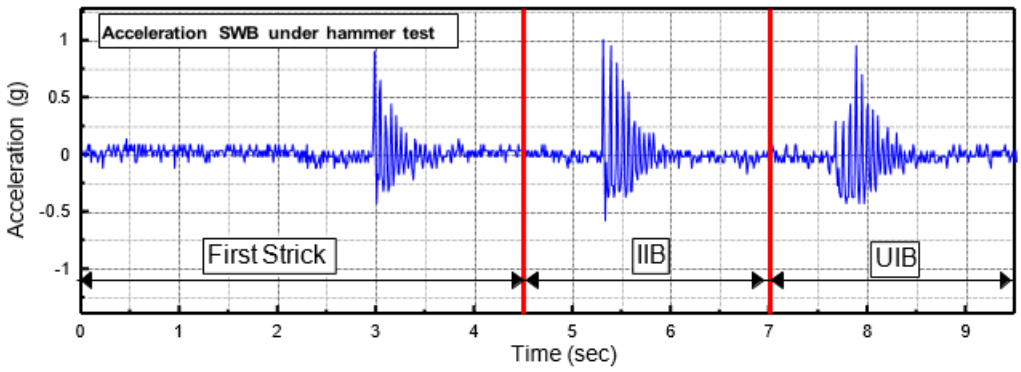

Figure 4.26: Acceleration For SWB at FB , IIB and UIB

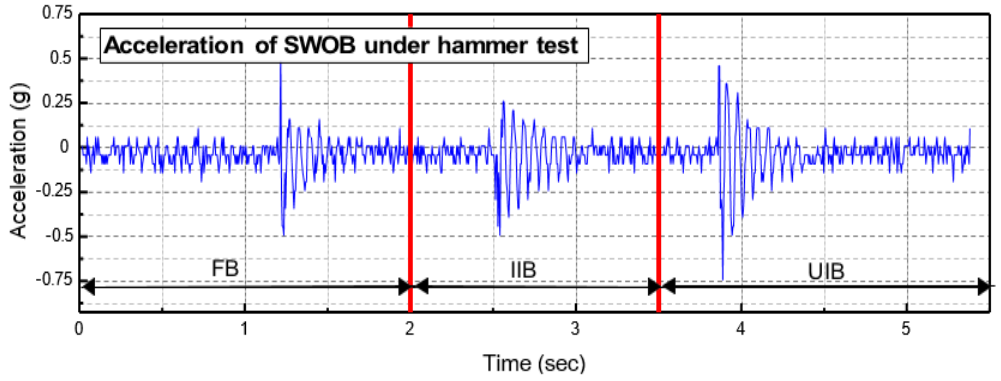

Figure 4.27: Acceleration For SWOB at FB , IIB and UIB

Table 12: Summary effect of impact response on fundamental period and damping.

Specimen		R_f (g)	f_n (Hz)	ξ %
SW	**FS**	1.34	37.5	3.1
	IIS	0.54	27.3	4.3
	UIS	0.37	18.8	5.1
SWO	**FS**	0.78	35.5	1.8
	IIS	0.52	33	3.3
	UIS	0.27	23	4.8
SWB	**FS**	2.71	50	5.5
	IIS	1.54	25	6.1
	UIS	0.78	20	7.8
SWOB	**FS**	2.34	30	2.7
	IIS	1.40	27.7	4.8
	UIS	0.68	23.1	7.4

4.4.6 Dynamic properties at different damage stage

Table 13 shows the results illustrate the consequences of low and high -velocity impacts on the walls at three stages: before testing, after initial impact strength failure, and after ultimate impact strength failure. Damping ratios were determined to gain a better understanding of the internal brick damage resulting from the impacts. It is observed that, before any impact, the resonance frequencies for the SWO and SWB configurations are higher than those for the SW configurations. This trend continues through the dynamic test conducted after ultimate failure. Similarly, the dynamic elastic modulus measured prior to impact testing is greater for the SWO and SWB walls compared to the SW and SWOB walls. However, following ultimate failure, the dynamic elastic modulus of the SWO configuration decreases relative to that of the SW, whereas the SWB configuration maintains a higher dynamic elastic modulus compared to the SWOB configuration. Overall, the data reveal that the damping ratios of all wall types increase with the application of impact strength, underscoring that walls incorporating jute fibers —especially those with bamboo or glass textile reinforcement—demonstrate enhanced energy dissipation capabilities, a critical factor for seismic resilience.

Figure 4.30 presents the damping values recorded at three different stages: the first impact, after initial impact strength (IIB) failure, and after ultimate impact blows (UIB) failure. The first impact has been considered as the reference (100%) to evaluate subsequent variations in damping and dynamic elastic modulus (EM_d). The results indicate a significant increase in damping, with values rising by 238.5% after IIB and 330.8% after UIB. Concurrently, the EM_d exhibited a notable reduction, decreasing by 43.42% after IIB and 19.42% after UIB, highlighting the progressive structural deterioration due to repeated impacts. The incorporation of bamboo reinforcement led to a substantial enhancement in damping characteristics. Specifically, damping increased from 1.7% to 2.1% in SWO and SWOB, while SW and SWB experienced a rise from 2.3% to 3.1%. This increase in damping suggests that bamboo-reinforced walls absorbed more energy during impact, contributing to improved dissipation of dynamic loads. However, this improvement in damping was accompanied by a reduction in stiffness, as indicated by the decrease in EM_d. The

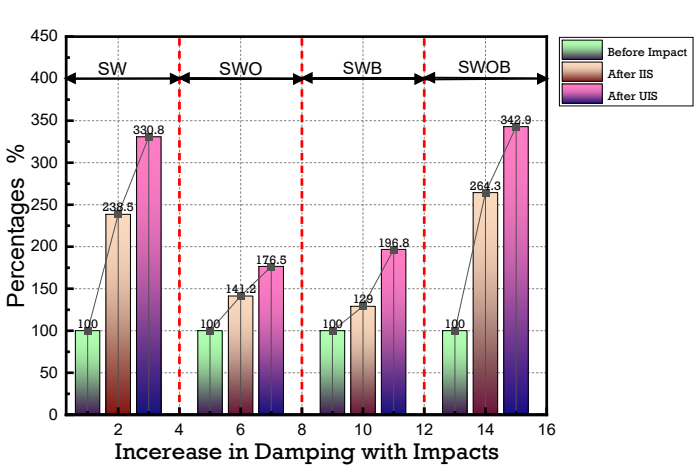

(a)

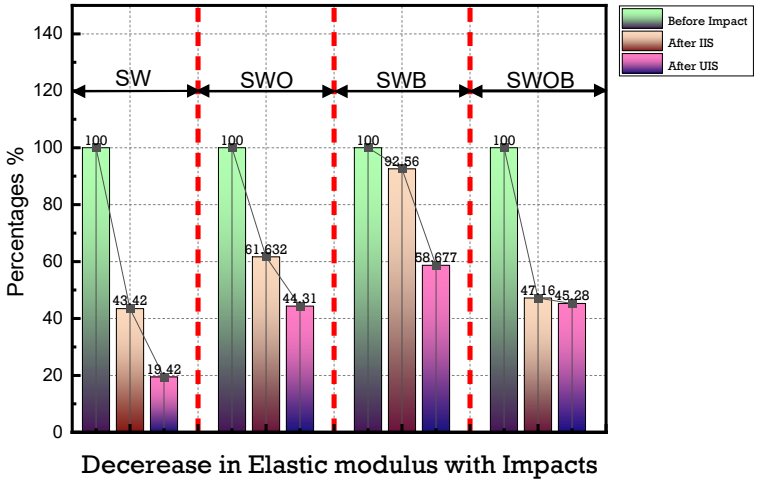

(b)

Figure 4.30: Percentage decrement against impact (a) Damping (b) Dynamic Elastic Modulus.

EM_d of SW and SWB dropped from 17.5 GPa to 12.1 GPa, signaling the formation and propagation of cracks, which weakened the structural integrity of the walls. Similarly, in SWO and SWOB, EM_d decreased from 8.8 GPa to 7.8 GPa, further reinforcing the observation that bamboo reinforcement alters the dynamic response of masonry structures. Overall, the results emphasize the critical role of bamboo reinforcement in enhancing damping capacity while acknowledging its impact on stiffness reduction. The observed trends highlight the trade-off between energy. Dissipation and structural rigidity, which is a key factor in designing impact-resistant masonry walls. Figure 4.31 illustrates the inverse relationship between resonance frequency and damping. As the resonance frequency decreases, the damping ratio increases, which can be attributed to the development of cracks within the masonry wall. When cracks form, the effective stiffness of the wall diminishes, leading to a lower resonance frequency, while the increased energy dissipation associated with crack propagation results in a higher damping ratio. For instance, in the simple wall (SW) configuration, the resonance frequency dropped from 3617.2 Hz to 1198 Hz, While the damping ratio increased from 2.3% to 4.3%. Similarly, for the simple wall with a central opening (SWO), the frequency decreased from 2488.5 Hz to 1584.5 Hz, with a corresponding increase in damping from 1.7% to 5.3%. These trends clearly demonstrate that as damage accumulates and cracks develop, the dynamic response of the wall shifts—stiffness decreases, leading to lower frequencies, while damping increases to absorb more energy. Such findings underscore the

Table 13; Low and High velocity impact on dynamic properties of deteriorating reinforced and unreinforced brick masonry walls.

Specimen		RF_t Hz	EM_d (GPa)	ξ %
SW	Before impact	3617.2	17.5	2.3
	After IIB	2374	7.6	3.1
	After UIB	1198	3.4	4.3
SWO	Before impact	2488.5	8.8	1.7
	After IIB	1777.8	5.5	2.4
	After UIB	1584.5	3.9	3.0
SWB	Before impact	3772.5	12.1	3.1
	After IIB	3473	11.2	4.0
	After UIB	3128.5	7.1	6.1
SWOB	Before impact	2108	7.8	2.1
	After IIB	1286	5	3.7
	After UIB	957.15	3	4.8

importance of effective reinforcement strategies, like bamboo reinforcement, to maintain structural integrity under impact and seismic load.

Note

A decrease in the elastic modulus indicates a reduction in the stiffness of the masonry wall system. As the structure experiences impact loading or repeated stress cycles, micro cracking and internal damage occur within the material, leading to a lower ability to resist deformation. Simultaneously,

an increase in damping reflects a greater capacity of the system to absorb and dissipate energy rather than store it elastically. This behavior is typically associated with nonlinear material response and energy loss through internal friction, cracking, or interface slip. In the context of this study, the combination of reduced stiffness and increased damping suggests that the walls are transitioning from an elastic state to a more damaged and dissipative phase, which is a common response in brittle masonry elements subjected to out-of-plane dynamic loading.

A decrease in the elastic modulus indicates a reduction in the stiffness of the masonry wall system. As the structure experiences impact loading or repeated stress cycles, micro cracking and internal damage occur within the material, leading to a lower ability to resist deformation. Simultaneously, an increase in damping reflects a greater capacity of the system to absorb and dissipate energy rather than store it elastically. This behavior is typically associated with nonlinear material response and energy loss through internal friction, cracking, or interface slip. In the context of this study, the combination of reduced stiffness and increased damping suggests that the walls are transitioning from an elastic state to a more damaged and dissipative phase, which is a common response in brittle masonry elements subjected to out-of-plane dynamic loading.

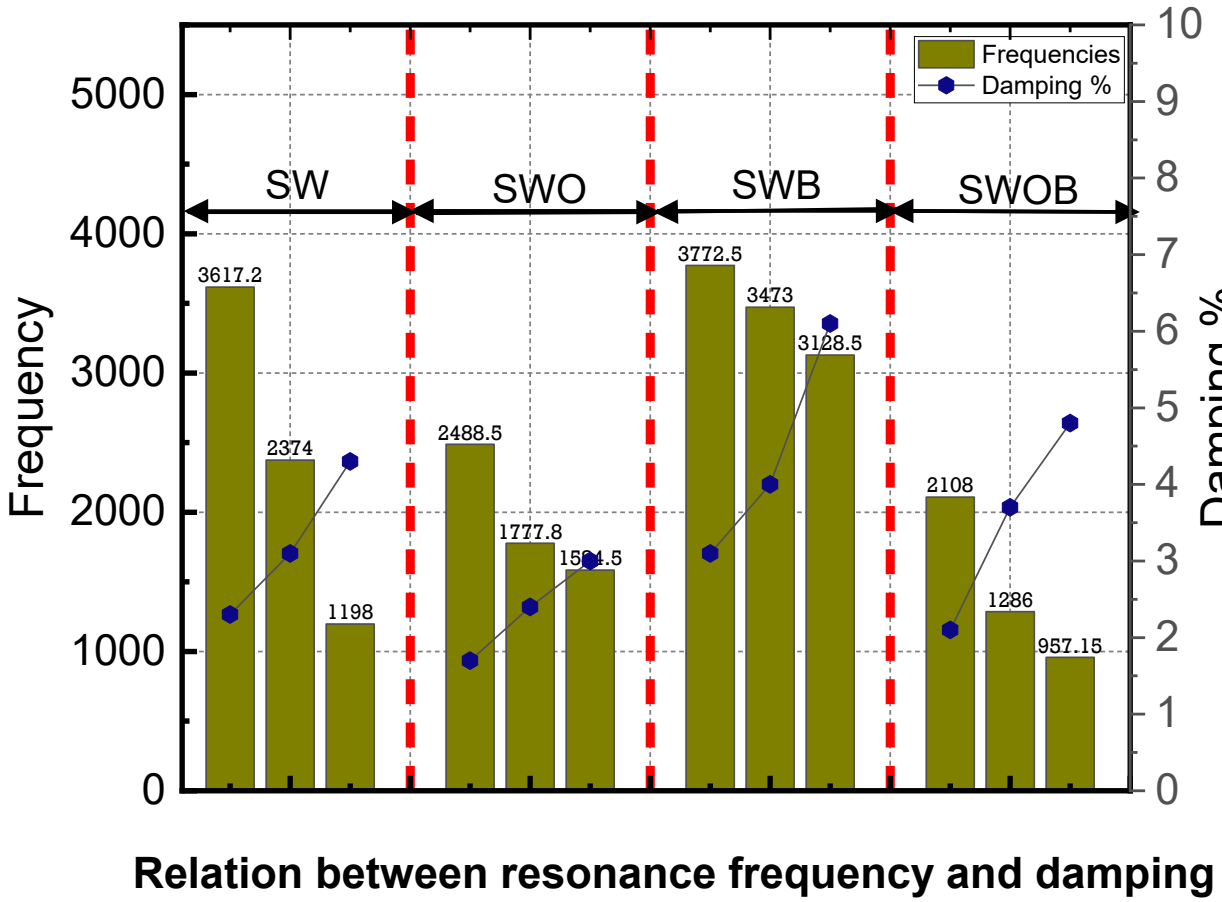

Figure 4.31; Relationship between Resonance frequency and Damping

4.4.7 Comparison of experimental and radical frequencies:

1. **Composite Material Properties:**

Effective Young's Modulus (Rule of Mixture)

$$E_{eff} = \sum V_i E_i = V_b E_b + V_{ba} E_{ba} + V_p E_p$$

$$V_b = 0.30, E_b = 7GPa; \quad V_{ba} = 0.080, E_{ba} = 20\ GPa; \quad V_p = 0.62, E_p = 25\ GPa;$$

$$E_{eff} = (0.30 * 7) + (0.08 * 2) + (0.62 * 25) = 18.4GPa$$

Effective Density:

$$\rho_{eff} = \sum V_i \rho_i = (0.30 * 1900) + (0.80 * 600) + (0.62 * 2000) = 1840 kg/m^3$$

Poisson's Ratio:

$$v_{eff} = 0.22$$

Flexural Rigidity:

$$D = \frac{E_{eff}^3}{12(1 - v_{eff}^2)} = \frac{18.4x10^9 * (0.04143^3)}{12(1 - 0.22^2)} = 114{,}560$$

<table>
<tr><td> 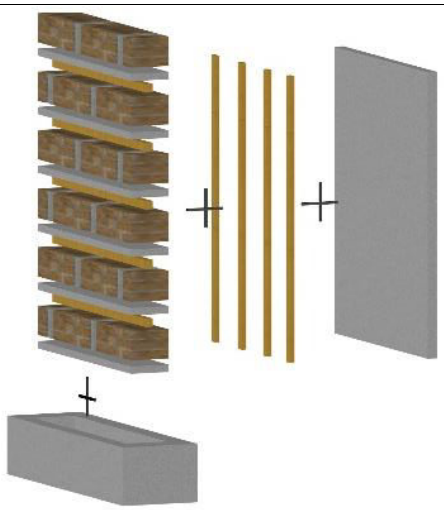 </td><td> 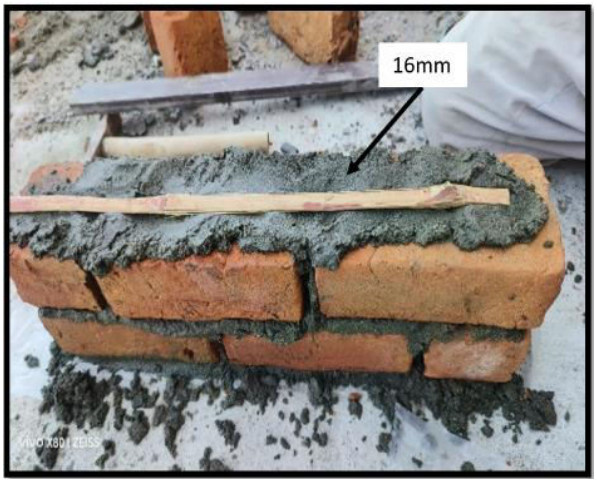
</td></tr>
<tr><td>(a)</td><td>(b)</td></tr>
<tr><td> 
</td><td>  </td></tr>
<tr><td>(c)</td><td>(d)</td></tr>
<tr><td colspan="2">Figure 4.32: (a) Geomatric composition of the composite system, (b) Placement bamboo reinforcemnt in the layers of wall specimens, (c) Placement of the bamboo reinforcement on the back side of the wall specimen, (d) Wall specimen is covered with plaster and bamboos are complete Embeded.</td></tr>
</table>

2. Plate Vibration Equations (Fixed Boundaries)
   Governing Equation:

$$D\nabla^4\omega + \rho_{eff}t\frac{\vartheta^2\omega}{\vartheta t^2} = 0$$

   Natural Frequency Solution:

$$f_m = \frac{1}{2\pi}\sqrt{\frac{K_{mm}}{M_{mn}}}$$

   Where modal stiffness $K_{mm}$and massM_{mn} are:

$$K_{mm} = \iiint_V \in^T C_\in dV, \quad M_{mn} = \rho_{eff}\iiint_V \Phi_m^2\Psi_n^2\varsigma_k^2 dV$$

   With eigenvalues λ_{mn}:

$$\lambda_{11} = 3.50, \quad \lambda_{12} = 6.98, \quad \lambda_{22} = 7.00, \quad \lambda_{13} = 8.00, \quad \lambda_{23} = 9.00,$$
$$\lambda_{33} = 10.0$$

3. Frequency Spectrum Calculation
   Fundamental Factor:

$$T = \frac{1}{2\pi a^2}\sqrt{\frac{D}{\rho_{eff}^t}} = \frac{1}{2\pi(0.610)^2}\sqrt{\frac{114{,}560}{1840 * 0.04143}} = 16.58Hz$$

Modal Frequencies:

$$f_{11} = (3.50)^2 * 16.58 = 203Hz$$

$$f_{12} = (6.98)^2 * 16.58 = 808Hz$$

$$f_{22} = (7.00)^2 * 16.58 = 812Hz$$

$$f_{13} = (8.00)^2 * 16.58 = 1061Hz$$

$$f_{23} = (9.00)^2 * 16.58 = 1343Hz$$

$$f_{33} = (10.0)^2 * 16.58 = 1658Hz$$

$$f_{14} = (11.0)^2 * 16.58 = 2006Hz$$

$$f_{24} = (12.0)^2 * 16.58 = 2388Hz$$

$$f_{34} = (13.0)^2 * 16.58 = 2802Hz$$

$$f_{44} = (14.0)^2 * 16.58 = 3250Hz$$

$$f_{45} = (15.0)^2 * 16.58 = 3730Hz$$

$$f_{55} = (16.0)^2 * 16.58 = 4244Hz$$

4. Thickness-Shear Mode (4000Hz)
   Shear Modulus

$$G_{eff} = \frac{E_{eff}}{2(1+v_{eff})} = \frac{18.4}{2(1+0.22)} = 7.54GPa$$

Shear Wave Speed:

$$v_s = \sqrt{\frac{G_{eff}}{\rho_{eff}}} = \sqrt{\frac{7.54x10^9}{1840}} = 2024\ m/s$$

Fundamental Thickness-shear Frequency:

$$f_{ts} = \frac{v_s}{2t} = \frac{2024.5}{2 * 0.04143} = 24400Hz$$

5. Bamboo Reinforcement Impact:
   Stiffness Enhancement:

$$\Delta E = V_{bamboo}(E_{bamboo} - E_{mortar}) = 0.08 * (20-5) = 1.2GPa$$

Frequency Shift:

$$\frac{\Delta f}{f} = \frac{1}{2}\sqrt{\frac{\Delta E}{E_{eff}}} = \frac{1}{2}\sqrt{\frac{1.2}{18.4}} = 9.1\%$$

Table14: Summary of Results of experimental and radical frequencies		
Mode	Frequency(Hz)	Experimental Range(Hz)
(1,2)	808	1000
(1,3)	1061	1000-4000
(2,2)	812	

(2,3)	1343	
(3,3)	1658	
(1,4)	2006	
(2,4)	2388	
(3,4)	2802	
(4,4)	3250	
(4,5)	3730	4000
(5,5)	42044	

Thickness-shear Mode: 24400Hz (not observed in 1-4 kHz)

Keyway stiffness: Increased frequency by 400% vs surface mount

Bamboo Effect: +9.1% frequency shift.

Chapter 5

Conclusion and Recommendations

1. A significant reduction in resonance frequency was observed in all wall configurations post-impact, indicating a notable loss in effective stiffness due to crack propagation. For instance, SW dropped from 3617.2 Hz to 1198 Hz and SWO from 2488.5 Hz to 1584.5 Hz.
2. The damping ratio increased with damage; SW rose from 2.3% to 4.3%, and SWO from 1.7% to 5.3%, confirming increased energy dissipation through internal friction and micro-crack activity.
3. Bamboo-reinforced walls (SWB and SWOB) exhibited superior damping and higher energy absorption compared to unreinforced counterparts, albeit with a moderate trade-off in stiffness reduction.
4. Dynamic elastic modulus decreased post-impact, reflecting stiffness degradation, yet bamboo reinforcement mitigated this effect more effectively than in unreinforced walls.
5. No bamboo strips failed in diagonal shear testing, confirming the tensile and compressive reliability of the bamboo reinforcements.
6. A pronounced effect of bamboo mesh spacing was noted: diagonal tension strength improved by 96% with 5 in. spacing, modulus of rigidity by 82%, and energy absorption by 195%, showing that wider bamboo mesh spacing offers optimal performance.
7. In-plane axial compression tests, SWB had the highest strength (5.79 MPa) and stiffness (4.21 GPa), while SW and SWO showed the lowest performance (3.51 MPa and 3.4 MPa; 2.5 GPa stiffness).
8. Maximum displacement was also controlled better in SWB (2.69 mm), indicating improved deformation resistance.
9. Wall specimens with openings (SWO, SWOB) consistently showed reduced compressive strength and stiffness, underscoring structural vulnerability.

10. Failure modes across all configurations included vertical cracking, crushing, and splitting, but the presence of bamboo helped contain crack propagation.
11. These findings suggest that BRMMW not only enhances structural resilience and energy dissipation but also maintains adequate stiffness and load-bearing capacity, validating its use in earthquake-prone and vibration-sensitive environments.

References

[1] T. Hussain and M. Ali, "Improving the impact resistance and dynamic properties of jute fiber reinforced concrete for rebars design by considering tension zone of FRC," *Construction and Building Materials,* vol. 213, pp. 592-607, 2019.

[2] P. R. Mali and D. Datta, "Experimental evaluation of bamboo reinforced concrete beams," *Journal of Building Engineering,* vol. 28, p. 101071, 2020.

[3] A. K. Dash and S. Gupta, "Bamboo wall structure: a step towards sustainable construction," *Advances in civil and structural engineering—CSE, Institute of Research Engineers and Doctors,* pp. 11-14, 2014.

[4] B. Sharma and A. van der Vegte, "Engineered bamboo for structural applications," in *Nonconventional and vernacular construction materials*: Elsevier, 2020, pp. 597-623.

[5] J. Vengala, H. Jagadeesh, and C. Pandey, "Development of bamboo structure in India," in *Modern bamboo structures*: CRC Press, 2008, pp. 63-76.

[6] M. Paradiso, "Usage of bamboo powder a san additive in adobe bricks and bamboo canes frames for the reinforcement of adobe structure," in *Reactive Proactive Architecture*: Universitat Politecnica de Valencia, 2019, pp. 232-238.

[7] D. Dowling, B. Samali, and J. Li, "An improved means of reinforcing adobe walls-external vertical reinforcement," *University of Technology. Sydney, Australia,* 2005.

[8] P. Kumar, P. Gautam, S. Kaur, M. Chaudhary, A. Afreen, and T. Mehta, "Bamboo as reinforcement in structural concrete," *Materials Today: Proceedings,* vol. 46, pp. 6793-6799, 2021.

[9] T. M. A. Khan, D. A. Quadir, T. Murty, A. Kabir, F. Aktar, and M. A. Sarker, "Relative sea level changes in Maldives and vulnerability of land due to abnormal coastal inundation," *Marine Geodesy,* vol. 25, no. 1-2, pp. 133-143, 2002.

[10] M. T. Siraj *et al.*, "Synthetic and mineral fibers: fundamentals and composites applications," *Synthetic and Mineral Fibers, Their Composites and Applications,* pp. 1-29, 2024.

[11] H. Jagadeesh and P. Ganapathy, "Traditional bamboo based walling/flooring systems in building and research needs," in *Proceedings of the 5th International Bamboo Workshop and the 9th International Bamboo Congress Ubud, Bali, Indonesia*, 1995, pp. 20-32.

[12] A. K. Dash and S. Gupta, "Energy absorption behavior of bamboo concrete composite wall panel," *Journal of Building Engineering,* vol. 57, p. 104857, 2022.

[13] Z. Ming, "Bamboo based boards in China: an introduction. Bamboo, people and the environment," *INBAR Tech. Rep.,* pp. 140-154, 1995.

[14] J. J. Janssen, *Designing and building with bamboo*. International Network for Bamboo and Rattan Netherlands, 2000.

[15] V. Puri, P. Chakrabortty, S. Anand, and S. Majumdar, "Bamboo reinforced prefabricated wall panels for low cost housing," *Journal of Building Engineering,* vol. 9, pp. 52-59, 2017.

[16] A. K. Dash and S. Gupta, "A scientific approach to bamboo-concrete house construction," in *Advances in Structural Engineering: Materials, Volume Three*, 2015, pp. 1933-1942: Springer.

[17] V. Puri and P. Chakrabortty, "Behavior of sustainable prefabricated bamboo reinforced wall panels under concentrated load," in *International Conference on Sustainable Infrastructure 2017*, 2017, pp. 116-125.
[18] S. Paudel, "Engineered bamboo as a building material," in *Modern bamboo structures*: CRC Press, 2008, pp. 45-52.
[19] M. Aizaz, K. Shahzada, A. Gul, and M. Saqib, "Experimental study on the in-plane behavior of mud brick walls strengthened with bamboo strip mesh and dried jute thread," in *Structures*, 2024, vol. 68, p. 107238: Elsevier.
[20] A. Gunasti and A. S. Manggala, "Utilization of bamboo for concrete columns in earthquake-resistant simple houses in Indonesia," *Case Studies in Construction Materials,* vol. 20, p. e02941, 2024.
[21] A. Bala, S. Gupta, K. Paradeshi, and A. K. Dash, "Behavior of bamboo wall panel under bullet impact load," *Materials Today: Proceedings,* vol. 32, pp. 904-909, 2020.
[22] X. Wei and M. G. Stewart, "Model validation and parametric study on the blast response of unreinforced brick masonry walls," *International journal of impact engineering,* vol. 37, no. 11, pp. 1150-1159, 2010.
[23] J. Moroz, S. Lissel, and M. Hagel, "Performance of bamboo reinforced concrete masonry shear walls," *Construction and Building Materials,* vol. 61, pp. 125-137, 2014.
[24] S. Ahmed and M. Ali, "Use of agriculture waste as short discrete fibers and glass-fiber-reinforced-polymer rebars in concrete walls for enhancing impact resistance," *Journal of Cleaner Production,* vol. 268, p. 122211, 2020.
[25] M. Kucukvar and O. Tatari, "Towards a triple bottom-line sustainability assessment of the US construction industry," *The International Journal of Life Cycle Assessment,* vol. 18, pp. 958-972, 2013.
[26] Z. Alwan, P. Jones, and P. Holgate, "Strategic sustainable development in the UK construction industry, through the framework for strategic sustainable development, using Building Information Modelling," *Journal of cleaner production,* vol. 140, pp. 349-358, 2017.
[27] P. O. Akadiri, P. O. Olomolaiye, and E. A. Chinyio, "Multi-criteria evaluation model for the selection of sustainable materials for building projects," *Automation in construction,* vol. 30, pp. 113-125, 2013.
[28] D. T. Doan, A. Ghaffarianhoseini, N. Naismith, T. Zhang, A. Ghaffarianhoseini, and J. Tookey, "A critical comparison of green building rating systems," *Building and Environment,* vol. 123, pp. 243-260, 2017.
[29] J. Bredenoord, "Sustainable building materials for low-cost housing and the challenges facing their technological developments: Examples and lessons regarding bamboo, earth-block technologies, building blocks of recycled materials, and improved concrete panels," *Journal of Architectural Engineering Technology,* vol. 6, no. 1, pp. 1-11, 2017.
[30] A. K. Dash and S. Gupta, "Study of bamcrete wall panel in the traditional Assam Type house," *Journal of Building Engineering,* vol. 51, p. 104164, 2022.
[31] P. Li, H. Brouwers, and Q. Yu, "Influence of key design parameters of ultra-high performance fibre reinforced concrete on in-service bullet resistance," *International Journal of Impact Engineering,* vol. 136, p. 103434, 2020.
[32] W. Wang and N. Chouw, "Flexural behaviour of FFRP wrapped CFRC beams under static and impact loadings," *International Journal of Impact Engineering,* vol. 111, pp. 46-54, 2018.

[33] C. Camposeco-Negrete, "Optimization of cutting parameters for minimizing energy consumption in turning of AISI 6061 T6 using Taguchi methodology and ANOVA," *Journal of cleaner production,* vol. 53, pp. 195-203, 2013.
[34] T. M. Pham and H. Hao, "Prediction of the impact force on reinforced concrete beams from a drop weight," *Advances in Structural Engineering,* vol. 19, no. 11, pp. 1710-1722, 2016.
[35] A. Badr and A. Ashour, "Modified ACI Drop-Weight Impact Test for Concrete," 2005.
[36] M. Sassu, A. De Falco, L. Giresini, and M. L. Puppio, "Structural solutions for low-cost bamboo frames: Experimental tests and constructive assessments," *Materials,* vol. 9, no. 5, p. 346, 2016.
[37] D. Romagno and M. Sassu, "Low cost seismic constructions: Design and dissemination in developing socio-economic areas," in *INTED2009 Proceedings*, 2009, pp. 2808-2818: IATED.
[38] F. Tootoonchy, B. Asgarian, and F. Danesh, "Experimental in-plane behavior and retrofitting method of mud-brick walls," *International Journal of Civil Engineering,* vol. 13, no. 2, pp. 191-201, 2015.
[39] T. L. Michiels, "Seismic retrofitting techniques for historic adobe buildings," *International Journal of Architectural Heritage,* vol. 9, no. 8, pp. 1059-1068, 2015.
[40] W. W. Mendis, G. De Silva, and G. S. De Silva, "Performance of un-reinforced burned clay brick masonry walls retrofitted with locally available materials," *Journal of the National Science Foundation of Sri Lanka,* vol. 47, no. 1, 2019.
[41] S. Kaminski, A. Lawrence, D. Trujillo, and C. King, "Structural use of bamboo: Part 2: Durability and preservation," *Structural Engineer,* vol. 94, no. 10, pp. 38-43, 2016.
[42] M. Blondet, J. Vargas, C. Sosa, and J. Soto, "Using mud injection and an external rope mesh to reinforce historical earthen buildings located in seismic areas," in *Proceedings of 9th international conference on structural analysis of historical constructions, Mexico City, Mexico*, 2014, vol. 252.
[43] M. Froli, G. Mariani, I. Ngoma, and M. Sassu, "A pilot test on the problem of joining steel plates to bamboo rods," 2003.
[44] M. Sassu, R. Domenica, N. Ignasio, P. Nicola, and B. Rita, *A proposal for low-cost earthquake-resistant bamboo buildings*. TEP-Tipografia Editrice Pisana, 2010.
[45] L. Jayanetti and P. Follett, "Briefing: Earthquake-proof house shakes bamboo world," in *Proceedings of the Institution of Civil Engineers-Civil Engineering*, 2004, vol. 157, no. 3, pp. 102-102: Thomas Telford Ltd.
[46] M. Sassu, M. Andreini, A. De Falco, and L. Giresini, "Bamboo trusses with low cost and high ductility joints," 2012.
[47] M. Sassu, M. Andreini, A. De Falco, and L. Giresini, "An innovative low cost solution for bamboo trusses with high-ductility connections," *Advanced Materials Research,* vol. 875, pp. 406-410, 2014.
[48] M. Blondet and C. Esparza, "Analysis of shaking table-structure interaction effects during seismic simulation tests," *Earthquake engineering & structural dynamics,* vol. 16, no. 4, pp. 473-490, 1988.
[49] D. Torrealva, "Seismic design criteria for adobe buildings reinforced with geogrids," in *Proceedings of 15th world conference on earthquake engineering, Lisbon, Portugal*, 2012.
[50] E. T. Puspitasari, S. M. Dewi, and D. A. Soehardjono, "Experimental Study of Flexural Capacity Strength In-Plane Load On Wall Panels Using Autoclaved Aerated Concrete Block and Bamboo Reinforcement," *GEOMATE Journal,* vol. 24, no. 103, pp. 17-25, 2023.

[51] M. Teguh and N. Rahmayanti, "Flexural behavior of confined masonry walls using interlocking concrete blocks subjected to out-of-plane loads," *GEOMATE Journal,* vol. 20, no. 81, pp. 179-184, 2021.
[52] S. M. Dewi, "Enhancing bamboo reinforcement using a hose-clamp to increase bond-stress and slip resistance," *Journal of Building Engineering,* vol. 26, p. 100896, 2019.
[53] S. Tambe, R. Kumar, M. Arrawatia, and A. K. Ganeriwala, "How safe are our rural structures? Lessons from the 2011 Sikkim Earthquake," *Current Science,* pp. 1392-1397, 2012.
[54] N. Quinn, D. D'Ayala, and T. Descamps, "Structural characterization and numerical modeling of historic Quincha walls," *International Journal of Architectural Heritage,* vol. 10, no. 2-3, pp. 300-331, 2016.
[55] A. Bala, A. K. Dash, S. Gupta, and V. Matsagar, "Behavior of bamboo wall panel at elevated temperature," in *Wood & Fire Safety: Proceedings of the 9th International Conference on Wood & Fire Safety 2020 9*, 2020, pp. 281-287: Springer.
[56] M. Blondet, M. Serrano, A. Rubiños, and E. Mattsson, "Training in earthquake resistent adobe brick construction in the Peruvian Andes," in *16th world conference on earthquake engineering*, 2017.
[57] C. Y. T. Ming, W. K. Jye, and H. A. I. Ahmad, "Mechanical properties of bamboo and bamboo composites: A Review," *J. Adv. Res. Mater. Sci,* vol. 35, no. 1, pp. 7-26, 2017.
[58] U. Anwar, M. Paridah, H. Hamdan, S. M. Sapuan, and E. Bakar, "Effect of curing time on physical and mechanical properties of phenolic-treated bamboo strips," *industrial crops and products,* vol. 29, no. 1, pp. 214-219, 2009.
[59] K. Rassiah, M. M. Ahmad, and A. Ali, "Mechanical properties of laminated bamboo strips from Gigantochloa Scortechinii/polyester composites," *Materials & Design,* vol. 57, pp. 551-559, 2014.
[60] S. Lakkad and J. Patel, "Mechanical properties of bamboo, a natural composite," *Fibre science and technology,* vol. 14, no. 4, pp. 319-322, 1981.
[61] A. Majumder, F. Stochino, I. Farina, M. Valdes, F. Fraternali, and E. Martinelli, "Physical and mechanical characteristics of raw jute fibers, threads and diatons," *Construction and Building Materials,* vol. 326, p. 126903, 2022.
[62] A. San Bartolomé, D. Quiun, and L. Zegarra, "Effective system for seismic reinforcement of adobe houses," in *13th world conference on earthquake engineering*, 2004, vol. 3321.
[63] M. Nili and V. Afroughsabet, "Combined effect of silica fume and steel fibers on the impact resistance and mechanical properties of concrete," *International journal of impact engineering,* vol. 37, no. 8, pp. 879-886, 2010.
[64] W. Zhang, S. Chen, N. Zhang, and Y. Zhou, "Low-velocity flexural impact response of steel fiber reinforced concrete subjected to freeze–thaw cycles in NaCl solution," *Construction and Building Materials,* vol. 101, pp. 522-526, 2015.
[65] M. P. Salaimanimagudam, C. R. Suribabu, G. Murali, and S. R. Abid, "Impact response of hammerhead pier fibrous concrete beams designed with topology optimization," *Periodica Polytechnica Civil Engineering,* vol. 64, no. 4, pp. 1244-1258, 2020.
[66] W. Zhang, S. Chen, and Y. Liu, "Effect of weight and drop height of hammer on the flexural impact performance of fiber-reinforced concrete," *Construction and Building Materials,* vol. 140, pp. 31-35, 2017.

[67] Y. Pan, C. Wu, X. Cheng, V. C. Li, and L. He, "Impact fatigue behaviour of GFRP mesh reinforced engineered cementitious composites for runway pavement," *Construction and Building Materials,* vol. 230, p. 116898, 2020.
[68] A. R-89, "Measurement of properties of fiber reinforced concrete," *Reported by ACI Committee,* vol. 544, 1999.
[69] T. Z. Batran, M. K. Ismail, and A. A. Hassan, "Behavior of novel hybrid lightweight concrete composites under drop-weight impact loading," in *Structures*, 2021, vol. 34, pp. 2789-2800: Elsevier.
[70] M. Ziada, S. Erdem, Y. Tammam, S. Kara, and R. A. G. Lezcano, "The effect of basalt fiber on mechanical, microstructural, and high-temperature properties of fly ash-based and basalt powder waste-filled sustainable geopolymer mortar," *Sustainability,* vol. 13, no. 22, p. 12610, 2021.
[71] E. K. Schrader, "Impact resistance and test procedure for concrete," in *Journal Proceedings*, 1981, vol. 78, no. 2, pp. 141-146.
[72] T. Rahmani, B. Kiani, M. Shekarchi, and A. Safari, "Statistical and experimental analysis on the behavior of fiber reinforced concretes subjected to drop weight test," *Construction and Building Materials,* vol. 37, pp. 360-369, 2012.
[73] H. Okail, A. Abdelrahman, A. Abdelkhalik, and M. Metwaly, "Experimental and analytical investigation of the lateral load response of confined masonry walls," *HBRC journal,* vol. 12, no. 1, pp. 33-46, 2016.
[74] J. M. Branco and J. P. Araújo, "Structural behaviour of log timber walls under lateral in-plane loads," *Engineering Structures,* vol. 40, pp. 371-382, 2012.
[75] A. Ganbaatar, T. Mori, S. Matsumoto, and R. Inoue, "Reinforced effect on brick wall using timber wall as a retrofitting method," *Buildings,* vol. 12, no. 7, p. 978, 2022.
[76] J.-W. Baek, J.-H. Kwon, S.-M. Kang, and H.-G. Park, "Cyclic loading test for brick masonry veneer anchored to reinforced concrete walls," *Journal of Building Engineering,* vol. 96, p. 110369, 2024.
[77] S. Burnett, M. Gilbert, T. Molyneaux, G. Beattie, and B. Hobbs, "The performance of unreinforced masonry walls subjected to low-velocity impacts: Finite element analysis," *International Journal of Impact Engineering,* vol. 34, no. 8, pp. 1433-1450, 2007.
[78] K. Senthil, A. Thakur, A. Singh, M. Iqbal, and N. Gupta, "Transient dynamic response of brick masonry walls under low velocity repeated impact load," *International Journal of Impact Engineering,* vol. 174, p. 104521, 2023.

Appendix

Matlab code used in calculations:

```
% Complete MATLAB Code for Acceleration Signal Analysis and PSD Plotting

% Assumptions:

% - You have a .txt file with acceleration data (one column or more)

% - We're using the 3rd column as acceleration (change if needed)

% - Sampling Frequency (Fs) is known or estimated


% Step 1: Load Acceleration Data

filename = 'acceleration_data.txt';  % Replace with your actual filename

data = load(filename);              % Load the data


% Step 2: Extract Acceleration Signal (Assuming 3rd Column)

acc = data(:,3);                    % Column 3 = Acceleration in m/s^2


% Step 3: Define Sampling Frequency (Hz)

Fs = 1000;  % Change based on your actual sampling rate


% Step 4: Time Vector Creation (optional, for plotting)

N = length(acc);                    % Total number of samples

t = (0:N-1)/Fs;                     % Time vector in seconds
```

```
% Step 5: Plot Raw Acceleration Signal
figure;
plot(t, acc, 'r', 'LineWidth', 1.2);
xlabel('Time (s)');
ylabel('Acceleration (m/s^2)');
title('Raw Acceleration Signal');
grid on;

% Step 6: Compute Power Spectral Density using Welch Method
[PSD, f] = pwelch(acc, hamming(1024), 512, 1024, Fs);  % You can tweak parameters

% Step 7: Plot PSD (in dB)
figure;
plot(f, 10*log10(PSD), 'b', 'LineWidth', 1.5);
xlabel('Frequency (Hz)');
ylabel('Power/Frequency (dB/Hz)');
title('Power Spectral Density (PSD)');
grid on;

% Step 8: Optional - Identify Peak Frequency
[max_val, max_idx] = max(PSD);       % Maximum PSD value
peak_freq = f(max_idx);              % Frequency at which it occurs
```

```
% Display peak frequency
fprintf('Dominant Frequency: %.2f Hz\n', peak_freq);

% Step 9: Save Plots (optional)
saveas(gcf, 'PSD_plot.png');        % Saves current figure as PNG

% Step 10: Summary Output
fprintf('Total Samples: %d\n', N);
fprintf('Sampling Frequency: %d Hz\n', Fs);
fprintf('Max Acceleration: %.2f m/s^2\n', max(acc));
fprintf('Min Acceleration: %.2f m/s^2\n', min(acc));
```